ISTANBUL MEDENIYET UNIVERSITY
INSTITUTE OF GRADUATE STUDIES
DEPARTMENTS OF MOLECULAR BIOLOGY AND GENETICS

Comparative Evaluation of Mycosporine-like Amino Acids Producing Psychrotolerant *Klebsormidium* Strains Isolated from Extreme Regions (Antarctica, Arctic, Alpine, Alaska, Atacama) and Film Production from Antarctic *Klebsormidium* sp. ASYA19

Master's Thesis

Barış Ballık

January 2024

ISTANBUL MEDENIYET UNIVERSITY
INSTITUTE OF GRADUATE STUDIES
DEPARTMENTS OF MOLECULAR BIOLOGY AND GENETICS

Comparative Evaluation of Mycosporine-like Amino Acids Producing Psychrotolerant *Klebsormidium* Strains Isolated from Extreme Regions (Antarctica, Arctic, Alpine, Alaska, Atacama) and Film Production from Antarctic *Klebsormidium* sp. ASYA19

Master's Thesis

Barış Ballık

Supervisor

Prof. Dr. Turgay Çakmak

January 2024

THESIS JURY APPROVAL

This M.Sc. thesis titled "Comparative Evaluation of Mycosporine-like Amino Acids Producing Psychrotolerant *Klebsormidium* Strains Isolated from Extreme Regions (Antarctica, Arctic, Alpine, Alaska, Atacama) and Film Production from Antarctic *Klebsormidium* sp. ASYA19", written by Barış Ballık at the Department of Molecular Biology and Genetics was accepted by our jury.

JURY MEMBERS **SIGNATURES**

Supervisor:

[Prof. Dr. Turgay ÇAKMAK]

Istanbul Medeniyet University

Other Jury Members:

[Prof. Dr. Murat KAZANCİ]

Istanbul Medeniyet University

[Prof. Dr. Nüzhet Cenk SESAL]

Marmara University

Date of Defense: 10/01/2024

STATEMENTS

Style and Reference Manual Statement

Having reviewed this thesis written under my supervision, I confirm that it has been written in accordance with APA Manual of Style and used its in text reference format consistently throughout the entire text.

Prof. Dr. Turgay ÇAKMAK

Declaration of Originality

I hereby declare that all information in this dissertation has been obtained and presented in accordance with academic rules and ethical conduct. I also declare that, as required by these rules and conducts, I have fully cited and referenced all material and results that are not original to this work.

Barış Ballık

ACKNOWLEDGEMENTS

First of all, I would like to thank my advisor Prof. Dr. Turgay Çakmak, who supported me during my thesis study, always tried to help me, and helped my personal development by sharing his knowledge and experience with me.

I also would like to express my gratitude to Prof. Dr. Murat Kazanci, who provided a lot of opportunity for conducting experiments in his laboratory and contributed to my research interpreting study results.

Afterward, I am extremely grateful to Prof. Ulf Karsten, who allowed me to benefit from the facilities and experiences of his laboratory at the University of Rostock, where I did my internship in the 2023 summer term within the scope of Erasmus. I would also like to express my endless gratitude to Dr. Azam Omidi, Niklas Plag, and Prof. Klaus Herburger, who added their valuable experience and physical contributions to my thesis during this process.

Moreover, I would like to express my endless gratitude to all my laboratory colleagues, especially Mihraç Görünmek, Kader Bozuklu, Büşra Duygun, Onur Aras, and Gamze Çamur, for their physical contributions, efforts, and knowledge transfer to me and my thesis.

Lastly, I would like to thank my family members for their financial and moral support, who have always supported me in achieving my professional goals. In particular, I would like to express my gratitude to my sister Büşra Ballık, and my girlfriend Ümay Aslan for their endless morale and motivation during my thesis process.

On the other hand, I would like to express my endless gratitude for the scholarship provided to me by the Directorate of Science Fellowships and Grant Programmes (BIDEB) In addition, I am grateful to the Scientific and Technological Research Council of Turkey (TUBITAK) for strengthening my thesis and scientific activities by giving many seminars.

This study was supported by the Scientific and Technological Research Council of Turkey (TUBITAK) Grant No: 112Y136 (Project Title: Mycosporin-Like Amino Acids of Microalgae Isolated from Horseshoe Island (Antarctica): Extraction, Purification and Evaluation of Economic Potential).

LIST OF SYMBOLS

A: Absorbance

cm: Centimeter

°C: Degree Celsius

g: Gram

g: g-force or rcf

μ: Growth Rate

km: Kilometer

L: Liter

M: Meter

μg: Microgram

μL: Microliter

μm: Micrometer

mg: Milligram

mL: Milliliter

min: Minute

M: Molarity

nm: Nanometer

NA: Not available

%: Percentage

rcf: The relative centrifugal force

rpm: Revolutions per minute

v/v: Volume by volume

w/w: Weight by weight

W: Watt

LIST OF ABBREVIATIONS

BBM: Bold-Basal Medium

CKB: Crude klebsormidium biomass

DAD: Diode array detector

DPPH: 2,2-difenil-1-pikrilhidrazil

DSC: Differential scanning calorimetry

EPS: Extracellular polymeric substances

FT-IR: Fourier-transform infrared spectroscopy

HPLC: High liquid pressure chromatography

MAA: Mycosporine-like amino acids

NCBI: National Center for Biotechnology Information

PAR: Photosynthetic active radiation

PVA: Polyvinyl alcohol

SEM: Scanning Electron Microscopy

TFA: Trifluoroacetic acid

TGA: Thermogravimetric analysis

UV: Ultraviolet

UVR: Ultraviolet radiation

YII: Effective quantum yield rate

TABLE of CONTENTS

LIST of FIGURES

LIST OF TABLES

ABSTRACT

Comparative Evaluation of Mycosporine-like Amino Acids Producing Psychrotolerant *Klebsormidium* Strains Isolated from Extreme Regions (Antarctica, Arctic, Alpine, Alaska, Atacama) and Film Production from Antarctic *Klebsormidium* sp. ASYA19

Ballık, Barış

Master Thesis, Molecular Biology and Genetics Department, Molecular Biology and Genetics Program

Supervisor: Prof. Dr. Turgay ÇAKMAK

Jan 2024. 107 Pages.

Microalgae are eukaryotic organisms with superior photosynthesis abilities that can cope with almost all extreme conditions on Earth. These photosynthetic organisms even spread in polar regions where ultraviolet radiation (UVR) is more intense than in other regions as a result of the depletion of the ozone layer. Neutralization of the harmful effects of UVR by UV-absorbing compounds has been developed by many microalgae as a defense mechanism under long-term UVR exposure. Mycosporine-like amino acids (MAAs) are a family of more than 40 different types of compounds with maximum absorption between 268 – 362 nm. These compounds are well known for their UV-absorbing role in various organisms, including microalgae, and are observed to be of evolutionary importance. These compounds are most pronounced in the *Klebsormidium* genus in the algae world. This thesis covers the comparative evaluation of the MAA production potential and other physiological responses of *Klebsormidium* strains isolated from various extreme regions. Additionally, it involves the production of bioplastics with UV-blocking capacity from the MAA-induced biomass of the *Klebsormidium* sp. ASYA19.

The physiological responses to UV-B of six different *Klebsormidium* strains (*Klebsormidium* sp. ASYA 19, *Klebsormidium* flaccidum ASYA 18, *Klebsormidium flaccidum, Klebsormidium crenulatum, Klebsormidium deserticola* and *Klebsormidium* subtile) isolated from different extreme conditions (Antarctica, Arctic, Alpine, Alaska, and Atacama) were evaluated based on their growth and photosynthetic performance. Moreover, *Klebsormidium* sp. ASYA19 has high biomass accumulation at 15°C compared to other species and high MAA production

capacity like other *Klebsormidium* strains. Bioplastic film with UV-blocking capacity was obtained from *Klebsormidium* sp. ASYA19 using the solvent casting method. Optimization studies were carried out by evaluating the mechanical properties and film-forming capacities of the bioactive films. As a consequence of optimization steps, the concentration of 5% *Klebsormidium* biomass was found to be appropriate. The film obtained from Crude *Klebsormidium* Biomass (CKB) was reinforced with certain glycerol and PVA ratios. Mechanical characterization parameters such as tensile stress, elongation (%), and young modulus of all the obtained films were determined by mechanical testing. Thermal and chemical characterization of the bioactive films were measured utilizing TGA-DSC, and FT-IR analysis. Additionally, the MAA-induced UV-blocking effect and microalgae-based antioxidant effect were determined by spectrophotometric methods.

The results show that *Klebsormidium* strains isolated from different regions revealed different physiological responses to UV-B. In particular, fluorimetric growth parameters and quantum yield data show that polar *Klebosrmidium* strains are not growth-limited against UV-B and show effective photosynthetic performance. At the same time, polar *Klebsormidium* strains, which have high photosynthetic efficiency and growth rate against UV-B, produced less MAA than other strains. In addition, as a result of MAA purification by HPLC, two different types of MAAs were detected in these strains, providing absorption at wavelengths of 323.5nm (Prasiolin) and 318nm (unknown) having a retention time of 1.9 min.

A water solution of 5% CKB has a film-forming capacity itself; however, the addition of 75% PVA results in improved mechanical properties when compared to the other groups tested. On the other hand, it was observed that the UV-blocking effect of the bioactive films decreased as the additive ratio increased. It has been observed that the antioxidant effect does not change significantly when concentrations change.

Klebsormidium species, a filamentous member of green algae, have evolutionary importance in the terrestrial transition of photosynthetic microorganisms and have been the subject of many scientific studies to date. This algal genus, which has the ability to maintain its vital activity in many extreme conditions from polar regions to deserts, has become the representative of the Streptophyte group, especially in terms of researching MAA synthesis. At the same time, the richness of its biochemical

composition and the fact that it has characteristic features such as a superficial water-repellent layer, unlike other algae, have recently made this genus a target for biotechnological product development. The results obtained in this thesis show that the UV-resistance mechanisms of polar *Klebsormidium* strains to UV radiation lay on photosynthesis. With their unique anatomical features, those strains can be employed to produce goods and feedstocks for bioactive material production as shown with *Klebsormidium* sp. ASYA19.

Keywords: Antarctica, Arctic, Alpine, Alaska, Atacama, Bioplastic, Klebsormidium, MAA, Microalgae,

ÖZET

Ekstrem bölgelerden (Antarktika, Arktik, Alpler, Alaska, Atacama) izole edilen psikrotolerant *Klebsormidium* suşları tarafından üretilen Mikosporin benzeri aminoasitlerin karşılaştırmalı değerlendirilmesi ve Antarktik *Klebsormidium* sp. ASYA19'dan film üretimi

Ballık, Barış

Yüksek Lisans Tezi, Moleküler Biyoloji ve Genetik Bölümü, Moleküler Biyoloji ve Genetik Programı

Danışman: Prof. Dr. Turgay ÇAKMAK

Ocak, 2024. 107 Sayfa.

Mikroalgler, Dünya üzerindeki neredeyse tüm zorlu koşullarla baş edebilen, üstün fotosentez yeteneklerine sahip ökaryotik organizmalardır. Bu fotosentetik organizmalar, ozon tabakasının incelmesi sonucunda ultraviyole radyasyonun (UVR) diğer bölgelere göre daha yoğun olduğu kutup bölgelerinde bile yayılım göstermektedir. UVR'nin zararlı etkilerinin UV emici bileşiklerle nötralizasyonu, birçok mikroalg tarafından uzun süreli UVR'ye maruz kalma altında bir savunma mekanizması olarak geliştirilmiştir. Mikosporin benzeri amino asitler (MAA'lar), maksimum emilimi 268 – 362 nm arasında olan 40'tan fazla farklı bileşik türünden oluşan bir ailedir. Bu bileşikler, mikroalgler de dahil olmak üzere çeşitli organizmalarda UV emici rolleriyle iyi bilinmektedir ve evrimsel öneme sahip oldukları gözlemlenmektedir. Bu bileşikler en çok alg dünyasındaki *Klebsormidium* cinsinde belirgindir. Bu tez, çeşitli ekstrem bölgelerden izole edilen *Klebsormidium* suşlarının MAA üretim potansiyelinin ve diğer fizyolojik tepkilerinin karşılaştırmalı olarak değerlendirilmesini kapsamaktadır. Ek olarak, *Klebsormidium* sp. ASYA19'un MAA kaynaklı biyokütlesinden UV engelleme kapasitesine sahip biyoplastiklerin üretimini de içermektedir.

Farklı aşırı koşullardan (Antarktika, Arktik, Alp, Alaska ve Atakama) izole edilen altı farklı Klebsormidium suşlarının (*Klebsormidium* sp. ASYA 19, *Klebsormidium flaccidum* ASYA18, *Klebsormidium flaccidum, Klebsormidium crenulatum, Klebsormidium deserticola* ve *Klebsormidium subtile*) UV-B'ye karşı fizyolojik yanıtlar büyüme ve fotosentetik performansları üzerinden değerlendirilmiştir. Ayrıca *Klebsormidium* sp. ASYA19, diğer türlere göre 15°C'de yüksek biyokütle birikimine

ve diğer Klebsormidium suşları gibi yüksek MAA üretim kapasitesine sahiptir. UV engelleme kapasitesine sahip biyoplastik film, solvent döküm yöntemi kullanılarak *Klebsormidium* sp. ASYA19'dan elde edilmiştir. Biyoaktif filmlerin mekanik özellikleri ve film oluşturma kapasiteleri değerlendirilerek optimizasyon çalışmaları yapılmıştır. Optimizasyon adımları sonucunda %5 *Klebsormidium* biyokütle konsantrasyonunun uygun olduğu görülmüştür. Ham *Klebsormidium* Biyokütlesinden (CKB) elde edilen film belirli gliserol ve PVA oranlarıyla katkılandırılmıştır. Elde edilen tüm filmlerin çekme gerilimi, uzama (%) ve elastisite modülü gibi mekanik karakterizasyon parametreleri mekanik testlerle belirlenmiştir. Biyoaktif filmlerin termal ve kimyasal karakterizasyonu, TGA-DSC ve FT-IR analizi kullanılarak ölçülmüştür. Ayrıca MAA kaynaklı UV bloke edici etki ve mikroalg bazlı antioksidan etki spektrofotometrik yöntemlerle belirlenmiştir.

Sonuçlar, farklı bölgelerden izole edilen *Klebsormidium* suşlarının UV-B'ye farklı fizyolojik tepkiler ortaya çıkardığını göstermektedir. Özellikle florimetrik büyüme parametreleri ve kuantum verim verileri, polar *Klebosrmidium* suşlarının UV-B'ye karşı büyümenin sınırlı olmadığını ve etkili fotosentetik performans sergilediğini göstermektedir. Aynı zamanda fotosentetik etkinliği ve UV-B'ye karşı büyüme hızı yüksek olan polar *Klebsormidium* suşları diğer suşlara göre daha az MAA üretmiştir. Ayrıca HPLC ile MAA saflaştırması sonucunda bu suşlarda 323,5 nm (Prasiolin) ve 318 nm (bilinmiyor) dalga boylarında absorpsiyon sağlayan ve 1,9 dakika alıkonma süresine sahip iki farklı MAA tipi tespit edilmiştir.

%5 CKB'lik bir su çözeltisinin kendisi de film oluşturma kapasitesine sahiptir; ancak %75 PVA eklenmesi filmin test edilen diğer gruplarla karşılaştırıldığında mekanik olarak önemli ölçüde geliştirildiğini göstermektedir. Diğer taraftan katkı oranı arttıkça biyoaktif filmlerin UV engelleyici etkisinin azaldığı gözlenmiştir. Konsantrasyonlar değiştiğinde antioksidan etkinin önemli ölçüde değişmediği gözlemlenmiştir

Yeşil alglerin flamentli bir üyesi olan *Klebsormidium* cinsleri fotosentetik mikroorganizmaların karasal geçişinde evrimsel bir öneme sahip olup bugüne kadar birçok bilimsel çalışmanın konusu olmuştur. Kutup bölgelerinden çöllere kadar birçok aşırı koşulda yaşamsal faaliyetini sürdürme yeteneğine sahip olan bu alg cinsi özellikle MAA sentezinin araştırılması açısından Streptofit grubunun temsilcisi olmuştur. Aynı zamanda biyokimyasal kompozisyonunun zenginliği ve yapısında diğer alglerden

farklı olarak yüzeysel su itici tabaka gibi karakteristik özellikler barındırması son zamanlarda bu cinsi biyoteknolojik ürün geliştirme konusunda hedef yapmaktadır. Bu tezde elde edilen sonuçlar, polar *Klebsormidium* türlerinin UV radyasyonuna karşı UV direnç mekanizmalarının fotosenteze dayandığını göstermektedir. Benzersiz anatomik özellikleriyle bu suşlar, *Klebsormidium* sp. ASYA19 ile gösterildiği gibi biyoaktif malzeme üretimi için mal ve hammadde üretmek amacıyla kullanılabilir.

Anahtar kelimeler: Antarktika, Arktik, Alp, Alaska, Atakama, Biyoplastik, Klebsormidium, MAA, Mikroalg

1. INTRODUCTION

1.1 General Overview of Algae: Characteristics and Adaptations

Microalgae, a diverse group of photosynthetic microorganisms, are the primary producers forming the basis of the food chain. These microscopic organisms thrive in a wide variety of habitats, from freshwater lakes to vast areas of the ocean. Microalgae are highly adaptable organisms that have evolved to survive in environments ranging from calm ponds to harsh extreme habitats such as hot springs and polar ice caps (Levine, I.A. and Fleurence, J., 2018).

One of the most prominent features of microalgae is their extraordinary photosynthetic efficiency, which exceeds that of higher plants. This efficiency is achieved thanks to their effective use of solar energy. They contain various pigment compounds that enable them to make their photosynthetic systems efficient, and their intracellular distribution varies according to environmental conditions. While chlorophyll a is found universally in all microalgae, other accessory pigments such as chlorophyll b, c, and phycobiliproteins predominate among different groups, adapting to specific light conditions. This diversity of pigments not only aids photosynthesis but also provides these organisms with a variety of colors in harmony, from the dark blues and greens of cyanobacteria to the golden hues of diatoms (MacIntyre et al., 2002).

In terms of reproduction, microalgae exhibit both asexual and sexual reproductive strategies, which increases their capacity to proliferate under various conditions. Asexual reproduction, mostly through binary fission, leads to rapid population growth, especially in nutrient-rich environments, where microalgae can use this advantage and spread rapidly into the environment. Conversely, sexual reproduction contributes to genetics and biodiversity by equipping microalgae populations to cope with environmental conditions that change negatively over time. These different reproductive strategies make it easier for these microorganisms to adapt and survive in different conditions of the world (Gastineau, Romain et al., 2014).

The ability of microalgae to adapt to various environmental conditions is evidenced by the responses resulting from physiological and biochemical processes. For example, microalgae can change their metabolic pathways in response to nutrient

deficiency, allowing them to grow and reproduce even in nutrient-depleted environments. Moreover, many microalgae species have evolved some survival mechanisms to survive in extreme conditions such as high salinity, intense light, or extreme temperatures (Shetty et al., 2019). These adaptations include the deposition of osmolytes to maintain the cell's turgor pressure at normal levels, the synthesis of heat shock proteins such as Hsp proteins, and the production of protective compounds such as mycosporine-like amino acids (MAAs) to protect against ultraviolet radiation. These MAAs have been the focus of researchers especially recently due to their potential applications in biotechnology and pharmaceuticals, underlining the importance of microalgae beyond their ecological roles (Mimouni et al., 2012).

Streptophytes such as *Klebsormidium* strains, exhibit unique features and adaptations that distinguish them in aquatic and terrestrial ecosystems (Škaloud et al., 2014). *Klebsormidium* represents a genus of filamentous microalgae which consist of cells that connect end-to-end and form long, thread-like chains, and cell morphologies vary depending on the habitat in the identified strains. This structural formation allows them to occupy a variety of niches, from moist soil surfaces to freshwater and marine environments. At the same time, thanks to this superior adaptation they have, they can quickly dominate the flora they are in. An important adaptation of filamentous microalgae is their ability to form mats or biofilms, which provides a competitive advantage in nutrient absorption from the environment and resistance to physical stressors. In this way, *Klebsormidium* shows exceptional resilience in habitats where conditions fluctuate, such as shallow water bodies subject to drying or freezing. They have mechanisms to resist desiccation and freezing, which is partially attributed to the production of MAAs and extracellular polymeric substances (Kumari et al., 2022). At the same time, they have superficial artificial repellent layers, which are similar to the wax layer of higher plants (more primitive), which makes the microalgae of this family group resistant to desiccation stress. With these abilities, *Klebsormidium* not only survives in extreme conditions but also contributes to primary productivity by stabilizing sediments, thus fulfilling its role in the ecosystem.

Microalgae have a remarkable ability to accumulate valuable compounds such as lipids, pigments, and carbohydrates, which have attracted significant attention in various industrial applications (Singh et al., 2011). For example, while lipid contents

are being investigated for biofuel production, pigments such as beta-carotene and xanthophyll attract attention in the food and cosmetic industries for their antioxidant properties. The rapid growth rates of microalgae and their ability to thrive in controlled environments make them a sustainable alternative to conventional crops in terms of these high-value compounds (Sathasivam et al., 2019).

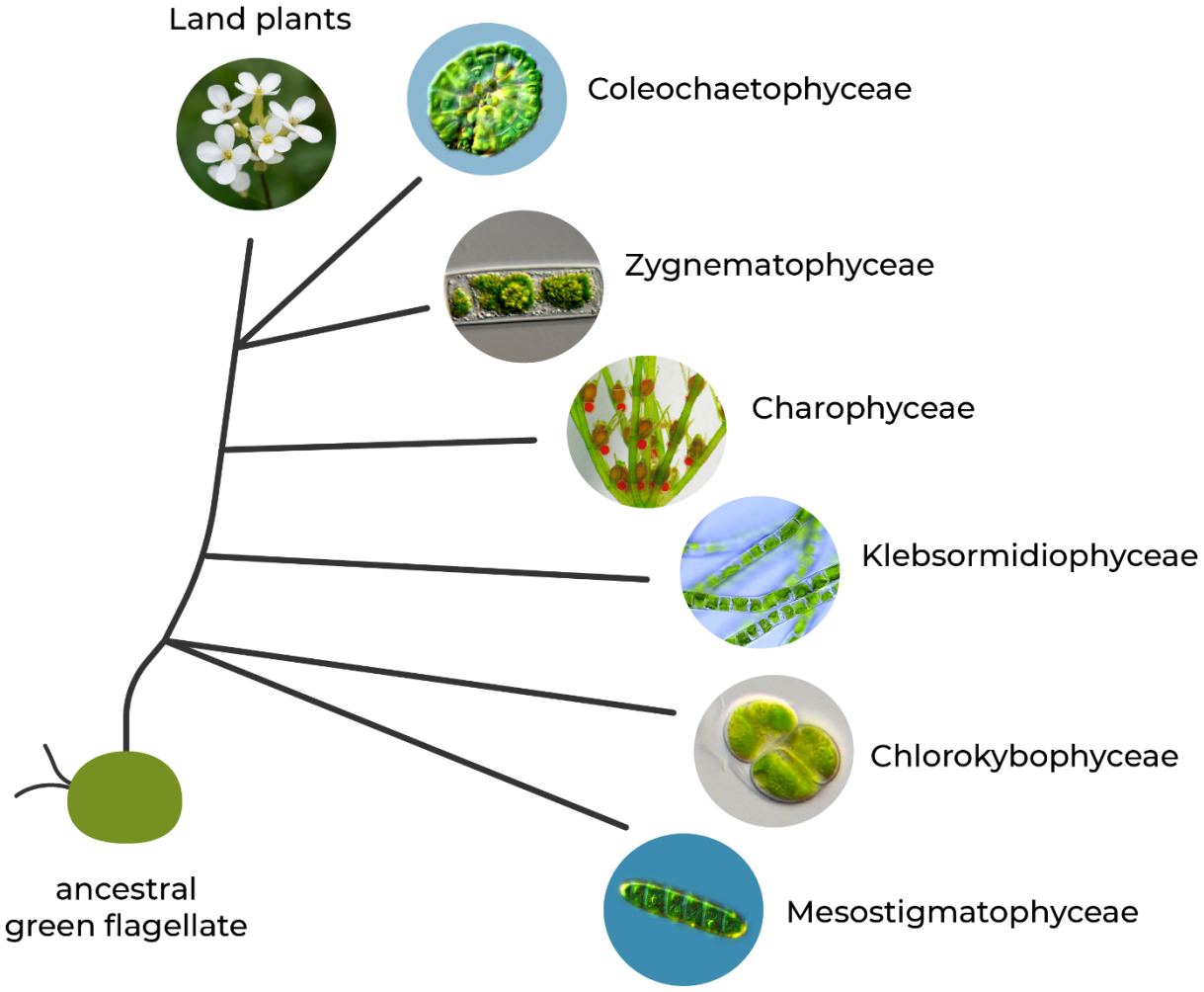

Figure 1: Overview phylogeny of the lineage of Streptophyte

1.2. Fundamentals of Ultraviolet Radiation and Photoprotection Mechanisms in Algae

The ongoing discourse surrounding global warming and the depletion of the stratospheric ozone layer has gained prominence in recent years. Despite efforts like the Montreal Protocol slowing the rate of ozone layer degradation, Earth continues to receive increasing levels of UV radiation (UVR) (Wu et al., 2013). This radiation,

encompassing short wavelengths with high energy, is primarily categorized into three types: UV-A (320-400 nm), constituting about 7% of the Earth's solar radiation; UV-B (280-320nm), which now impacts the Earth's surface more due to ozone layer thinning, albeit still less than 1%; and UV-C (100-280nm), entirely absorbed by the atmosphere (Neale P. J., 2000). Organisms exposed to these energetic wavelengths have evolved various strategies to mitigate their harmful effects. Higher plants, for instance, rely on phenylpropanoids and flavonoids, animals on melanin pigments, and cyanobacteria and algae on MAAs and other similar metabolites to bolster their biochemical defenses against photodamage (Cockell, C. S., & Knowland, J., 1999).

Exposure to intense UV radiation is known to hinder growth, metabolism, and reproduction in animals, plants, and microorganisms (Weihs et al., 2013). Photosynthetic organisms face severe damage to crucial processes like photosynthesis, leading to photoinhibition. This disruption is due to UV-induced alterations in vital protein structures, DNA damage, and other molecular impairments (Sinha, R. P., & Häder, D. P., 2002), (Joshi et al., 2018). To survive these harsh conditions, Earth's organisms have adopted two primary strategies (Sen, S., & Mallick, N., 2021). One involves using the physical environment for adaptation, such as benthic microalgae growing in macroalgae-shaded areas or migrating to lower-light regions. The other strategy involves metabolic evolution to enhance biochemical processes and photosynthetic efficiency. Hence, organisms have evolved appropriate mechanisms to either prevent potential damage or repair it. Algae typically combat excessive photosynthetically active radiation or UV chemically by either producing molecules to neutralize UV-induced metabolic toxins or synthesizing sunscreen components like MAAs to filter UV wavelengths (Vincent, W. F., & Roy, S., 1993). Additionally, other UV-absorbing organic metabolites produced by some microalgae sulfated polysaccharides and MAAs, help mitigate UV radiation's detrimental effects and preserve photosynthetic capabilities (Dionisio-Sese, M. L., 2010), (Santiesteban-Romero et al., 2022).

1.2.1.Mycosporine-like Amino Acids

MAAs are considered to be the most stable photoprotective compounds for microalgae, increasing cell tolerance against abiotic stresses such as temperature, osmotic stress, extreme salinity, and drought, as well as their absorption ability in the

broad UV spectrum. When MAAs are examined in terms of their photoprotective properties, unlike other pigments, by converting the absorbed radiation into harmless heat and releasing it, they act as an intracellular passive shield without causing any photochemical reaction (Oren et al., 2007). For these reasons, MAAs can prevent UV-based skin damage (Singh et al.,2021). The researchers demonstrated in an application they performed in human fibroblast cells that MAAs effectively prevented the occurrence of DNA damage by inhibiting the formation of thymine-thymine dimers against UV radiation (Zaki et al., 2018).

Naturally, MAAs have a low molecular weight, and the degree of quality of their photoprotective effects according to their size has attracted attention. It has been proven by scientists that a formula made with porphyria-334, a type of MAA, increases photoprotective activity when used as a sunscreen (Bhatia et al.,2010). On the other hand, MAAs have begun to be tested for use in alternative packaging products in the food industry. As a result of these trials, the use of MAAs, which are used at certain concentrations in active biocomposite products, as a protective additive to prevent the photochemical degradation of foods has been successfully demonstrated (Gan et al., 2022).

1.2.2.Carotenoids

Carotenoids, found in almost all photosynthetic organisms, are classified into carotenes and xanthophylls. They function primarily in the light-harvesting complex by absorbing the blue-green spectrum (400-500nm) and transmitting light to chlorophyll (Núñez-Pons et al.,2018). As lipophilic molecules with a C-40 polyisoprenoid structure, they act as chromophores. Secondary carotenoids also serve as photoprotectors against UV radiation. Studies have indicated an increase in intracellular carotenoid levels in response to UV-B exposure (Shen et al., 2017), and a correlation has been observed between carotenoid and MAA levels in response to UVR stress in certain microalgal species (Huang et al.,2018). For example, exposure of the macroalgal species *Pelvetia canaliculata* to UV-B resulted in a significant increase in carotenoid content (Hupel et al.,2011).

1.2.3. Sulfated Polysaccharides

Sulfated polysaccharides in microalgae play a crucial role in photoprotection, particularly against UV radiation. These compounds, characterized by their sulfate groups, are primarily located in microalgal cell walls and are known for their UV-absorbing and antioxidant abilities. Research has shown that these polysaccharides effectively absorb UV light, thus protecting microalgae from UV-induced oxidative stress (Plaza, Cifuentes, & Ibáñez, 2014). Additionally, their antioxidant activity is significant in reducing damage from reactive oxygen species (Kraan et al., 2012). Beyond UV absorption, sulfated polysaccharides aid in stabilizing the photosynthetic apparatus and enhancing repair mechanisms post-UV exposure (Skjånes, Rebours, & Lindblad, 2013). This multifaceted protection is essential for microalgae in high solar irradiance environments. The structural diversity of these polysaccharides reflects the evolutionary adaptation of microalgae to different light conditions (Borowitzka, 2012) and presents opportunities for industrial applications, including in sunscreens and protective coatings (Fan et al., 2014).

1.2.4.Phenolic Compounds

Phenolic compounds, functioning as secondary metabolites, protect algae and higher plants from high-energy rays. Their bioactivity is defined by phenol rings and attached radical groups in their structures (Ignat et al.,2011). These compounds, including phenolic acids, flavonoids, and tannins, have been investigated for their photoprotective properties, particularly under UV-B exposure (Heo et al., 2009). For example, phloroglucinol applied to mouse skin was found to be effective and safe in attenuating UV-B radiation (Piao et al., 2014). Owing to their antioxidant capacity and UV-B protective effects, phenolic compounds are increasingly used in cosmetic applications (Del Mondo et al., 2022).

1.3. Biochemical Properties and Diversity of MAAs

Mycosporine-like amino acids, commonly abbreviated as MAAs, are intracellular biomolecules notable for their low molecular weight (under 400 Da), colorless appearance, and solubility in water. These highly stable compounds, found across a wide geographical range, are known for their ability to absorb UV radiation. Chemically, MAAs are characterized by their aminocyclohexenone or aminocyclohexenimine rings, bonded to nitrogen substituents from amino acids or

imino alcohols. Structurally, there are two primary types of MAAs: those like mycosporine-glycine and mycosporine-taurine, formed when various amino acids conjugate with the cyclohexenone ring, and others such as palythine and shinorine, where the cyclohexenimine ring binds with glycine or methylamine at the third carbon and an amino acid or amino alcohol at the first carbon (Balskus, E. P., & Walsh, C. T., 2010), (Ishihara et al., 2017). Some MAAs, including commonly known ones like Porphyra-334 and palythine-serine, can also form covalent bonds with different oligosaccharides (Böhm et al., 1995), (Inoue-Sakamoto et al., 2018). The term "Mycosporin" refers to compounds with a ketone group at the C1 position, as seen in oxo-mycosporins or mono-substituted mycosporins. MAAs are distinct for their specific absorption spectrum, typically between 268-362 nm wavelengths (Lawrence et al.,2018). With high molar extinction coefficients (28,100–50,000 M^{-1} cm^{-1}) (Dunlap, W. C., & Shick, J. M., 1998), these biomolecules act as stable dampers in natural synthesis against UV-A and UV-B radiation. Named for their structural groups, MAAs' functions vary with these groups, and their synthesis is influenced by solar radiation intensity. Most MAAs are stable up to 60 °C and can withstand high pH levels (up to pH 11) (Bernillon et al., 1990).

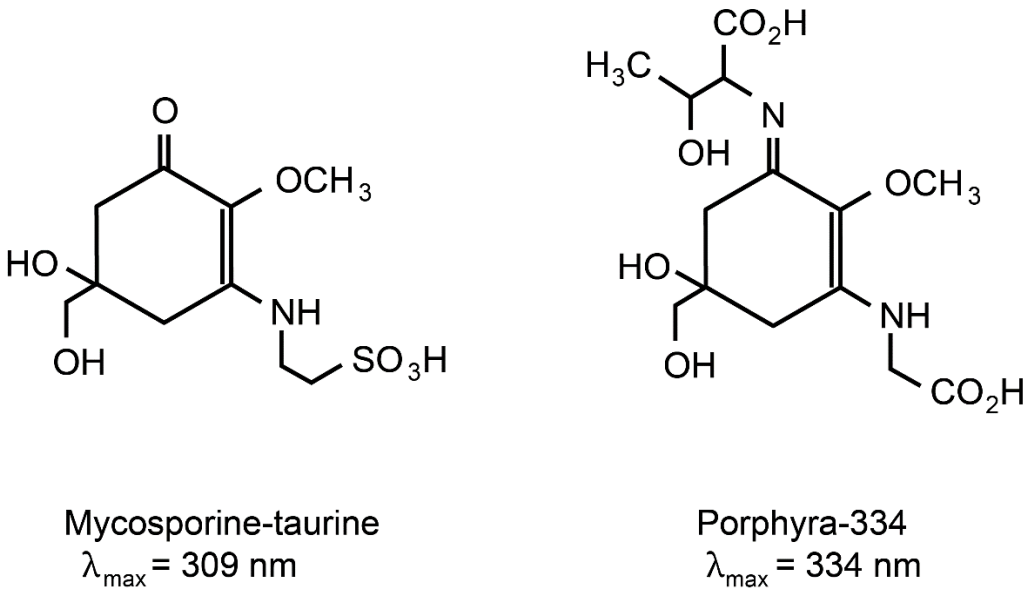

Figure 2: Mycosoporin-taurine, an example of an oxomycosporin containing a cyclohexenone ring in its structure, is given on the left, and Porphyra-334, which contains a cyclohexenime ring and amino acid group, is given on the right.

In studies conducted to date, 12 Aminocyclohexenone-type (such as Mycosporine-glycine, Mycosporine-taurine, Mycosporine-alanine) and 20 Aminocyclohexene imine-type (such as Porphyra-334, Shinorine, Palythine) MAAs have been identified. In addition, when sulfated Derivatized MAAs (such as Palythine-threonine sulfate, Palythine-serine sulfate, and Shinorine-pentoside) are taken into account, the number of identified MAAs exceeds 40 (Wada et al., 2015). These MAAs have predominantly been extracted from sources such as microalgae, macroalgae, cyanobacteria, fungi, and certain marine invertebrates. The variation in the type and diversity of MAAs observed is often influenced by the environmental conditions and geographic location of the organisms from which they are extracted. Notably, about 36% of the documented UV-absorbing compounds were derived from marine species found in Antarctic waters. Studies have highlighted the photoprotective role of MAAs like mycosporin-glycine,

shinorine, and asterina-330, which were extracted from cyanobacteria in Austrian Alpine freshwater sources, in shielding these microorganisms from intense radiation (Wada et al., 2013), (Singh et al.,2017). Similarly, the presence of shinorine and Porphyra-334 was reported in Microcystis aeruginosa, a species exposed to high solar and UV-B radiation, aiding in its survival and bloom formation (Babele et al.,2017).

Research conducted in a temple in Thailand uncovered two previously unknown MAA species, with absorption peaks between 320-329 nm, along with shinorine, Porphyra-334, mycosporin-Gly, and palythiol, in a cyanobacterial mat sample (Rastogi et al., 2015). Recent advancements have also led to the clarification of the chemical structure of prasiolin, found in Prasiola calophylla, with an absorption maximum of 324 nm (Shang et al., 2018). Additionally, a study focusing on terrestrial benthic microalgae species, specifically *Klebsormidium* sp. and *Interphylum* sp., led to the discovery of two novel MAA species, MAA1 and MAA2. These species, distinguishable by their molecular weights, are active in the UV-A range around 324 nm (Hartmann et al., 2016), (Hotter et al., 2018). In another investigation involving the Nostoc flagelliforme CCNUN1 strain under UV-B stress, a new mycosporin variant, mycosporin-2-(4-deoxygadusolyl-ornithine), was identified within the 312-334nm wavelength range (Hartmann et al., 2020).

1.4. Biosynthesis of MAAs

The process of synthesizing Mycosporine-like Amino Acids (MAAs) remains a topic of debate and is not yet fully understood. Some findings indicate that MAAs originate from the 4-deoxygadusol precursor, formed directly through the enzyme 3-dehydroquinate synthase from the shikimate pathway, which is involved in synthesizing aromatic amino acids (Portwichi et al., 2003), (Geraldes et al., 2020). In contrast, other research points to the significance of the pentose phosphate pathway in MAA production (Balskus et al., 2010), (Rosic et al., 2012) emphasizing the conversion of sedoheptulose-7-phosphate, a pentose phosphate pathway intermediate, into 4-deoxygadusol (Pope et al., 2015), (Katoch et al., 2016). Interestingly, even with the deletion of the cyclase-2-epi-5-epi-valiolone synthase (EVS synthase) gene in Anabaena variabilis, responsible for EVS synthase enzyme production that catalyzes EVS formation from SH-7P, shinorine production persisted (Spence et al., 2012). This

suggests that while the pentose phosphate pathway contributes to MAA diversity, it is not the primary pathway but rather complements the shikimate pathway.

The basic structure of MAAs is believed to arise from the convergence of these two pathways at the 4-DG stage, with the subsequent addition of glycine leading to the formation of mycosporin glycine, a precursor to many MAAs (Singh et al., 2009), (Singh et al., 2010). Mycosporin-glycine, an oxo-mycosporin, can then be transformed into imino-mycosporins through chemical or biochemical modifications, such as the addition of amino acid groups. This modification is carried out by enzymes like non-ribosomal peptide synthase-like (NRPS) or D-alanine ligase (Geraldes et al., 2020), (Balskus et al., 2010). The diversity in the amino acid side chains involved in MAA synthesis is key to the variation in their absorption spectra (Lawrence et al.,2018).

Recent genomic research has elucidated the genetic pathways involved in the biosynthesis of Mycosporine-like Amino Acids (MAAs) in various algal species, including Anabaena and *Chlamydomonas reinhardtii*. In *Anabaena variabilis*, specific genes like Ava_3858 and Ava_3857 are implicated in forming the cyclohexenone core, a critical component of MAAs (Portwich & Garcia-Pichel, 2003). Similarly, in *Chlamydomonas reinhardtii*, the CrMYB1 gene has been identified as playing a pivotal role in the initial stages of MAA synthesis, particularly in the shikimate pathway, which is key for producing aromatic amino acids (Barka et al., 2016). These findings in both cyanobacteria and green algae highlight the complexity of genetic mechanisms behind MAA biosynthesis.

In contrast, research on the genetic aspects of MAA biosynthesis in the genus *Klebsormidium* is relatively scarce. Known for its resilience in extreme environments, *Klebsormidium* is presumed to have unique genetic pathways for MAA production, potentially involving key genes in the shikimate pathway for synthesizing the cyclohexenone core. The exploration of these genetic pathways in *Klebsormidium* is essential, as it may reveal new insights into MAA biosynthesis in extremophile microalgae and open avenues for biotechnological applications (Holzinger & Karsten, 2013; Karsten & Holzinger, 2014). Despite the current gaps in understanding, the potential of *Klebsormidium* in MAA research remains significant, particularly for

developing natural products like sunscreens and antioxidants suited for extreme conditions.

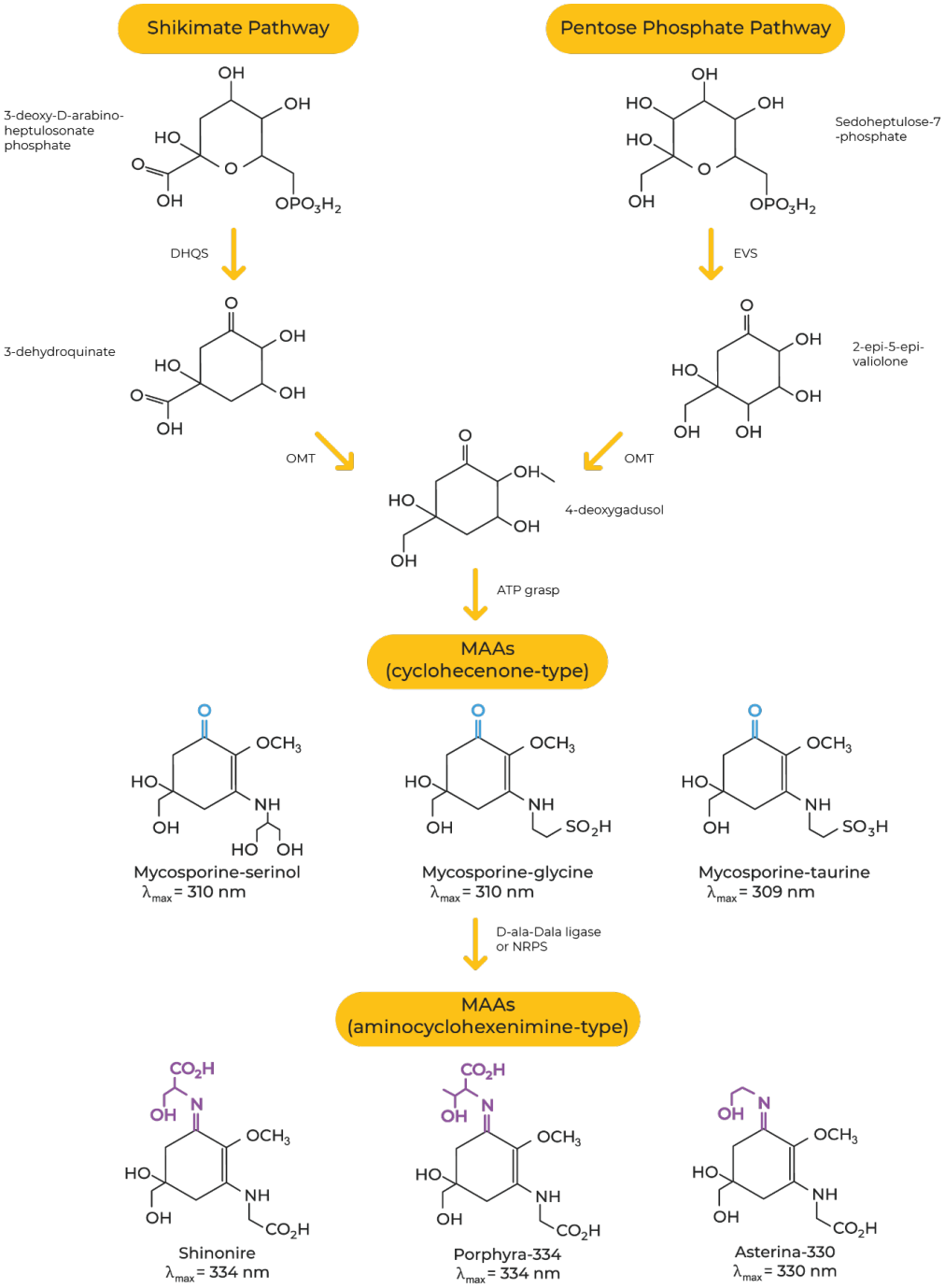

Figure 3: Detailed biosynthesis representation of mycosporine-like amino acids with precursor molecules formed in the shikimate and pentose phosphate pathways.

1.5. Ecological Significance of MAAs in Algae: Stress Response and Adaptation

MAAs found in different types of algae have an important place, especially in ecological adaptation and stress tolerance. In addition to their ability to protect against UV, they make important contributions to the cell in which they are synthesized in resisting different environmental conditions and ensuring the continuation of cell activities. These compounds, which also increase the ecological compatibility of the cell, are becoming more recognized today.

In microalgae, MAAs serve as a frontal defense against UV and intense light radiation by absorbing harmful rays to protect photosynthetic mechanisms that are sensitive to intense light (Carreto and Carignan, 2011). In addition, it has been revealed that MAAs play a role in the response to oxidative stress by providing critical protection against reactive oxygen species (ROS) that can accumulate under various environmental factors, especially temperature and salinity changes (Singh et al., 2010; Rastogi et al., 2014).

Studies conducted to date have revealed that MAAs are also upregulated against desiccation and salinity stress in microalgae and that they take part in the response to osmotic stress and cellular homeostasis (Ören, 1997). This positive response plays a critical role for terrestrial microalgae living in hypersaline environments with constantly changing humidity and salinity levels.

Klebsormidium is an intercontinental species and is an adaptive microalga that continues its vital activities from the high altitudes of the Alps to the harshest regions of the poles. Therefore, the synthesis of MAAs is key to their survival. *Klebsormidium* species tolerate severe desiccation and freezing conditions. It achieves remarkable tolerance to these conditions thanks to MAA-mediated photoprotection and antioxidant mechanisms (Holzinger & Karsten, 2013; Karsten & Holzinger, 2014). Moreover, in recent studies, valuable scientists have shown that *Klebsormidium* can adjust its MAA composition in response to changing environmental stress factors, revealing an evolutionary adaptation to harsh climates (Karsten et al., 2016).

1.6. MAA Variability: Distribution Patterns Across Extreme Habitats

The Antarctic continent, known for its geographical and ecological isolation, stands out as the world's coldest, driest, and windiest region, experiencing drastic temperature

fluctuations between +10 °C in summer and -60 °C in winter. These extreme conditions, with temperatures as low as -89.2 C°, have necessitated unique adaptation mechanisms for organisms to survive. The Southern Ocean, with temperatures ranging from +1.5 C° to -2 C°, serves as a habitat for diverse marine species. Additionally, Antarctica records the planet's highest UVR intensities, especially during early spring and summer, influenced by the thinning ozone layer (Convey et al., 2007), (Littlepage et al., 1965), (Cordero et al., 2022). Studies in this region have revealed that a significant portion of microalgae contains MAAs, crucial for UV protection, suggesting an evolutionary response predating the current ozone layer formation (Karentz et al., 1991). For example, in the species *Phaeocystis antarctica*, researchers have identified a potential photoprotective mechanism against UV damage (Smith Jr, W. O., & Gordon, L. I., 1997), (Döhler et al., 1995). The macroalgae *Pyropia columbina* in the sub-Antarctic region has shown increased MAA accumulation under heightened UV-A and UV-B exposure (Navarro et al., 2014), while other Antarctic macroalgae display species-specific MAA biosynthesis in response to different UV levels (Hoyer et al., 2002). Recent research on the red macroalgae *Curdiea racovitzae* from Antarctica has explored its potential as an industrial sunscreen ingredient (Rangel et al., 2020). Additionally, Studies in these regions have shown an increased concentration of MAAs in microalgae, suggesting an adaptive response to high UVR exposure. Antarctic microalgae like *Chlamydomonas nivalis* have demonstrated elevated MAA levels, providing crucial photoprotection under the intense polar sun (Vincent & Quesada, 2012).

In the Arctic region, similar to Antarctica, organisms face extreme cold and significant seasonal variations in sunlight exposure. Arctic microalgae have adapted to long periods of darkness and intense bursts of UV radiation during brief summers. A noteworthy example is the study of Arctic diatoms. Researchers have found that these diatoms produce a variety of MAAs in response to the heightened UV radiation during the prolonged daylight hours of Arctic summers (Zacher et al., 2007). This response is not only crucial for their survival but also for maintaining the primary productivity of the Arctic marine ecosystem. These MAAs enable the diatoms to continue photosynthesis efficiently, contributing to the carbon cycle and supporting the food web in these frigid waters.

Alpine regions, characterized by high altitude and increased UV radiation, present another challenging habitat for microalgae. Species such as *Klebsormidium sp.* exhibit a high content of MAAs, which aids in their survival and thriving in these UV-intense environments (Karsten & Holzinger, 2014). This indicates a direct correlation between altitude-related UV stress and MAA production.

The Alaskan environment, with its cold climate and varied light conditions, influences MAA production in local microalgal species. In this region, microalgae like *Chlorella sp.* show variability in MAA content, adapting to the seasonal fluctuations in light and temperature (Morgan-Kiss et al., 2006).

In the Atacama Desert, one of the driest places on Earth, microalgae face extreme UV radiation and aridity. The presence of MAAs in desert microalgae serves as a critical adaptation for surviving intense solar exposure and preventing desiccation. *Dunaliella salina* from the Atacama exhibits significant MAA production, reflecting an evolutionary adaptation to these harsh conditions (Garcia-Pichel et al., 1993).

1.7. MAAs: Beyond UV Protection to Antioxidant Activity and Potential Industrial Applications

MAAs, which generally stand out with their UV protective properties, are also being investigated for their antioxidant activities and potential in various industrial applications in recent studies. The reason for the recent increase in interest in MAAs is that their nature and functions are becoming more and more recognized day by day.

Recent studies have shown that MAA has a secondary role in clearing reactive oxygen species produced for various reasons in the metabolism of microalgae. In case of excessive oxidative stress, MAAs work like other antioxidant agents and play a primary role in helping the cell cope with stress and become an important component in the general stress response mechanism (Rastogi et al., 2015; De la Coba et al., 2009). Depending on their type, MAAs perform antioxidant functions, and these types are sometimes related to the stress conditions in the environment. In addition, these activities have affected potential application areas ranging from reducing oxidative stress in the marine ecosystem to human health and nutrition (Carreto and Carignan, 2011).

The versatile contribution potential of MAAs has been promising for the industry. Particularly their high UV absorption ability and antioxidant properties make them a promising candidate, providing an environmentally friendly, sustainable alternative to synthetic UV filters (Bandaranayake, 1998). In the cosmetic industry, MAAs are being studied in depth in anti-aging skin care products and are used to protect against skin diseases and oxidative damage that can be caused by UV.

On the other hand, the potential of MAAs in food preservation is exploited. Its antioxidative properties can be used to extend the shelf life of food by protecting against oxidative spoilage. Biotechnology, particularly the integration of MAAs into bioplastic production, is an emerging area of interest. Incorporating MAAs into bioplastics can increase UV resistance, improving the durability and functionality of these sustainable materials (Conde et al., 2000)

1.8. The Role of Klebsormidium Species in MAA Research and Application

Klebsormidium species are particularly adept at producing MAA when exposed to high UV radiation or desiccation. This ability is a fundamental adaptive strategy that allows them to live in diverse and often harsh environments, from alpine crusts to polar regions. Biosynthesis of MAAs in *Klebsormidium* is a topic of ongoing research focusing on understanding the specific pathways and genetic mechanisms involved. Insights into these processes are crucial not only for ecological studies but also for potential biotechnological applications (Holzinger and Karsten, 2013; Karsten et al., 2016).

In the ecological context, MAA production by *Klebsormidium* is vital for its survival and proliferation. These compounds play an important role in protecting algae from UV-induced damage and oxidative stress, allowing them to maintain photosynthetic efficiency and overall cellular integrity. Thus, the study of MAAs in *Klebsormidium* contributes to a better understanding of the adaptation strategies used by extremophilic algae, highlighting their flexibility and versatility.

The potential applications of *Klebsormidium*-derived MAAs are very broad and promising. In the pharmaceutical and cosmetic industries, these MAAs can be used for their protective properties against UV radiation and can contribute to the development of natural sunscreens and skin care products. Additionally, the antioxidant properties

of MAAs suggest their use in nutraceuticals and as natural food preservatives. In biotechnology, *Klebsormidium* MAAs can be explored to increase the UV resistance of bioplastics and other materials, meeting the growing demand for sustainable and environmentally friendly products.

1.9. The Rising Importance of Bioplastics in Sustainable Development

Bioplastic, which has entered our lives as an important concept in recent years, is one of the key concepts of sustainable development. It emerges as an alternative to harmful petroleum-derived substances and generally contains components of vegetable oils, starch, or photosynthetic organisms in its structure. Historically, bioplastics date back to the beginning of the 20th century with the development of materials such as celluloid and cellophane (Belgacem and Gandini, 2012). However, with the consumption frenzy that came with the modern age, increasing environmental concerns came to the fore and the concept of bioplastics came into our lives fully (Andrady and Neal). , 2009). Synthetic plastics' environmental impact, ranging from negatively affecting wildlife to increasing greenhouse gas emissions, has been the catalyst that increased the popularity of bioplastics (Thompson et al., 2009). Since synthetic plastics are inherently unsustainable, serious alternatives are needed. Bioplastic, an environmentally friendly alternative that reduces carbon footprint, is one of the most efficient green resources today that will encourage us to turn to it (Philp et al., 2013).

The development of some bioplastics based on PLA, PHA, and starch, produced after these concerns in the plastics industry, has expanded these applications beyond packaging. The increasing use of alternative products in industries such as agriculture and automotive, where traditional plastics are used extensively, has been promising in terms of their prevalence (Vroman and Tighzert, 2009; Siracusa et al., 2008). As current research advances, Bioplastic efficiency increases, which plays a role in expanding the potential and application areas of these materials (Emadian et al., 2017). Bioplastics, which are used against basic environmental challenges, are gradually reaching a standard on a global scale in reducing dependence on fossil-based plastics.

Recent developments show that petroleum-derived plastic packaged products increase the carbon footprint (Ali et al., 2023). Many years of efficiency improvement studies,

cost balance, and resource diversity have been limiting factors for bioplastics. That's why scientists have recently paid more attention to plant sources such as microalgae, which have a faster life cycle, than higher plants.

On the other hand, the dissemination and promotion of the use of petroleum-derived plastic products is seen as the biggest challenge in the development of green products. Another challenge is the ever-increasing demand and product costs. However, the widespread use of feasibility studies of environmentally friendly bioplastic products and international incentives given to the development of bioplastic-based products give hope for the future. The important thing here is to minimize the use of petroleum-derived products by differentiating product production processes in the bioplastic sector and trying new innovative models. The main vision for the future widespread adoption of biodegradable plastic in the modern environmental movement and manufacturing industry is to create fields of history, business, and scientific research supported by sustainable products (Chia et al.,2020).

1.10. Algal Biomass as a Resource for Bioplastic Production

The exploration of sustainable resources for bioplastic production has led to a growing interest in algal biomass, a renewable and eco-friendly raw material. Algae, encompassing a wide range of photosynthetic organisms, present a viable alternative to terrestrial biomass sources for bioplastics due to their unique advantages. Algae, both micro and macro forms, are renowned for their rapid growth rates and ability to thrive in diverse environments, ranging from freshwater to marine ecosystems. Unlike terrestrial plants, algae do not require arable land for cultivation, thereby not competing with food crops for resources. This aspect is crucial in the context of sustainable development, as it addresses the food versus fuel debate often associated with bio-based materials (Milledge et al., 2015).

One of the most significant advantages of using algal biomass for bioplastic production is its high yield and faster growth rates compared to traditional crops. Algae can also be cultivated in non-potable water, including wastewater, which adds to their sustainability quotient by aiding in water purification (Singh & Dhar, 2011). Moreover, algae absorb carbon dioxide during photosynthesis, contributing to carbon sequestration and helping mitigate climate change impacts (Brennan & Owende,

2010). Algal biomass is rich in carbohydrates, proteins, and lipids, making it a suitable feedstock for various bioplastic types. The polysaccharides in algae, such as starch and cellulose, can be converted into bioplastics like PLA and PHA. These bioplastics exhibit properties comparable to conventional plastics, including durability and versatility, making them suitable for a wide array of applications (Jung et al., 2013).

Recent technological advances in algal biotechnology have streamlined the process of converting algal biomass into bioplastics. Techniques like hydrolysis, fermentation, and polymerization have been optimized to enhance the efficiency of bioplastic production from algae (Koller et al., 2017). However, challenges remain, such as the need for cost-effective cultivation and harvesting methods and the development of efficient conversion processes to make algal-based bioplastics economically viable on a large scale. Incorporating algal biomass in bioplastic production aligns with the principles of the circular economy. It offers an avenue for recycling carbon and nutrients, especially when coupled with wastewater treatment. The environmental benefits extend beyond reducing dependence on fossil fuels; they also include the potential for biodegradable and compostable end products, contributing to waste reduction (Chen et al., 2016).

Especially in algae source-based bioplastic studies, researchers use solvent casting, electrospinning, and compression molding techniques as methods (Onen Cinar et al., 2020). Recent studies have shown that although Spirulina appears to be a potentially hydrophobic species suitable for bioplastic production and due to its cell wall charge, *Chlorella* can also be a good filler in a blended solution. On the other hand, some species such as *Nannocloropsis gaditana* and *Neochloris oleoabundans* have been reported in the literature as potential species to create new bioplastic composites using microalgal biomass (Johnsson, N., & Steuer, F.,2018), (Torres et al., 2015).

1.11. Processes and Technologies in Algal Film Production

The conversion of algae biomass into biopolymer films is an innovative approach in the field of sustainable materials, employing various methods like compression molding, electrospinning, and solvent casting. Each technique contributes uniquely to transforming this eco-friendly resource into practical bioplastic products. The process of creating algal bioplastic films begins with the extraction and preparation of

biopolymers from algae. This crucial first step involves mechanical or chemical disruption of algal cells to release key components such as alginates, carrageenan, and agar. The extracted biopolymers are then refined and processed, readying them for film production. Wijesekara et al. (2011) highlight the importance of this stage in ensuring the quality and suitability of the biopolymers for subsequent applications. Compression molding is one of the methods used to transform these biopolymers into films. It involves applying high pressure and temperature to press the biopolymers into the desired shape and thickness. While it offers simplicity and cost-effectiveness, especially for thicker films, its application is somewhat limited when it comes to producing very thin or highly uniform films. Electrospinning, on the other hand, provides a technique for creating ultra-fine fibers from algal biopolymers, which are then used to form thin films. This method allows for control over fiber morphology, making it ideal for applications requiring a high surface area, such as filtration membranes. Lee et al. (2012) emphasize its versatility and the high-quality films it can produce.

However, among these techniques, solvent casting emerges as a particularly advantageous method for algal film production. This process involves dissolving the biopolymer in a solvent, casting it into a flat surface or mold, and allowing the solvent to evaporate, leaving behind a uniform film. This technique stands out due to its precision in controlling film thickness and its adaptability to various biopolymer types. The resulting films are known for their smooth surfaces and consistent properties. However, as Pandey et al. (2010) note, solvent casting requires careful management of solvent use and recovery to mitigate environmental impacts.

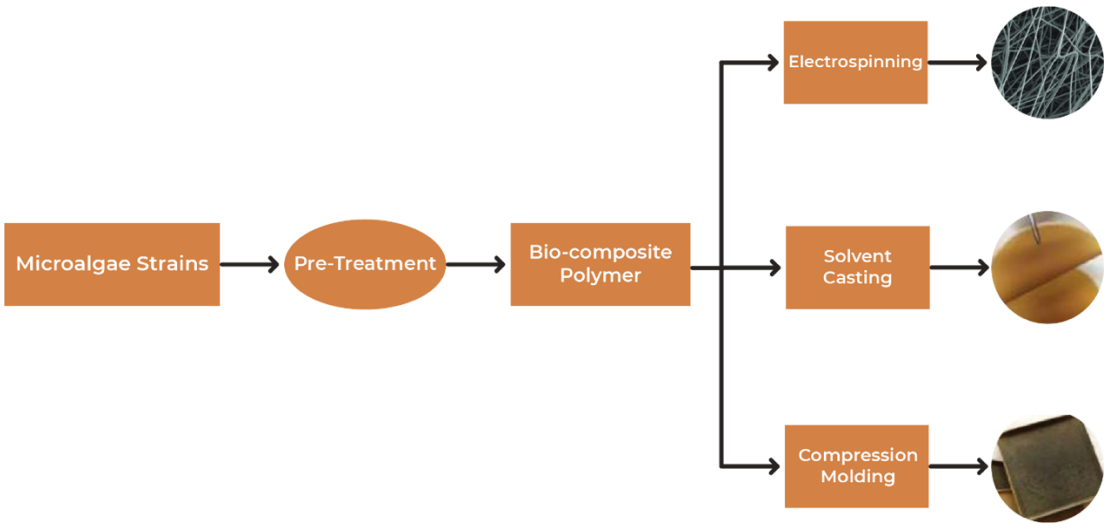

Figure 4: Different methods of producing bio-composite polymers from microalgae.

In conclusion, the production of biopolymers from algae biomass and their transformation into films is a field that combines sustainability with innovation. While techniques like compression molding and electrospinning have their own merits, solvent casting is particularly notable for its ability to produce high-quality films. As the field evolves, these processes are expected to become even more efficient and environmentally friendly, enhancing the role of algal bioplastics in sustainable material solutions.

1.12. Effects of Additives on the Functional Properties of Solvent-Casted Film

The incorporation of various additives into solvent-casted algal films significantly influences their functional properties, enhancing their applicability in diverse sectors. Additives play a crucial role in modifying the properties of bioplastic films. These can include plasticizers, fillers, colorants, stabilizers, and other functional agents. The choice and concentration of these additives are critical in determining the film's overall performance (Sirisha et al., 2016). Plasticizers are added to improve the flexibility and processability of bioplastic films. Commonly used plasticizers in algal bioplastics include glycerol, sorbitol, and polyethylene glycol. Studies have shown that the incorporation of glycerol in algal films significantly enhances their flexibility but may reduce their tensile strength and thermal stability (Rhim et al., 2013). Fillers like clay nanoparticles, cellulose nanocrystals, and carbon nanotubes are added to improve the mechanical strength and barrier properties of the films. For instance, research indicates

that adding cellulose nanocrystals to algal bioplastic films enhances their tensile strength and modulates their biodegradability (Saba et al., 2017).

The barrier properties of algal films, crucial for packaging applications, are significantly affected by additives. Studies have explored the use of nano-fillers like nano-clays to improve the moisture and gas barrier properties of the films. This enhancement is critical in extending the shelf-life of packaged goods (Zia et al., 2017). Additives can also influence the thermal stability and degradation behavior of algal films. For instance, thermal stabilizers are used to enhance the heat resistance of the films, which is essential for applications involving high-temperature processing or usage (Pandey et al., 2005). Incorporating colorants and UV stabilizers is important for aesthetic and functional reasons. UV stabilizers, particularly, play a vital role in preventing the degradation of films exposed to UV radiation, thus extending their lifespan (Nagarajan et al., 2016). The strategic incorporation of additives into solvent-casted algal films can tailor their properties to meet specific application requirements. While these modifications enhance the films' functionality, ongoing research focuses on ensuring that the additives do not compromise the biodegradability and eco-friendliness of the films.

On the other hand, algae are not used only as a filler in films obtained using the solvent casting method. At the same time, they can provide different functions to the material thanks to the unique metabolites they contain. Particularly algae are reported in the literature as a high source of antioxidants, which is an expected ability to ensure the continuity and stability of photosynthesis, which is their basic activity (Gopu et al.,2020). In addition, carotenoids and MAAs, whose concentrations vary depending on various factors in their metabolism, serve as natural UV filters. These properties pave the way for various biological functionalization opportunities in algae-based bioplastics. In addition, algae rich in neutral lipids and some special filamentous species such as *Klebsormidium* contain a precursor wax layer in their structures. This can act as a stabilizer in the biomaterial they are contained in.

1.13. Industrial and Commercial Viability of Algal Film

The versatility of algal films is evident in their various applications. In the packaging industry, they are especially beneficial for products where sustainable packaging is

prioritized. Their biodegradability is particularly useful in single-use applications, aligning with efforts to reduce plastic waste (Rhim et al., 2013). In agriculture, algal films serve as eco-friendly alternatives to conventional plastic mulches, contributing to soil health and reducing plastic residue. The biomedical field also benefits from the biocompatibility of algal films, making them suitable for applications such as drug delivery systems and biodegradable wound dressings (Sirisha et al., 2016).

Despite these advantages, the widespread adoption of algal films faces several challenges. Production costs, higher than those of traditional plastic films, are a significant barrier, primarily due to the expenses associated with algae cultivation and processing. Scalability is another challenge; meeting industrial demands while maintaining sustainability and quality is complex. Additionally, material property requirements for different applications remain a hurdle, necessitating ongoing research to enhance the strength, flexibility, and barrier properties of algal films (Singh et al., 2011).

1.14. The Potential of Klebsormidium Species as a Source of Bioplastic Film

Klebsormidium species are known for their robustness and ability to thrive in harsh environmental conditions, including extreme temperatures and varying levels of moisture. These algae have a high carbohydrate content, particularly in the form of cellulose and starch, which are essential raw materials for bioplastic production (Karsten & Holzinger, 2014). The presence of these biopolymers makes *Klebsormidium* an attractive biomass source for bioplastic film manufacturing. The process of turning *Klebsormidium* biomass into bioplastic involves several steps. Initially, the extraction of cellulose and starch from the algal biomass is conducted, which can be achieved through various mechanical and chemical methods. Subsequently, these extracted biopolymers undergo processes such as polymerization and plasticization to create a pliable and moldable material suitable for film production (Becker, 2007).

Klebsormidium-based bioplastics offer several advantages. These include biodegradability, reduced carbon footprint during production, and the avoidance of competition with food crops for agricultural land, a common concern with some bio-based plastics (Singh et al., 2011). Furthermore, the rapid growth rate of

Klebsormidium and its ability to grow in a variety of aquatic environments, including wastewater, make it a sustainable and cost-effective resource (Wang et al., 2008). Recent research has focused on optimizing the extraction and conversion processes of *Klebsormidium* biomass into bioplastics. Studies have explored various pre-treatment and hydrolysis methods to improve the yield and quality of the extracted biopolymers (Fu et al., 2013). Moreover, advancements in biotechnological techniques have enabled the modification of *Klebsormidium* strains to enhance their biopolymer production capabilities (Pittman et al., 2011). While the potential of *Klebsormidium* in bioplastic film production is promising, challenges remain in terms of large-scale cultivation, consistent biomass quality, and the economic feasibility of the overall process. Future research is likely to focus on genetic and metabolic engineering approaches to increase biopolymer yields, as well as the development of more efficient and sustainable processing technologies.

2. MATERIALS AND METHODS

2.1. Experimental Organisms and Growth Condition

2.1.1. Klebsormidium Strains

During the IV. Turkish National Antarctic Science Expedition, two algae species, *Klebsormidium* sp. ASYA19 *and Klebsormidium flaccidum* ASYA18 were sourced from a rock by a lakeside in Antarctica at coordinates 67°49'57.6"S 67°14'16.4 "W. Algal material was gently scraped from the rock with a sterile tool, and stored in sanitized containers close to the environmental temperature to keep the algae alive. They were initially identified using a light microscope, with further identification planned according to Mikhailyuk et al., 2014.

Once brought to the lab, the samples were mixed with clean fresh water and placed on 3N-BBM agar plates, as described by (Starr et al., 2004). To avoid bacterial interference, antibiotics were added to the agar. The plates were kept under conditions mimicking the Antarctic summer, with a 16:8-hour light-dark cycle at 4°C. After 2-3 weeks, clear algal colonies emerged. These colonies were individually transferred to new agar plates for further purification. Then, they were maintained in a liquid 3N-

BBM medium under the same conditions, making them ready for further study and experiments.

Klebsormidium deserticola, Klebsormidium crenulatum, Klebsormidium subtile, and *Klebsormidium flaccidium* species were obtained from the microalgae culture collection of Rostock University Applied Ecology and Phycology department thanks to the facilities provided by Prof. Ulf Karsten. *Klebsormidium deserticola* was isolated from open patches of shrub vegetation south of the Atacama region of Chile at coordinates 29°45'25"S 71°10'01"W (Samolov et al., 2019). *Klebsormidium subtile* was isolated from snow in Barrow Port, Alaska (71°17'42.8"N 156°46'24.1" W) and is preserved by the Culture Collection of Algae (SAG) with the code SAG 384-1. *Klebsormidium crenulatum* is also preserved by SAG with the code SAG 2415 and was isolated from Obergurgl 2,350 m a.s.l. alpine soil crust (46°51'02.7"N 11°00'53.6"E). Finally, *Klebsormidium flaccidium* is preserved in the CCCryo Culture Collection with the strain code 149-01 and was isolated from the South coast of Amsterdam, Danskegattet, Spitsbergen, Svalbard, Norway (79°44'33.0"N 10°50'00.0"E).

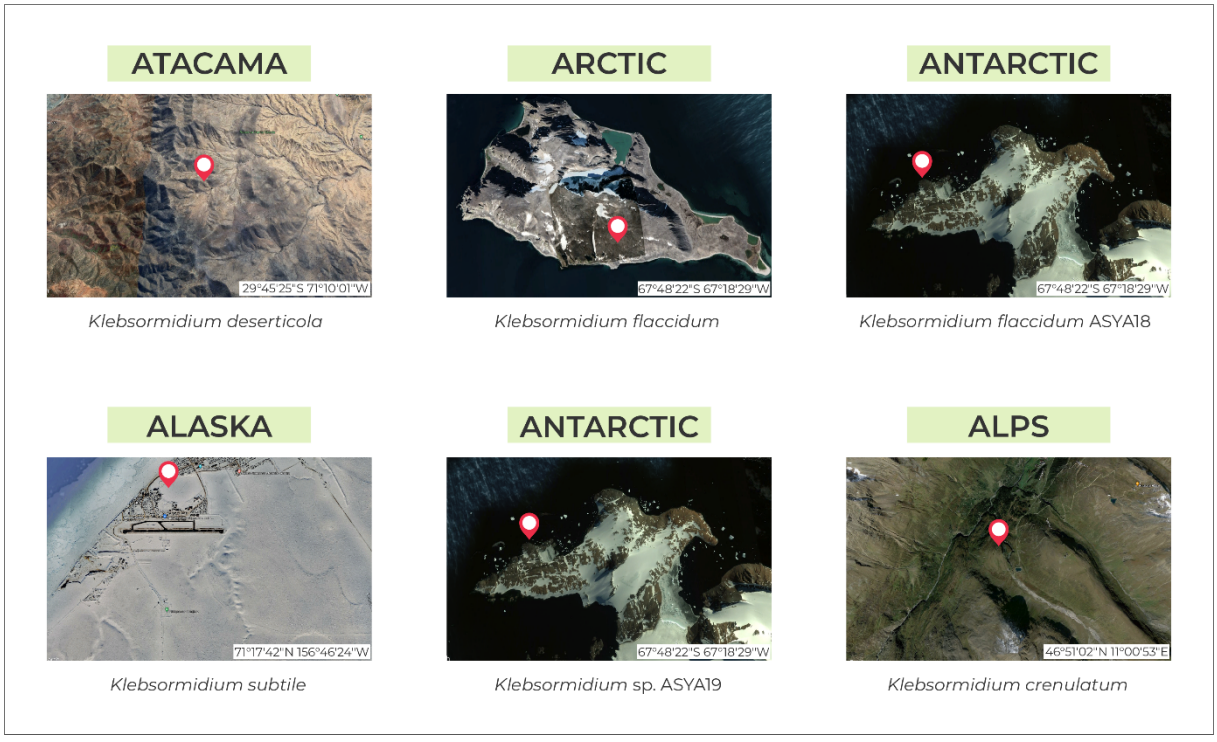

Figure 5: Regions and coordinates where Klebsormidium strains were obtained.

2.1.2. Growth Condition of Klebsormidium Strains

Axenic *Klebsormidium* isolates were collected from agar plates and planted in fresh 3-NBBM liquid medium. Subcultures were made every two weeks into new liquid 3-NBBM medium. All samples were grown at 15 °C, in an 8:16 h light/dark photoperiod, under a light intensity of 50 µmol photons $s^{-1}m^{-2}$. Cultivation was performed in 100 mL Erlenmeyer flasks with a 50 mL working volume. Samples were grown in a liquid medium at 15 °C in an incubation shaker cabinet (CERTOMAT BS-T, Sartorius) with continuous light. Identification of purified microalgae was achieved by both morphological and genomic analysis.

Table 1: Biochemical compositions of BMM Medium

BBM Medium (Bold's Basal Medium + soil extract + vitamins)				
Stock Solution (SL)	**Volume**	**Component**	**Concentration in SL**	**Conc. in final Medium**
SL 1	10 mL	$NaNO_3$	2.50 g . 100 mL^{-1}	2.94 . 10^{-3} M
SL 2	10 mL	$MgSO_4.7H_2O$	0.75 g . 100 mL^{-1}	3.04 . 10^{-4} M
SL 3	10 mL	NaCl	0.25 g . 100 mL^{-1}	4.28 . 10^{-4} M
SL 4	10 mL	K_2HPO_4	0.75 g . 100 mL^{-1}	4.31 . 10^{-4} M
SL 5	10 mL	KH_2PO_4	1.75 g . 100 mL^{-1}	1.29 . 10^{-3} M
SL 6	10 mL	$CaCl_2$	0.25 g . 100 mL^{-1}	1.70 . 10^{-4} M
SL 7	1 mL	$ZnSO_4.7H_2O$	8.82 g . L^{-1}	3.07 . 10^{-5} M
(trace		$MnCl_2.4H_2O$	1.44 g . L^{-1}	7.28 . 10^{-6} M
elements		MoO_3	0.71 g . L^{-1}	4.93 . 10^{-6} M
solutions)		$CuSO_4.5H_2O$	1.57 g . L^{-1}	6.29 . 10^{-6} M
		$Co(NO_3)_2.6H_2O$	0.49 g . L^{-1}	1.68 . 10^{-6} M
SL 8	1 mL	H_3BO_3	1.14 g . 100 mL^{-1}	1.85 . 10^{-4} M
SL 9	1 mL	$Na_2EDTA.2H_2O$	5.00 g . 100 mL^{-1}	1.71 . 10^{-4} M
		KOH	3.10 g . 100 mL^{-1}	5.53 . 10^{-4} M
SL 10	1 mL	$FeSO_4.7H_2O$	4.98 g . 1 L^{-1}	1.79 . 10^{-5} M
SL 11	50 mL	garden soil		
(soil extract)				
SL 12	1 mL	Vit. B_1 (Thiamine HCl)	0.100 g . 100 mL^{-1}	2.97 . 10^{-6} M
(vitamin mix)		Vit. H (Biotin)	0.025 mg. 100 mL^{-1}	1.02 . 10^{-9} M
		Vit. B_{12} (Cyanocobalamin)	0.015 mg . 100 mL^{-1}	1.11 . 10^{-10} M

- **For 3N-BBM, add a triple quantity of $NaNO_3$.**
- **For 1 L final culture medium, add the prepared stock solutions to 850 mL distilled water.**
- **Adjust medium to final pH of 5.5/6.5 and autoclave at 121°C for 20 min.**

Figure 6: Maintenance of stock cultures of Klebsormidium strains in a cold room (15°C) at Rostock University and in a climate cabinet in Fitotron SGC120 (15°C) at Istanbul Medeniyet University with an aeration system.

2.1.3. Identification of Klebsormidium Strains

The molecular identities of the isolated strains *Klebsormidium* sp. ASYA19 and *Klebsormidium flaccidum* ASYA18 were determined through standard genomic DNA extraction methods. We amplified and sequenced the entirety of the Internal Transcribed Spacer 1 (ITS1) region, as well as a segment of the ribulose-bisphosphate carboxylase large chain (rbcL2) gene. Upon analysis, both the complete ITS1 and the fragment of rbcL2 sequences for the two strains showed high similarity to reference sequences in the NCBI database. The partial sequences of rbcL2 for the strains were given the NCBI accession numbers ON817225.1 and ON729294.1, respectively. The identified strains have been deposited and are available for reference in the culture collection of Istanbul Medeniyet University. Detailed information about the strain, including its cultivation conditions and molecular data, can be accessed through the university's online collection portal: https://www.imuasya.org/collection.

On the other hand, the NCBI accession numbers of *Klebsormidium subtile*, *Klebsormidium crenulatum*, *Klebsormidium deserticola,* and *Klebsormidium flaccidum*, which were previously characterized, are EF372517.1, JN190354.1, MH971189.1 and x (not shared yet), respectively.

2.1.4. Temperature-Driven Growth Monitoring

To assess the growth dynamics of various Klebsormidium strains isolated from different regions, a systematic growth control was implemented. Strains examined included *Klebsormidium* sp. ASYA19 and *Klebsormidium flaccidum* ASYA18 (both from Antarctic regions), *Klebsormidium subtile* (sourced from Alaska), *Klebsormidium crenulatum* (from the Alps), *Klebsormidium deserticola* (originating from Atacama), and *Klebsormidium flaccidum* (from the Arctic). For each strain, 25 mL of the appropriate culture medium was inoculated into 50 mL Erlenmeyer flasks. The experiment was set up with three biological replicates for each strain at three distinct temperatures: 5°C, 15°C, and 23°C. To monitor biomass progression, samples were collected from each flask every three days. Cultures were diligently observed until they reached the stationary phase. This approach was designed to generate comprehensive data on the growth performance of each strain, particularly about biomass accumulation across the different temperature conditions.

Figure 7: Suitable conditions (5°C, 15°C, and 23°C) provided for the Temperature-Driven Growth Monitoring experiment of *Klebsormidium* strains and the image of the continuation of the experiment.

2.2. Investigation of UVR Exposure

2.2.1. Preliminary MAA scanning for UVR Treatment

To establish the experimental setup that will be explained in section 2.2.2, firstly, preliminary screening of Klebsormidium isolates taken from different regions was carried out to find out which UV source produced a more effective MAA response. In this preliminary screening, UV-B, UV-A, and UV-B+UV-A combined stresses were applied to Klebsormidium species that entered the late exponential phase, based on literature information (Maria Arroniz-Crespo et al., 2005). During the application, microalgae of selected species were added to 24-well plates at a density of 2.5 (A680 = 2.5) at a wavelength of 680nm in each well and were exposed to stress. The plates are covered with stretch film to prevent water loss and ensure UV permeability. The samples were harvested at 24, 48, and 78 hours after the application and stored at -80 degrees. The photosynthetic active radiation (PAR) rate to be used was determined as 50 µmol in all groups, and it was aimed to induce only MAA in the cells with UVR. The stress group found to be most efficient (only UV-B treatment) will be the main stress factor for MAA purification from other physiological tests and strains.

2.2.2. Maximization of MAAs and Measurement of Other Physiological Responses in Klebsormidiums

UV-B stress, which was selected as a result of the preliminary MAA screening conducted in the previous section for six different Klebsormidium species, was determined as the main stress factor of this study. The experiment set lasts seven days, as clearly shown in the figure above. It starts with the first two-day control conditions, then continues with a 3-day UV-B application, and finally ends with a 2-day re-control condition application. The first two days are intended to adapt the microalgae to be used in the experiment to the experimental conditions. The last two days are designed to show how long it takes for cells to recover after UV-B application. The control group was maintained under 50 µmol photons $s^{-1}m^{-2}$ light intensity at 23 °C for 7 days. The experimental setup was prepared by blending some of the MAA studies conducted to

date and determining appropriate conditions (Ryan et al., 2002), (Gröniger et al., 1999).

Table 2: Visual expression of the experimental set to be used in the study.

2 days	3 days	2 days
PAR (50 µmol photons $s^{-1}m^{-2}$)	UV-B (2 Wm^{-2})	PAR (50 µmol photons $s^{-1}m^{-2}$)

2.2.2.1 Extraction of MAAs

The microalgae were freeze-dried using a CD plus freeze-drier from Christ (Germany) and then ground into powder using a mortar and pestle. Mycosporine-like amino acids (MAAs) were extracted from the powdered algal samples (10 mg dry weight) by immersing them in 1 mL of 25% methanol solution (HPLC grade) in a 45°C water bath for 4 hours. Regular vortexing was applied Throughout the water bath using a Vortex-Genie 2 from Scientific Industries (USA) to enhance extraction efficiency. Following this, the samples underwent centrifugation at 13,000×g for 15 minutes using a Biofuge pico centrifuge from Heraeus (Germany), and the methanolic supernatants were transferred to new microtubes. These supernatants were then evaporated to dryness using a Speed Vacuum Concentrator (RVC 2–25 CD plus, Christ, Germany). The resulting dried pellets were reconstituted in 1 mL of HPLC water. After vortexing the aqueous homogenates for 30 seconds, they were centrifuged again at 13,000×g for 15 minutes. Finally, the resulting aqueous supernatants were filtered through a 0.45 µm filter (WhatmanTM, Germany) and transferred to HPLC vials for injection into the HPLC column (Borburema et al., 2022).

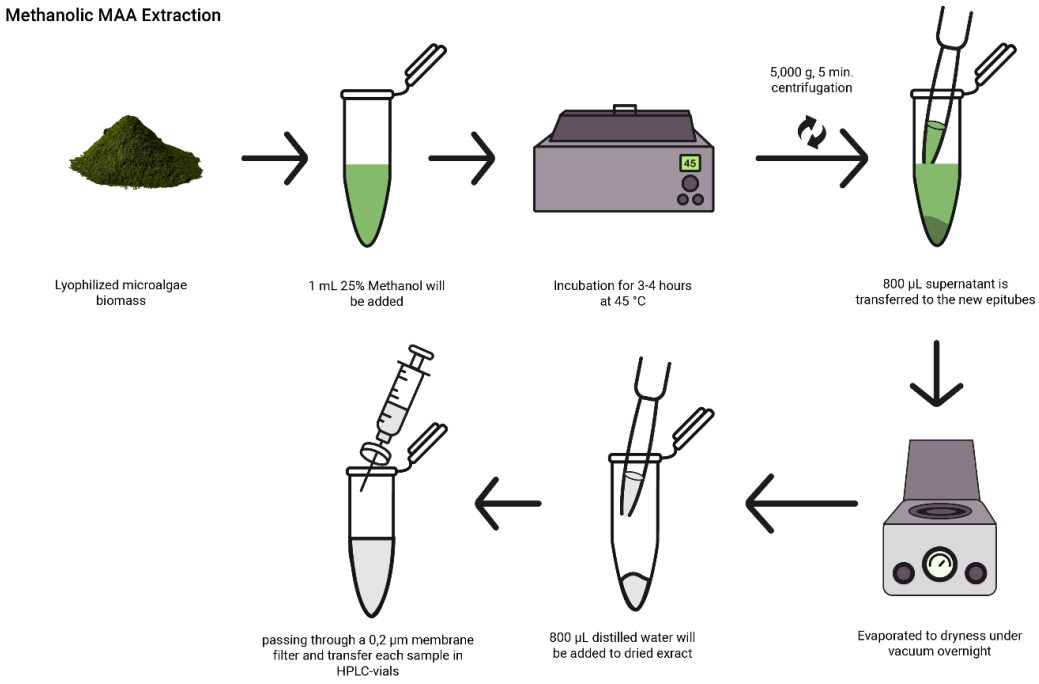

Figure 8: Visual representation of the methanolic MAA extraction process.

2.2.2.2 Spectrophotometric Assessment of MAAs

The extracted MAA sample was placed in a 96-well UV-star microplate suitable for spectrophotometry. The plate was then analyzed using a BioTech Cytation 5 Cell Imaging Multimode Reader, with a scanning range of 250-750nm, following the procedure outlined by Rastogi et al. (2014)."

Figure 9: Image of the experimental conditions used to monitor the MAA produced by different *Klebsormidium* strains under UV-B and control conditions for 7 days.

2.2.2.3 Purification of MAAs

Samples were assessed for the presence and quantity of Mycosporine-like amino acids using the 1220 Infinity II HPLC system (Agilent Technologies, Germany) paired with

a diode array detector (DAD) set at 330 nm, covering a spectrum of 240–400 nm. The analysis employed a Phenomenex Synergie 4µm fusion RP column (C18, 4 µm, 250 × 3mm, Phenomenex, Germany) along with an associated guard cartridge (RP-18 4 × 3 mm I.D., Phenomenex). The eluent used comprised 2.5% methanol and 0.1% acetic acid, delivered at a rate of 0.5 mL per minute under 150 bar pressure, with the column maintained at 30°C. Each injection involved a 10 mL volume. The resultant chromatograms were matched with known biological standards, specifically palythine, asterina-330, shinorine, and porphyra-334, to discern the MAAs based on retention time and absorbance pattern. Quantification was achieved by comparing the area under the curve of the sample peaks with that of known MAA concentrations in the reference standards, and the results were expressed in mg per g of dry weight (Borburema, Henrique DS, et al., 2022)

2.2.2.4 Fluorescence Measurements

Growth performance data of the control group and different Klebsormidium species exposed to UV were monitored by fluorimetric measurement for 7 days. We conducted fluorescence measurements using a growth fluorometer, as described by (Karsten et al.,1996). We chose bright blue light-emitting diodes (LEDs from Nichia) with a dominant wavelength of 470 nm to stimulate the chlorophyll fluorescence. Single-use Petri dishes were used with lids (sourced from Licefa) as containers for incubation. Measurements commenced with cultures in their logarithmic growth phase, which were previously acclimated to the given abiotic settings. These settings remained consistent during the determination of growth rates. Under aseptic conditions, 20 mL of each culture (with an initial cell count corresponding to the lower detection limit which is 120-70mv) was dispensed into the Petri dishes, which were subsequently sealed using parafilm (manufactured by Pechiney Plastic Packaging). Since the lighting and measurement apparatus was positioned beneath the Petri dish, cells had to settle and undergo dark adaptation before the inaugural fluorescence reading. Individual measurements were quickly taken by placing the Petri dish into the measurement device, ensuring no disturbance that might resuspend the cells, thus maintaining freely floating cells at the Petri dish base, optimal for detection. For every species cultivated in a 16-hour light to 8-hour dark rhythm, chlorophyll fluorescence was consistently logged every 24 hours. We conducted fluorescence measurements

using a growth fluorometer, as described by Karsten et al. (1996). We chose bright blue light-emitting diodes (LEDs from Nichia) with a dominant wavelength of 470 nm to stimulate the chlorophyll fluorescence.

To determine the growth rate μ, we used the formula $Ft = F0e\mu t$, where F0 represents the initial fluorescence and Ft is the fluorescence after a specific number of days (t). This calculation is valid only during exponential growth. To verify that the cultures were in this phase, we graphed the logarithmic fluorescence values against time (Gustavs et al., 2009).

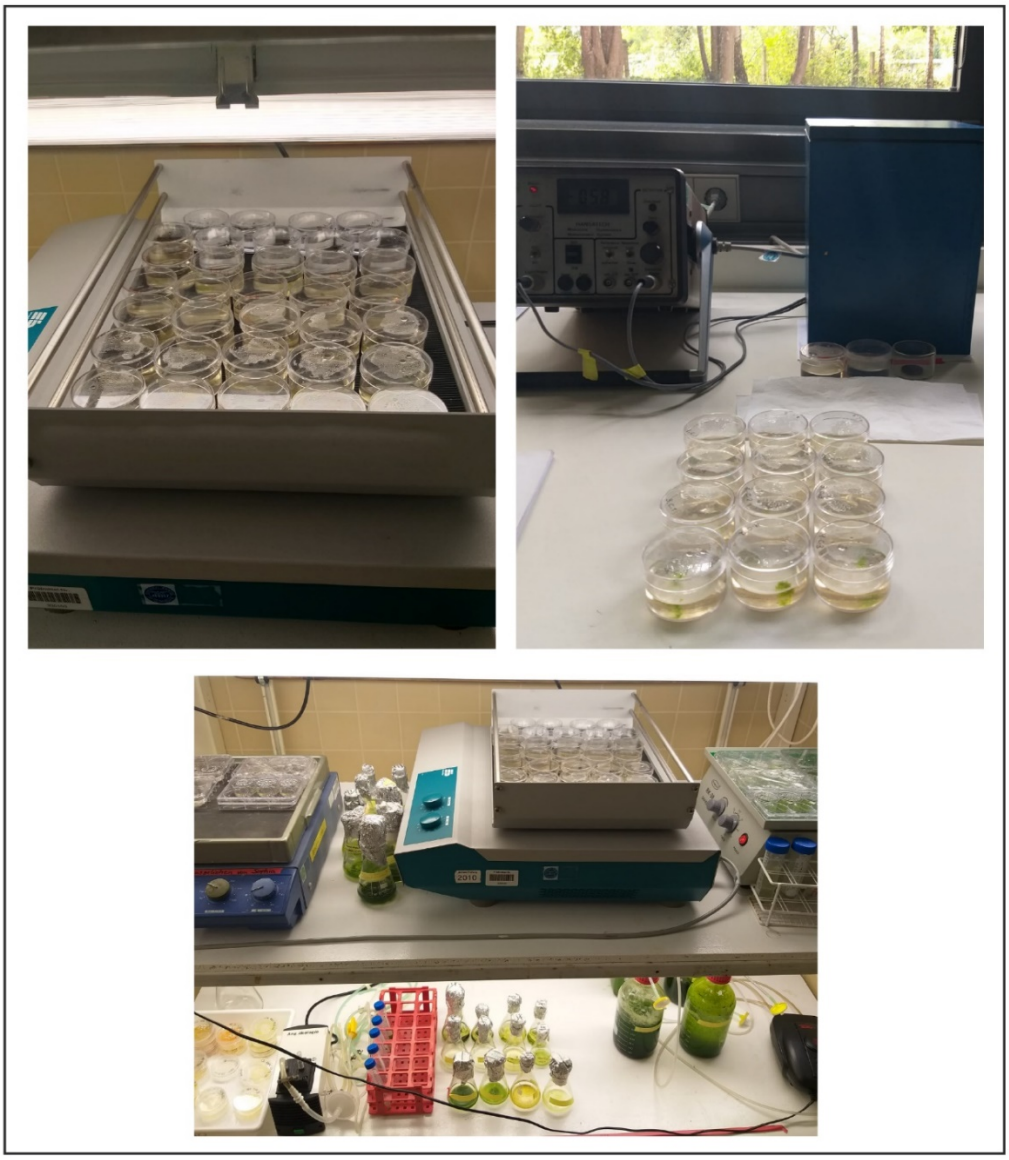

Figure 10: Conditions for carrying out fluorimetric measurement and images of measuring samples with the device.

2.2.2.5 PAM Measurements and Morphological Analysis

We utilized a mobile pulse amplitude-modulated fluorometer (PAM 2000, Walz, Effeltrich, Germany) to measure the in vivo chlorophyll fluorescence. This device captures fluorescence signals from the chlorophyll-a within the photosystem II. To compute the effective photosynthetic quantum yield (Y), we applied the formulas presented by Genty et al.,1989 and Weis and Berry 1987: $Y = (Fm - Ft) / Fm = Fv / Fm$

Where:

- **Y** is the effective photosynthetic quantum yield.
- **Fm** represents the maximal fluorescence induced by a saturating white light pulse.
- **Ft** stands for the current steady-state fluorescence induced by a weak red light in light-adapted samples.

For this study, a 7-day experimental setup was employed. During the initial two days, the Klebsormidium strains were maintained under control conditions to serve as a baseline. Subsequently, for the next three days, the strains underwent UV-B exposure to investigate the potential morphological changes induced by UV-B light. The final two days of the experiment were dedicated to reverting the conditions to control settings to observe any recovery or further alterations in cell morphology. Samples were collected at three designated time points over the seven days. These samples were then prepared for light microscopic examination, with observations made at 100x magnification. Differences in cell morphology between the control, UV-B-exposed, and post-UV-B exposure phases were meticulously documented to discern the effects of UV light on the strains.

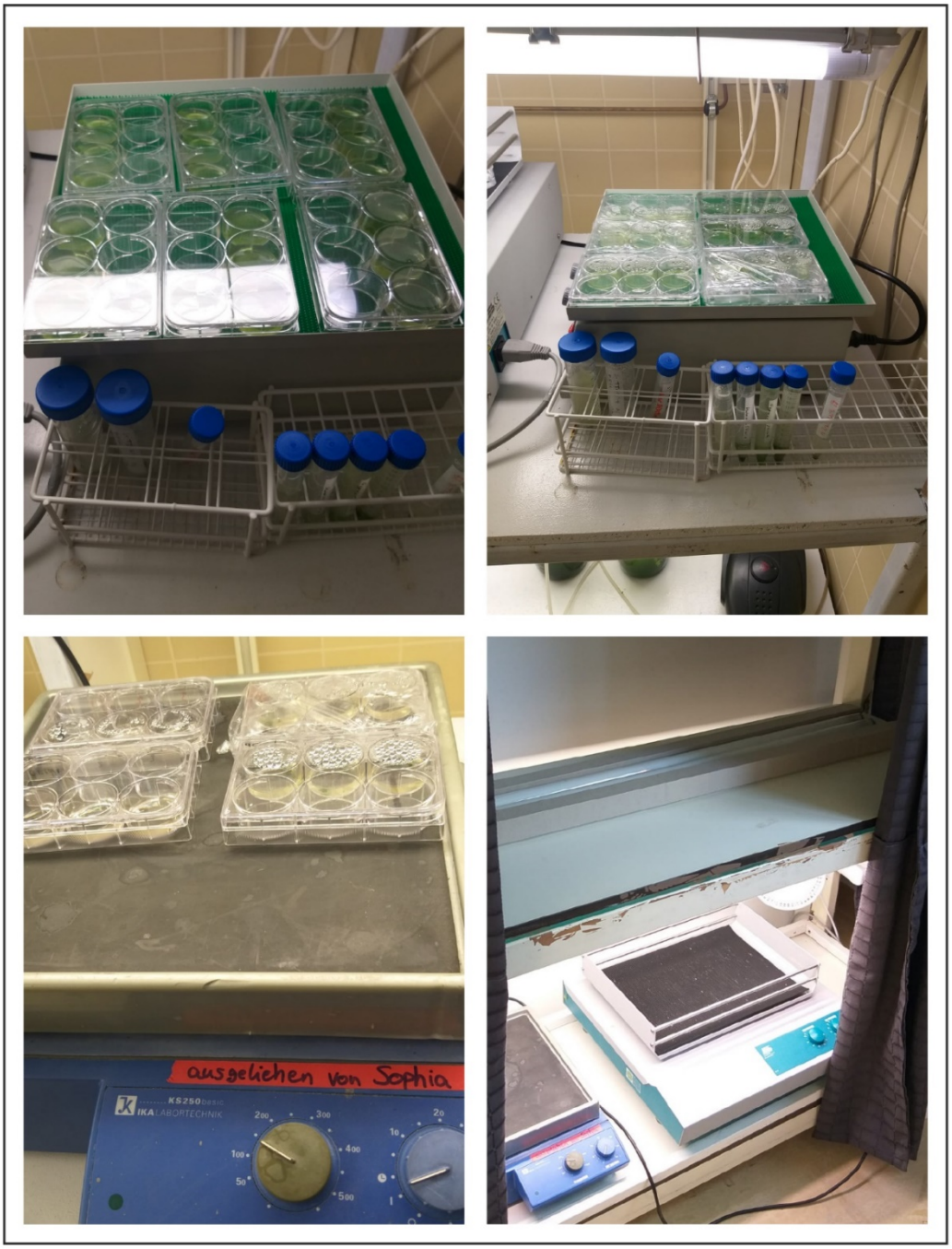

Figure 11: Image of experimental conditions used to monitor the photosynthetic performance of different Klebsormidium strains with PAM under UV-B and under control conditions for 7 days.

2.3. Bioplastic Production with UV-Blocking Capacity

2.3.1 Growth Conditions and Harvesting of Klebsormidium sp. ASYA 19

Klebsormidium sp. ASYA 19 was grown in a meticulously regulated photobioreactor to guarantee uniform growing conditions. The freshwater-supporting 3NBBM medium was utilized, and its pH was fine-tuned to 7.2 using 0.1N NaOH. LED lamps delivered a consistent light intensity of 200 µmol photons m^{-2} s^{-1}, catering to the photosynthetic demands of the algae and enhancing biomass rich in MAAs. The temperature was stabilized at 15°C, chosen for its suitability for the algal strain's growth. The photobioreactor introduced a continuous stream of sterile-filtered air, supplying necessary carbon dioxide and ensuring a homogenous culture by preventing cell settling. A tenth of the thriving culture was shifted to a new 3N-BBM medium every week. Regular checks on algal health and growth were performed by measuring optical density at 680 nm and by counting cells each week. Post a cultivation cycle of 21 days, cells that had been subjected to elevated light intensity were gathered from the photobioreactor. These cells were promptly preserved in a -80°C freezer to retain their condition and metabolic characteristics. Before their intended use in experiments, the stored cells were lyophilized to produce dry biomass, readying them for subsequent tests.

Figure 12: Detailed illustration of the bioprocess from the isolation of *Klebsormidium* sp. ASYA19 to the production of Bioactive film.

2.3.2 Experimental Setup

In this research, a range of mixtures were meticulously crafted to examine the influence of glycerol, PVA, and Crude *Klebsormidium* Biomass (CKB) on the attributes of bioplastics. The initial test used a blend containing just 5% CKB. Subsequent tests included mixtures of the same 5% biomass with different glycerol concentrations: 15% (w/w), 30% (w/w), and 45% (w/w). In parallel, other mixtures combined the 5% biomass with varying PVA levels: 25% (v/v), 50% (v/v), and 75% (v/v). A control group was also made using only 100% PVA, without any biomass. The primary goal of these various mixes was to pinpoint the best conditions for creating bioplastic films using the solvent-casting technique. The capability of CKB to form films was initially assessed at concentrations of 2.5%, 5%, 7.5%, and 10%. Preliminary tests indicated that the 5% CKB film was chosen due to its superior mechanical traits. It was also noted that all concentrations, except the 2.5% one, displayed the ability to form films.

Table 3: Illustration of experimental groups created with certain concentrations of films obtained with Crude Klebsormidium Biomass, PVA, Glycerol

Groups	Glycerol (w/w)	PVA (v/v)
5% Crude Klebsormidium Biomass	15%	-
	30%	-
	45%	-
	-	25%
	-	50%
	-	75%
PVA		100%

2.3.3 Preparation of Bioactive Film

Initially, 5% of raw *Klebsormidium* Biomass was measured and mixed in 20mL of doubly distilled water. This mixture was then agitated on a magnetic stirrer at a speed

of 400 rpm and a temperature of 20°C for three days. In the group containing glycerol and PVA, these compounds were added to the microalgae biomass. For the final 20 minutes of stirring, before casting, the solution's temperature was raised to 40°C at the same stirring speed to activate these additives, as noted by Tedeschi et al. (2021). Once the mixing process concluded, the mixture was allowed to stand for 10 minutes to release trapped gases. It was then poured into a 9cm diameter plastic petri dish and left to air dry at a temperature of 15°C in a setting with 60% relative humidity. Once fully dried, the resultant films were carefully detached from the petri dishes using both a spatula and a scalpel.

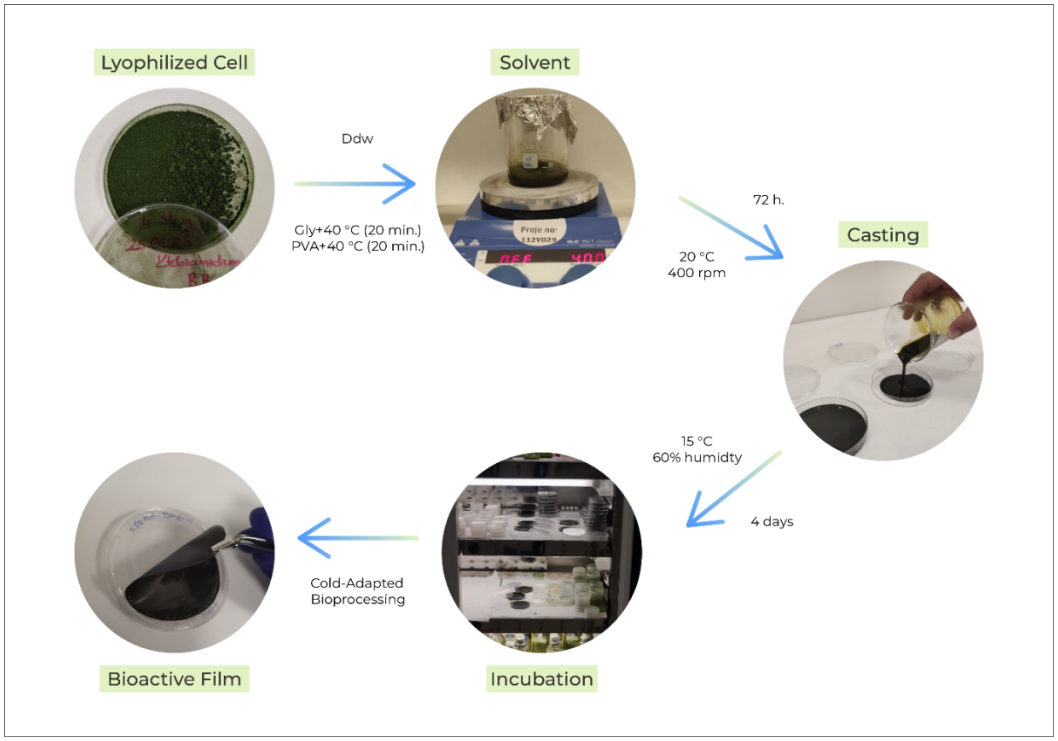

Figure 13: Detailed illustration of bioactive film production

2.3.4 Characterization of Bioactive Film

2.3.4.1 Mechanical Properties of the Films

Bioplastics' mechanical attributes were assessed using a custom-made tabletop tensile tester with a 5 kN capacity and a rate of 2.33 mm/min. These tensile evaluations were conducted under conditions of 21 ± 2°C temperature and 62 ± 2% relative humidity. Test samples, sized 30 mm by 5 mm, were prepared in compliance with ASTM D882-10 standards. Data was gathered from a minimum of five samples and then averaged.

Before testing, the film was conditioned for 48 hours at an environment of 23°C and 50% relative humidity. Key parameters like Young's modulus, tensile strength, and elongation upon breaking were deduced from the resulting stress-strain graphs (Nunes et al., 2013)."

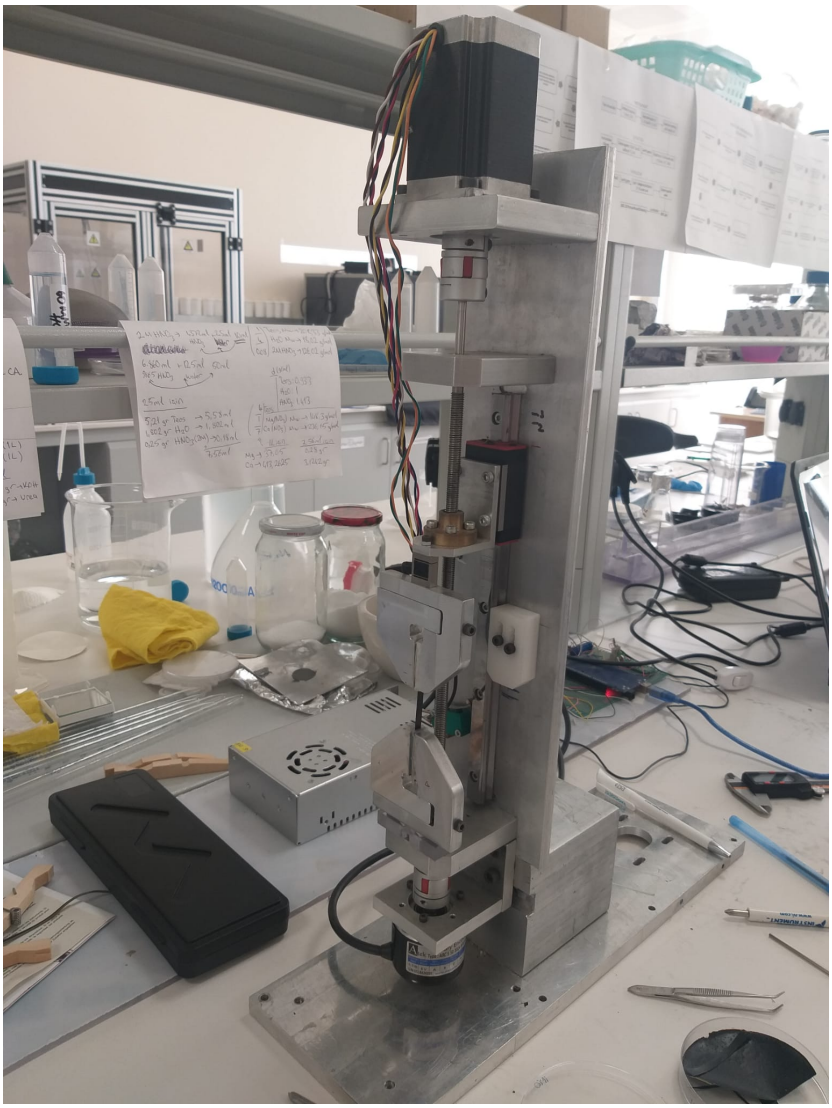

Figure 14: Image of the mechanical testing process of bioactive films obtained from *Klebsormidium* biomass.

2.3.4.2 Chemical Characterization

Fourier Transform Infrared (FTIR) Spectroscopy The chemical structure of the CKB, CKB /Glycerol, and CKB/ PVA bioplastic was studied using a Bruker Vertex spectrometer (Massachusetts, USA) with an Attenuated total reflection (ATR) at a resolution of 4 cm^{-1}.

2.3.4.3 Thermal Characterization

2.3.4.3.1. DSC (Differential Scanning Calorimetry)

The bioplastics' thermal characteristics and crystallization patterns were analyzed using differential scanning calorimetry, utilizing the PERKIN ELMER DSC 8500 model. Bioplastic samples weighing between 8-10 mg were tested in an aluminum container with a heating gradient of 10 °C/min, ranging from -50°C to 400°C, in a nitrogen environment. This was done to ascertain the films' thermal resilience. The protocol involved multiple heating and cooling cycles: starting with a hold at -50°C for one minute, heating from -50°C to 400°C at a rate of 10°C/min, then cooling from 400°C down to -50°C at 20°C/min, and finally maintaining the sample at -50°C for another minute. Each sample underwent this measurement cycle three times for consistency (Mathiot et al., 2018).

Figure 15: DSC Calorimeter (PERKIN ELMER, DSC 8500) equipped with cooler.

2.3.4.3.2. TGA (Thermogravimetric Analysis)

Samples weighed 8-10 mg were heated between 25 and 400°C at 10°C/min using the PERKIN ELMER, STA6000 device. Measurements are repeated in triplicate for each sample.

2.3.4.4. Scanning Electron Microscopy (SEM) Analysis

To assess the morphology of the crafted bioactive films, samples were cut into squares measuring 2x2 mm^2. These samples were then positioned on aluminum stubs with the aid of adhesive carbon tape. For optimum electron imaging, the samples were scanned with the ESEM module on the SEM (THERMO SCIENTIFIC QUATTRO S) device. Surface morphology and porosity were then observed using a Scanning Electron Microscope set at a voltage range of 10-15 kV. Various magnifications were used to capture images, and specialized software was utilized to deeply analyze attributes such as surface irregularities and the distribution of pores.

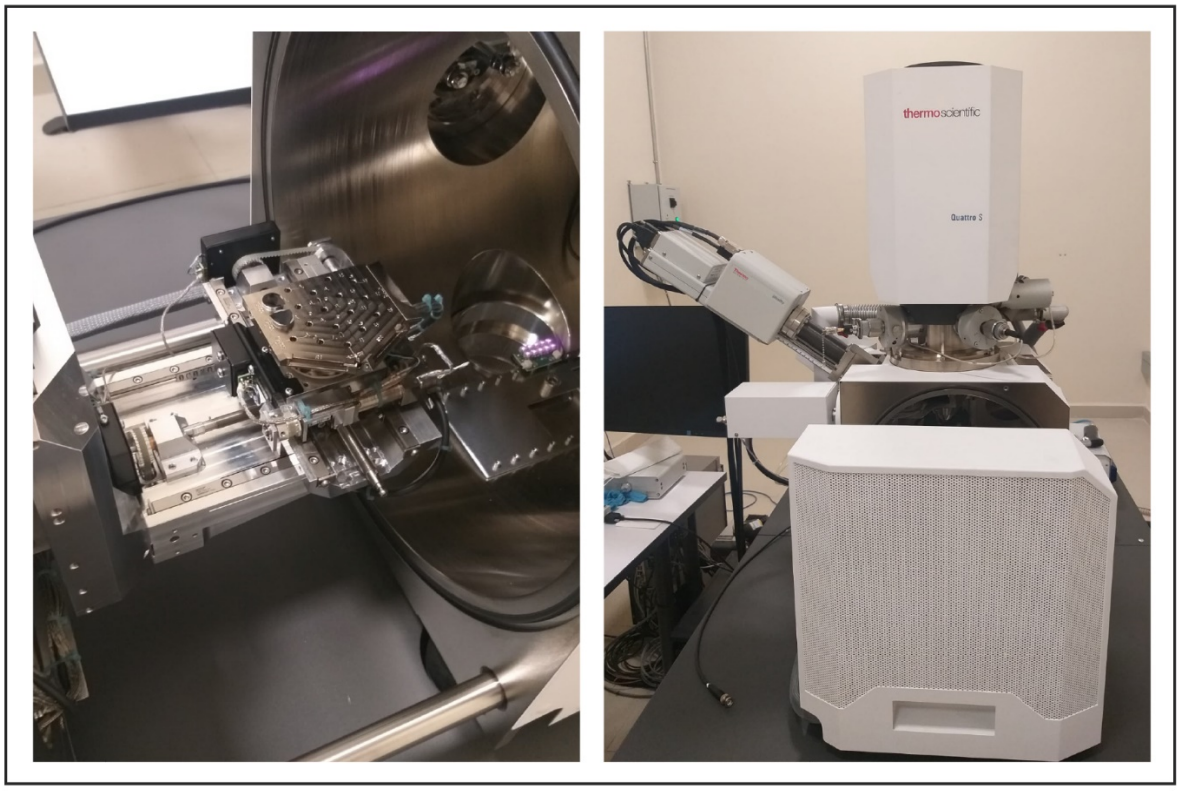

Figure 16: SEM (THERMO SCIENTIFIC QUATTRO S) device and placing the film obtained from *Klebsormidium* into the sample chamber.

2.3.4.5. DPPH Radical Scavenging Capacity

To examine the film samples, 5 mg of each film was dissolved in 1 mL of distilled water. Subsequently, 1 mL of ethanol was added. The mixture underwent centrifugation at 5000 rpm for 10 minutes to separate and obtain the transparent supernatant. To gauge its absorbance at 517 nm (labeled as Ag), 1 mL of this supernatant was mixed with 5 mL of a DPPH(0.2 mM) ethanol solution with a concentration of 0.01 mM. This was then kept in a dark environment for half an hour. For a reference point (denoted as Ac), 1 mL of the supernatant was combined with 5 mL of pure ethanol. Another reference setup, aimed at getting the A0 value, blended a solvent of 0.5 mL distilled water and 0.5 mL ethanol with 5 mL of the 0.01 mM DPPH ethanol solution, which was then left in the dark for 30 minutes (Brand-Williams et al., 1995). 50µg/mL concentration Ascorbic acid was used, as a standard, for comparative analysis.

2.3.4.6. UV Blocking Capacity of Microalgae Biomass and Bio-active Film

Firstly, to detect MAA efficiency in the biomass of *Klebsormidium* sp. ASYA19 grown in the photobioreactor under the above-mentioned conditions for 1 month was evaluated. Then, MAA was extracted from the film samples obtained from the Klebsormidium biomass specified in the experimental design to determine the UV-blocking capacity. The MAA extraction and spectrophotometric scans to be used are explained in detail in sections 2.2.2.1 and 2.2.2.2.

2.3.4.7. Evaluation of Water Content, Swelling Degree, and Solubility of the Film

Employing the method outlined by Jamróz E, film samples sized 3 cm x 3 cm were first weighed after being dried at 70°C for 24 hours, leading to a weight recorded as W2. These samples were then soaked in distilled water at 25°C over 24 hours and reweighed, obtaining a weight named W3. Excess moisture was removed using filter paper. Post another drying cycle at 70°C for 24 hours, the weight of the residue from the non-dissolved film was marked as W4 (Jamróz et al., 2018). The metrics were then computed using the equations:

•Water content (%) = [(W1- W2) / W3] x 100%

• Swelling Ratio (%) = [(W3- W2) / W2] x 100%

• Solubility (%) = [(W2- W4) / W2] x 100%

Figure 17: Incubation images of film samples during Water Content, Swelling Degree, and Solubility tests.

2.3.4.8. Assessment of Density of the Film

1 cm by 1 cm samples were preserved to determine the density of films with different concentrations of glycerol and PVA adducts (Jamróz et al., 2018). The films were stored in a desiccator with calcium sulfate desiccator (0% relative humidity) and silica gel for 20 days and then their final weight was weighed. Dry matter densities were calculated using the equation where A is the film area (1 cm^2), d is the film thickness (cm), and m is the dry mass of the film (g). Film density was expressed as follows: density (g/cm^3) = m / (A × δ)

Figure 18: Image of films after 20 days of incubation in a desiccator with 0% relative humidity for measuring film densities.

2.3.4.9. Contact Angle Determination

To assess the wettability of bioactive films, the static contact angle was determined through the Dataphysics OCA 15. 10 µL water droplet, sourced from Milli-Q, was

applied to the film surface and subsequently imaged. SCA 20_U software was utilized to process this image and ascertain the contact angle (CA). The relationship used to derive the CA is CA (θ) = arctan (2h/D), where D denotes the droplet's base width and h signifies its elevation.

3. RESULT & DISCUSSION

3.1.Temperature-Driven Growth Monitoring

As shown in Fig.19 In order to evaluate the impact of temperature on Klebsormidium strains, the microalgae were incubated at 5°C, 15°C, and 23°C. All cultures were started with 0.1g/L biomass concentration. *Klebsormidium* sp. ASYA19 showed the best growth with a specific growth rate of 0.143 and reached 2.10g/L biomass at the end of 24 days of incubation at 5°C. *Klebsormidium subtile* reached its maximum biomass with a value of 1.23 g/L on the 21st day of incubation. The specific growth rate was calculated as 0.12 for this strain. Other strains did not show considerable growth at 5°C. The specific growth rate was calculated as 0.11 for *K.deserticola* and *K.flaccidum*; and 0.1 for *Klebsormidium* sp. ASYA18, and 0.09 for *K. crenulatum*. Thereby the Antarctic strain *Klebsormidium* sp. ASYA19 is pronounced for its growth at freezing temperatures.

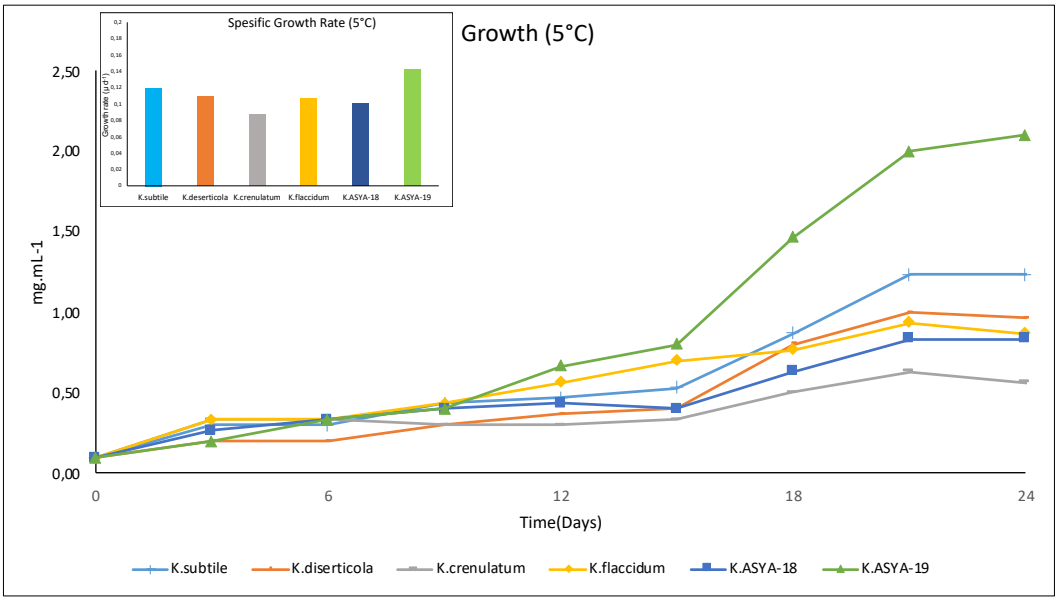

Figure 19: Detailed illustration of the line graph of biomass increases (a) and growth rate (b) of *K.subtile, K.diserticola, K.crenulatum, K.flaccidum, K.flaccidum ASYA 18* and *K. ASYA 19* at 5°C in $mg.mL^{-1}$

It is observed that all strains remain in the lag phase until the 6th day. It is seen that there is an exponential increase, especially after the 12th day, and the increase in biomass did not change after the 21st day, that is, all strains entered the stationary phase. In addition, it is clearly seen in the graphs that, compared to other growth conditions, the condition in which all species had the least biomass accumulation was determined as 5°C. It was observed that 5°C was a temperature at which all *Klebsormidium* strains could grow, but it was not optimum and obviously revealed that the growth of some strains was suppressed.

As can be seen in Fig.20, *Klebsormidium* sp. ASYA 19, *Klebsormidium flaccidum* ASYA 18, *K.deserticola,* and *K.flaccidum* have a higher growth rate with 0,18, 0,16, 0,14, and, 0,15 respectively at 15°C than other temperatures, and this temperature is even optimum for these strains. Moreover, figure x illustrates that *K. crenulatum* has almost the same growth rate at 15°C and 23°C with 0,15. *Klebsormidium* sp. ASYA 19 also has a dominant growth rate against other strains, as at 15°C with 0,18, and this rate was observed as the highest growth rate compared to all strains and temperatures. *K.deserticola* again had the lowest growth rate with 0,14 at 15°C, and this growth trend repeated at 23°C with 0,12.

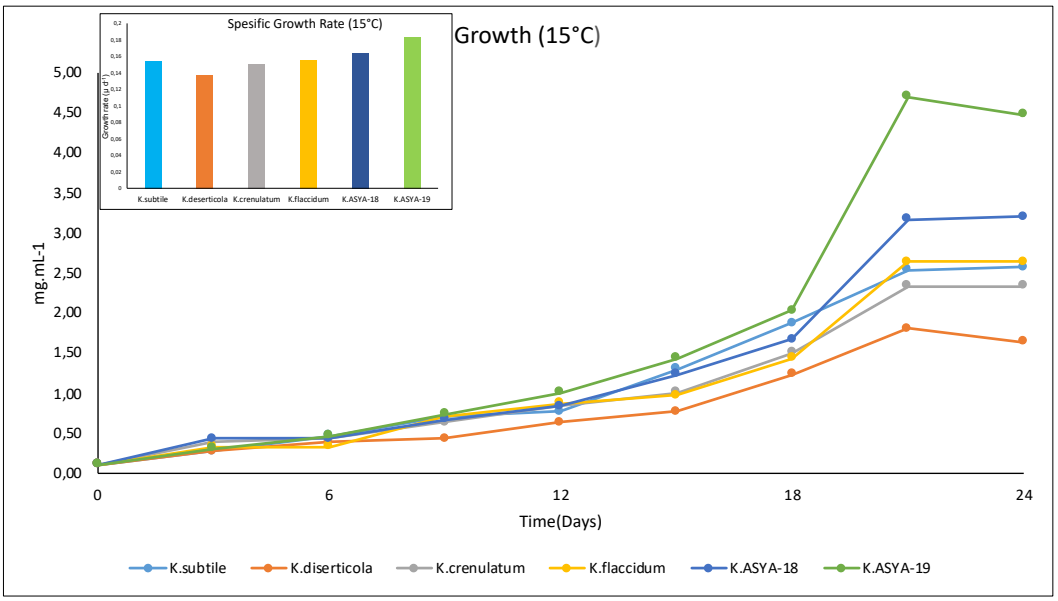

Figure 20: Detailed illustration of the line graph of biomass increases (a) and growth rate (b) of *K.subtile, K.deserticola, K.crenulatum, K.flaccidum, K.flaccidum ASYA 18* and *K. ASYA 19* at 15°C in mg.mL^{-1}

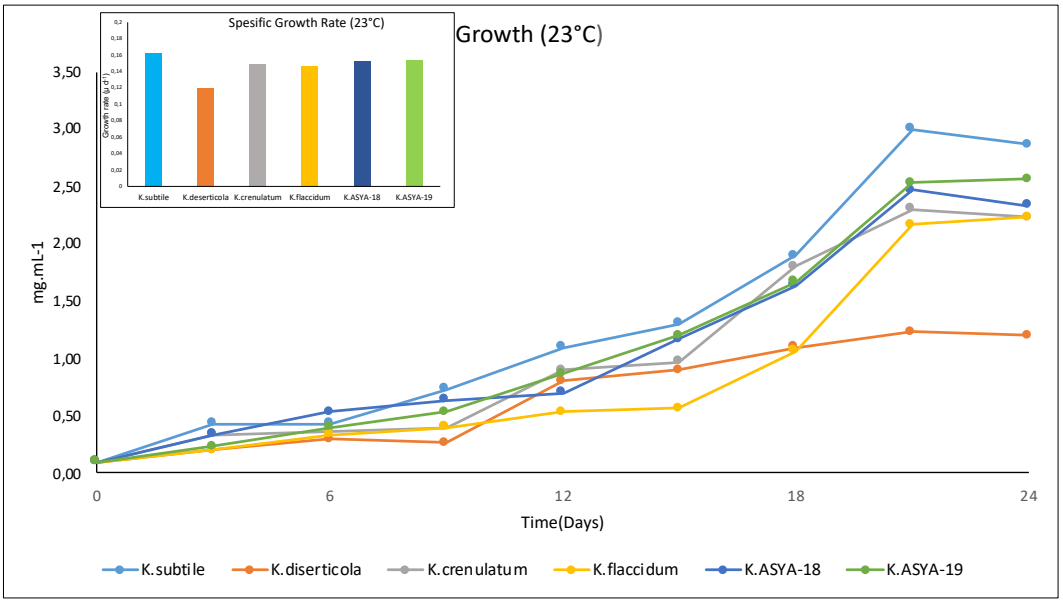

Figure 21: Detailed illustration of the line graph of biomass increases (a) and growth rate (b) of *K.subtile, K.deserticola, K.crenulatum, K.flaccidum, K.flaccidum ASYA 18* and *K. ASYA 19* at 25°C in mg.mL^{-1}

At 23°C, there is a similar distribution among strains. To elaborate, *K.subtile*, showed a slightly better growth rate (0,16) than, *Klebsormidium* sp. ASYA 19 (0,15), but when all temperatures were considered combined, the leading growth-based species was *Klebsormidium* sp. ASYA 19 (15°C). Additionally, *Klebsormidium* sp ASYA 19 surpassed other strains by accumulating 4.70 g/L biomass at the end of the 21st day. Another prominent result is that *K.flaccidum, K.crenulatum, and Klebsormidium flaccidum* ASYA 18 show a very similar growth rate at 23°C with 0,15. In addition, these 3 strains accumulated almost similar biomass, reaching 2.30 g/L biomass after 24 days. The growth rates of all strains were evaluated, and it was observed that all strains started to increase exponentially on the 9th day. On the other hand, while the lag phase was mostly observed for the strains in the first 6 days of biomass increase, all strains entered the stationary phase after the 21st day. Additionally, at 23°C (room temperature) *Klebsormidium* sp. It has been determined as the optimum growing

temperature for all species except ASIA 19. Therefore, it was decided that room temperature would be the common temperature used to conduct all other experiments.

Six different *Klebsormidium* strains isolated from five different regions (Antarctic, Arctic, Alps, Alaska, and Atacama) showed different growth rates at different temperatures. These microalgae even showed optimal growth rates at temperatures higher than the original environmental conditions. For example, in a study, *Klebsormidium* isolated from Antarctica the optimum growth condition of UMACC 227 was determined as 14°C, which proved that the strain was a psychrotolerant rather than a psychrophilic species (Teoh et al., 2004). On the other hand, in another study, Chlamydomonas species isolated from Antarctica were studied. In these studies, it was determined that this species was more sensitive to temperature, unlike its temperate variants, and it was revealed that it grew in a narrow temperature range (Teoh et al., 2013). On the other hand, it was determined many years ago that Chlorella species have a wide growth range (Kessler et al., 1985). Additionally, the growth of Antarctic microalgae over wide temperature ranges has been reported many times (Seaburg et al., 1981). Evidence shows that *Klebsormidium* strains taken from extreme regions continue their physiological activities over wide growth ranges, although not optimally. They probably carry these abilities in their adaptable nature, highly equipped biochemical composition, and genetic codes (Ryšánek et al., 2016).

3.2. Preliminary MAA scanning for UVR Treatment

Klebsormidium strains were exposed to e(UV-A), f(UV-B), and g(UV-A+UV-B) treatments for 24, 48, and 72 hours and the MAA potentials of the strains were evaluated spectrophotometrically. As a result of the evaluation, the general effects of UV-A and UV-B on *Klebsormidium* strains in terms of MAA accumulation were observed. In this experiment, it was clearly seen that while UV-A was not a significant MAA-increasing factor in *Klebsormidium* strains, UV-B was the major environmental factor that increased MAA accumulation in cells at different concentrations. In addition, the results obtained with UVR application were compared with the control group (without UVR), and the control groups of other *Klebsormidium* strains, except *K.crenulatum*, did not accumulate MAA.

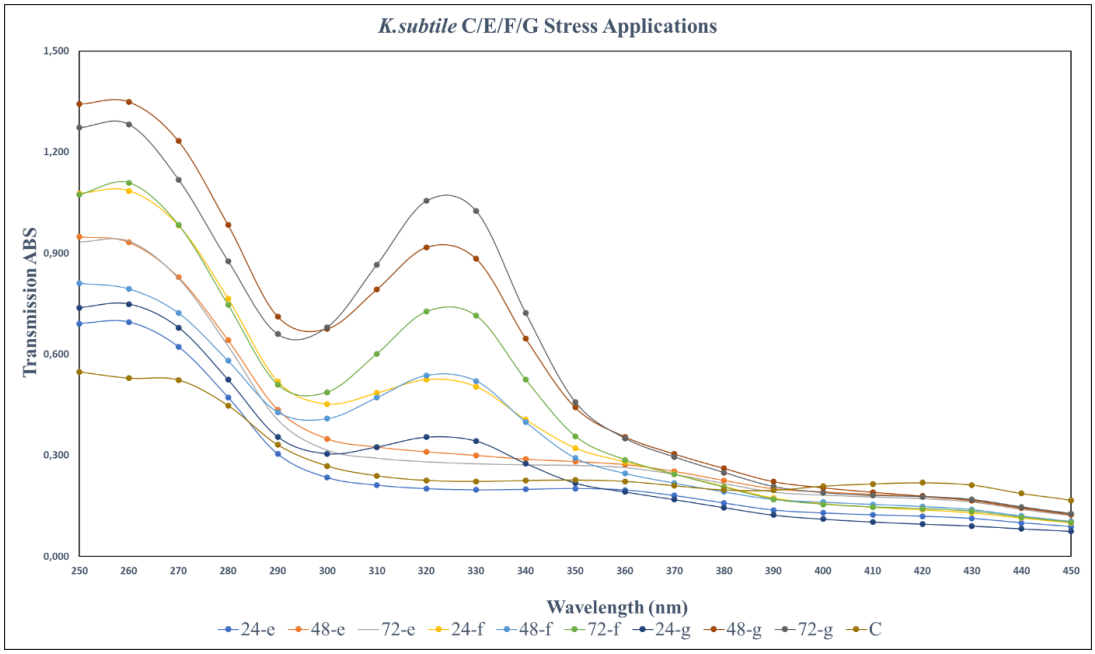

Figure 22: Spectrophotometric demonstration of *K.subtile*'s MAA accumulation obtained by exposure to e(UV-A), f(UV-B), and g(UV-A+UV-B) treatments for 24, 48, 72 hours

As shown in Fig.22, the maximum MAA accumulation of *K.subtile* was in the 320-330 nm wavelength range in the 72-hour g group application. Peak density decreased gradually at 48g and 72f, respectively. The 24th application hours of these two stress groups were less efficient in stimulating MAA compared to the 48 and 72-hour UVR applications. It has also been observed that UV-A is not a significant factor for increasing MAA accumulation by *Klebsormidium subtile*. In addition, the control group result shows that *K.subtile* did not accumulate MAA without UV applications. Moreover, all peaks were found between 320-330 nm wavelength at all hours of all UVR groups. This can be explained as follows: UV-A and UV-B applications did not reveal any difference in MAA derivatization in *K. subtile.*

On the other hand, as shown in detail in Fig.23, group f was a more efficient inducer of MAA for the *K.deserticola* strain. When the parameters that increase MAA production are examined, the 72-hour f group application is followed by the 48-hour g group and 72-hour g group stress factors, respectively. UV-A was not a significant parameter in *K.deserticola* and all UV-A treatment groups showed the same

absorbance value as the control group in the 320-330 nm wavelength range. This again shows that UV-A is not an efficient MAA-inducing factor for this strain.

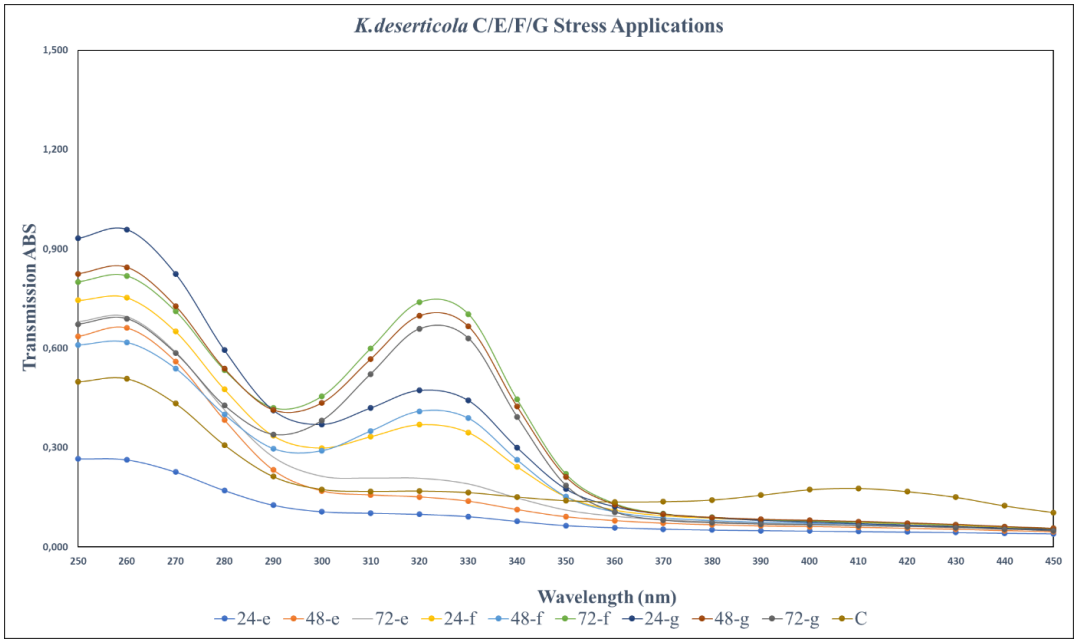

Figure 23: Spectrophotometric demonstration of *K.deserticola*'s MAA accumulation obtained by exposure to e(UV-A), f(UV-B), and g(UV-A+UV-B) treatments for 24, 48, 72 hours

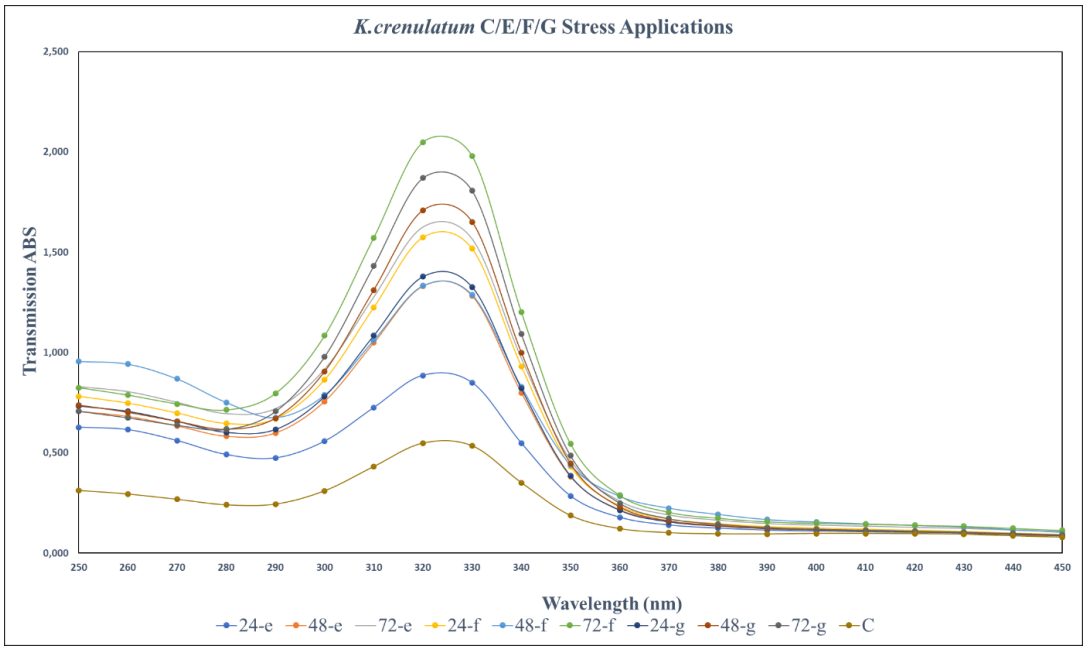

Figure 24: Spectrophotometric demonstration of *K.crenulatum*'s MAA accumulation obtained by exposure to e(UV-A), f(UV-B), and g(UV-A+UV-B) treatments for 24, 48, 72 hours

Klebsormidium crenulatum was the strain that reached the highest absorbance value among other species in terms of MAA, which was around 2,000 absorbance. Although this strain reaches the highest MAA accumulation value as a result of 72 hours of UV-B application, 72-g, 48-g, and 72-e treatment groups, respectively follow 72-f closely. Unlike other strains, *K.crenulatum* also responded to UV-A, and its response in UV-A groups was almost similar to its response in UV-B stress application. Interestingly, in UV-B and UV-A applications, the peak point was around 320 nm, where MAA was maximum, and MAA accumulation was not detected at different nm. Secondly, MAA has already been detected in this strain to a significant extent in the control group. The control group remained at the lowest rate in terms of MAA production when compared to other stress groups, but when compared to other *Klebsormidium* strains, it was even higher than the MAA produced by many strains after UVR application.

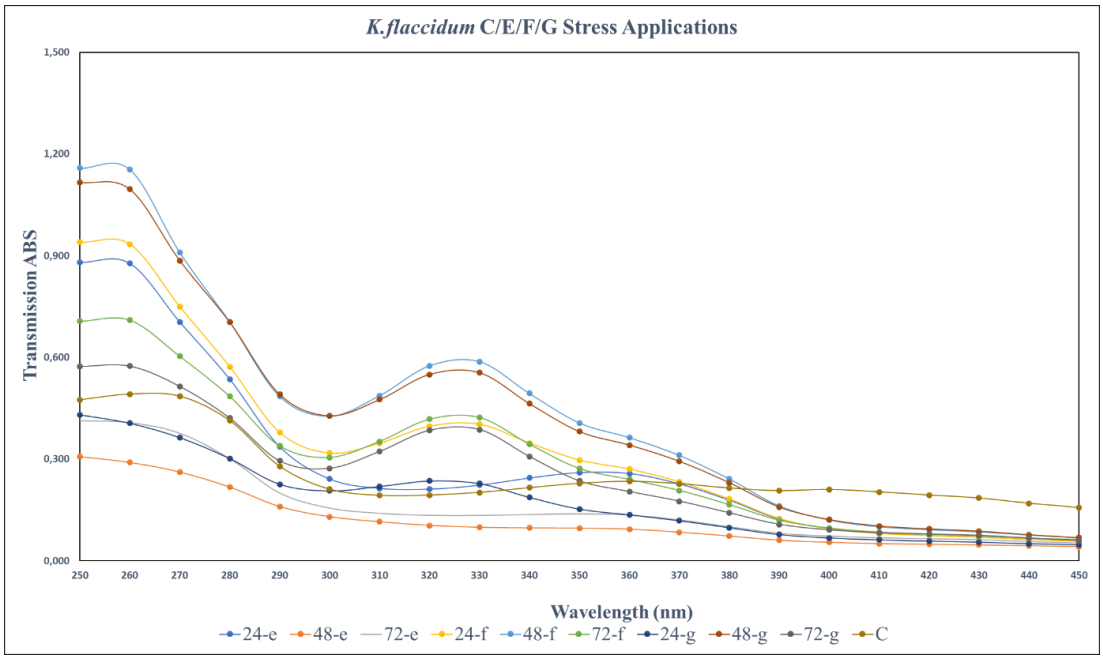

Figure 25: Spectrophotometric demonstration of *K.flaccidum*'s MAA accumulation obtained by exposure to e(UV-A), f(UV-B), and g(UV-A+UV-B) treatments for 24, 48, 72 hours

K.flaccidum showed the highest MAA production in 48-f, and 48g UV applications, respectively. 72f,72g come right after them. These results show that UV application was not a factor that would increase MAA production in *K.flaccidum* after 48 hours. In addition, this strain did not respond to UV-A in terms of MAA, and the peaks in the 320-330nm wavelength range that appeared in UV-B application were not detected after UV-A application. *K.flaccidum* was another strain that did not accumulate MAA in the control group, and when its peaks were evaluated, it produced less MAA than *K.crenulatum, K.subtile*, and *K. deserticola.* strains. Like the majority of other Klebsormidium strains, the peaks detected were again between 320-330.

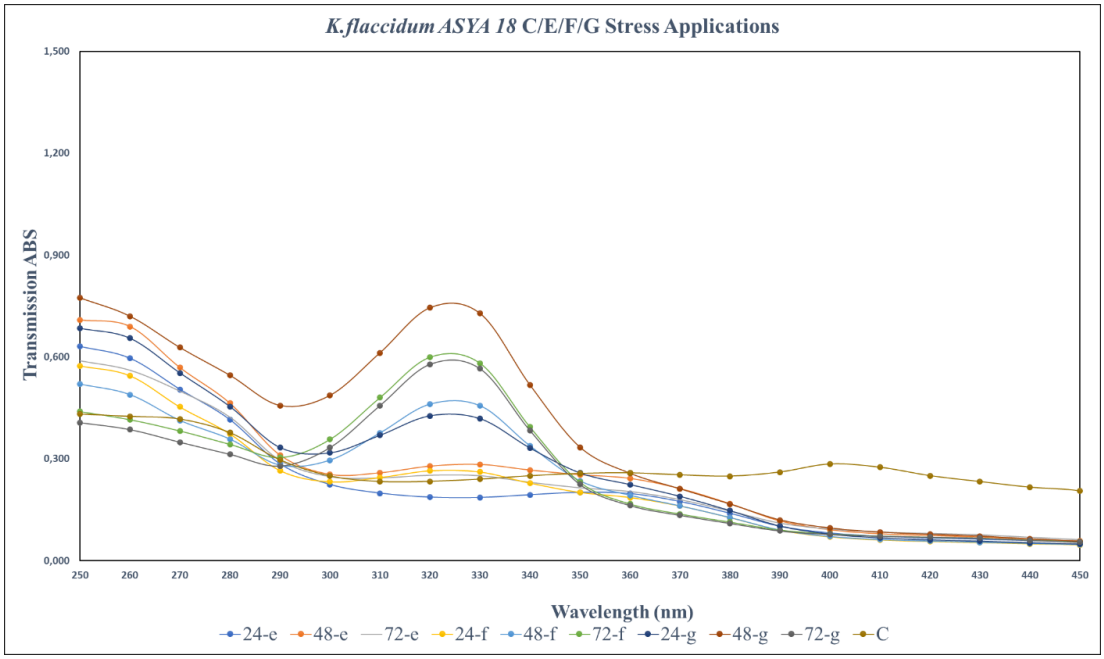

Figure 26: Spectrophotometric demonstration of *K.flaccidum* ASYA 18 MAA accumulation obtained by exposure to e(UV-A), f(UV-B), and g(UV-A+UV-B) treatments for 24, 48, 72 hours

As can be seen in Fig.26, *Klebsormidium flaccidum* ASYA 18 showed a similar MAA distribution in response to UV stress as *K.flaccidum*. MAA response was not observed in the control group of this strain, which produced the most MAA in 48 hours of UV-A+UV-B application. Similar to *K.flaccidum*, *K.flaccidum* ASYA 18, whose MAA production did not increase in UV-A, increased MAA production in the 72-f and 72-g groups, respectively, after the 48-g group. Considering the total absorbance ratio, it was ahead of *K.flaccidum* in terms of MAA production. However, considering the

stress conditions under which it is most efficient in terms of MAA production, it still lags behind *K.subtile, K.deserticola,* and *K.crenulatum*

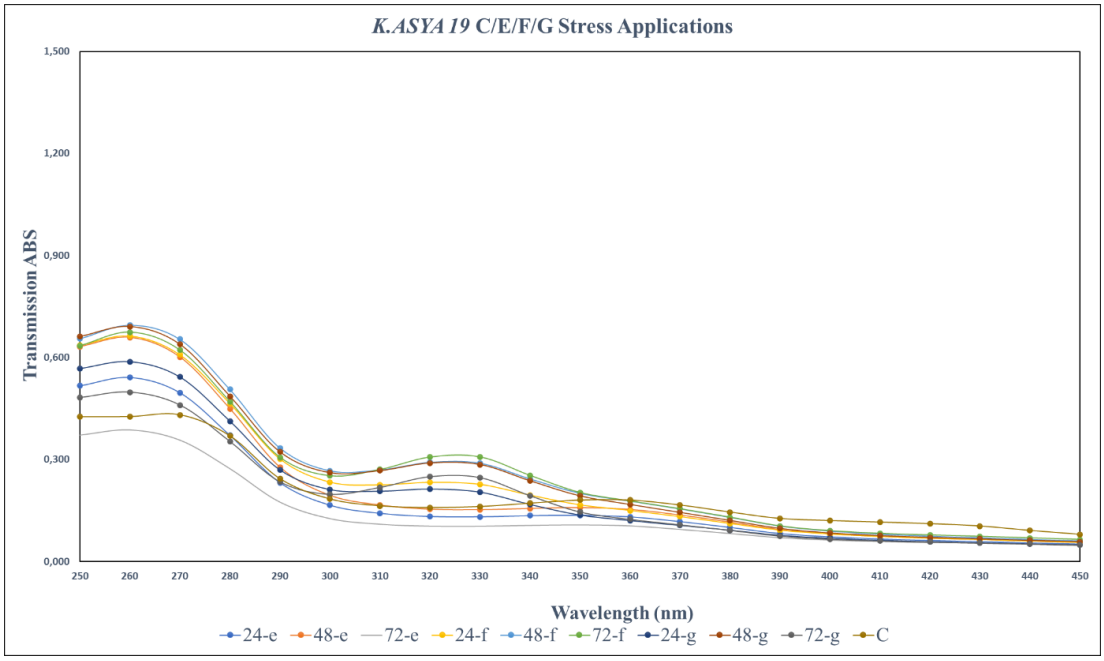

Figure 27: Spectrophotometric demonstration of K. ASYA 19 MAA accumulation obtained by exposure to e(UV-A), f(UV-B), and g(UV-A+UV-B) treatments for 24, 48, 72 hours.

Lastly, the effect of UV-A and UV-B, separately and in combination, on MAA increase was evaluated for *Klebsormidium* sp ASYA 19. Findings show that K. ASYA 19 did not produce any MAA response against UV-A, and its MAA production response against UV-B was the lowest compared to other species. In addition, the wavelength of MAA production for K. ASYA 19 was detected between 320-330 nm, and at these peaks, 72 hours of UV-B application was the most important potential stress condition. In addition, MAA production was not found in the control group.

Preliminary screening was performed with some UVR stress combinations to maximize the potential detection of MAAs in *Klebsormidium* strains and to measure other physiological responses against UVR. The results show that *Klebsormidium* strains isolated from different regions have the potential to produce MAA. However, the MAA rates they accumulate in their metabolism are different from each other, and the types of UV to which they respond may sometimes differ. For example, while only *K.crenulatum* responded to UV-A, all strains produced MAA against UV-B. In studies

conducted to date, researchers have shown that MAAs are synthesized in marine and tropical organisms to alleviate the lethal effects of cells against UV-B (Karentz et al., 1991). In addition, MAA studies conducted to date have proven that MAAs are produced in different types of microalgae (Gleason et al., 1993). The results obtained show that UV-B has a high potential to increase MAA production in *Klebsormidium* strains, and especially these strains are mostly dependent on strong stress conditions such as UV for MAA production except for *K.crenulatum*.

3.3. Maximization of MAAs and Measurement of Other Physiological Responses in Klebsormidiums

3.3.1 Spectrophotometric Assessment of MAAs

Klebsormidium strains were scanned spectrophotometrically for 7 days. In this experiment, two groups were used: UV and control groups, and the UV group refers to being exposed to UV-B application on the 3rd, 4th, and 5th days. As a result of MAA screening, it was observed that MAA increased with UV-B application in all strains, and it was noted that other strains, except *K.crenulatum*, did not produce MAA under control conditions.

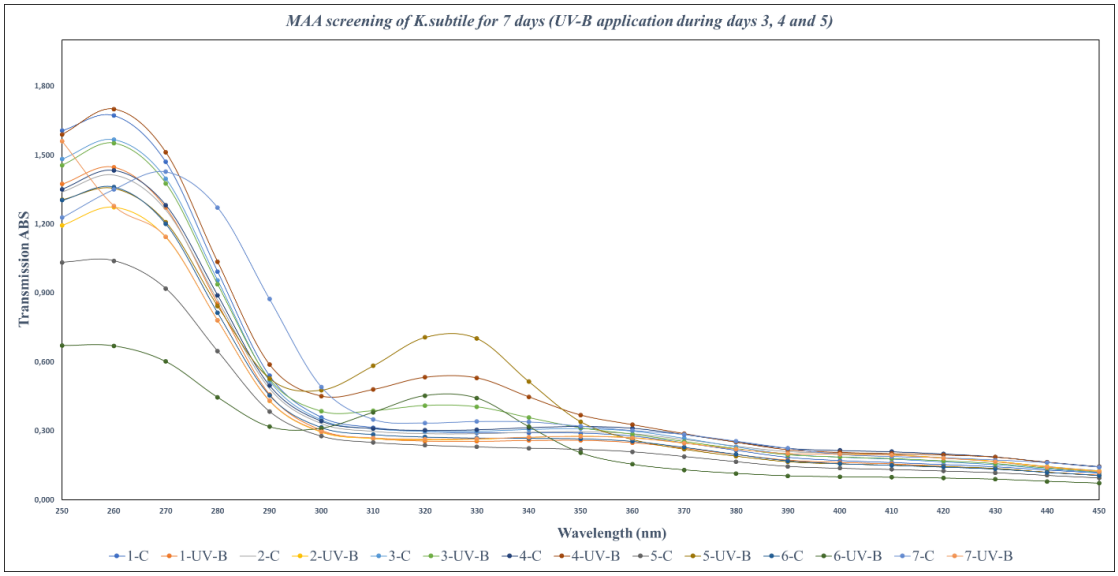

Figure 28: Spectrophotometric demonstration of *K.subtile* MAA accumulation obtained by exposure to f(UV-B) treatments for 7 days with the control group

As a result of the 7-day MAA screening conducted in *K.subtile*, it was observed that the highest MAA accumulation was on the 5th and 4th days, respectively. These days

are the 72nd and 48th hours of UV-B application, respectively. These results are correlated with the preliminary screening data, but after these days, the prominent value was on the day, followed by the 3rd day, that is, the 24th hour of UV-B application. After the UV-B application ended, *K.subtile* continued to produce a significant amount of MAA in its structure, and then, on the 7th day, MAA synthesis showed a decline similar to control conditions. No peak was observed between 320-330nm in the control groups compared to the UV groups. However, almost all groups exhibit high peaks between 260-270 nm, which is indicative of the gadusol molecule, which is the MAA precursor and has absorption at 268 nm.

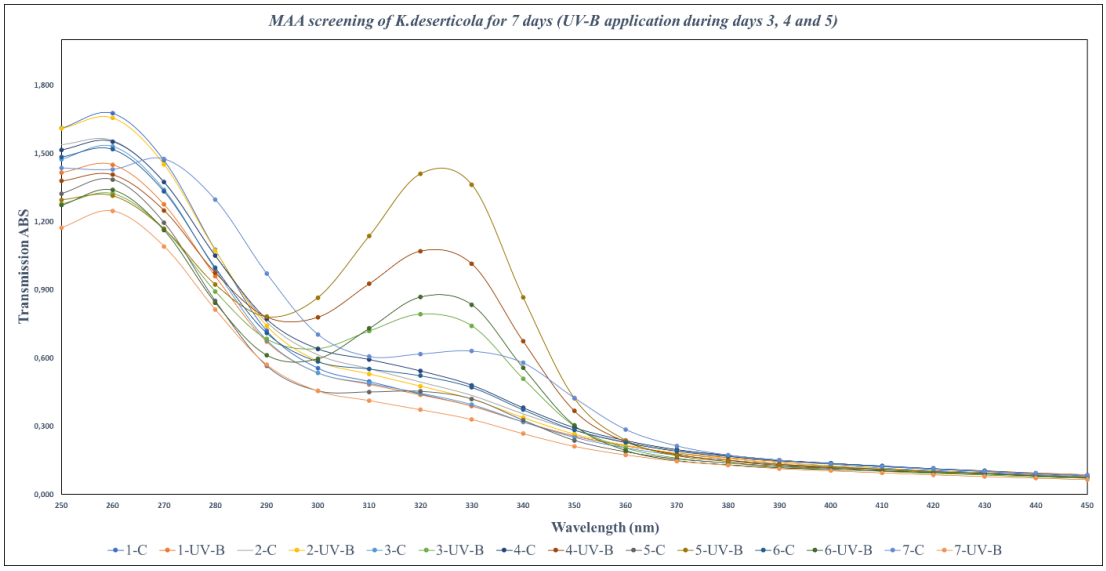

Figure 29: Spectrophotometric demonstration of *K.deserticola* MAA accumulation obtained by exposure to f(UV-B) treatments for 7 days with the control group

A similar spectral scan result was detected in *K.deserticola* against UV-B in terms of MAA as in *K.subtile*. The highest values are on the 5th and 4th days, respectively, when UV-B was applied, followed by the 6th day after UV-B application. Finally, after 24 hours of UV-B application, MAA production is observed at 320-330 nm, as in *K.subtile*. Gadusol synthesis was again seen in high amounts in the 260-270 nm range, but this time, unlike *K.subtile*, there was a low synthesis of precursor molecules compared to the MAA type produced. Additionally, no MAA peak was observed in control groups independent of UVR.

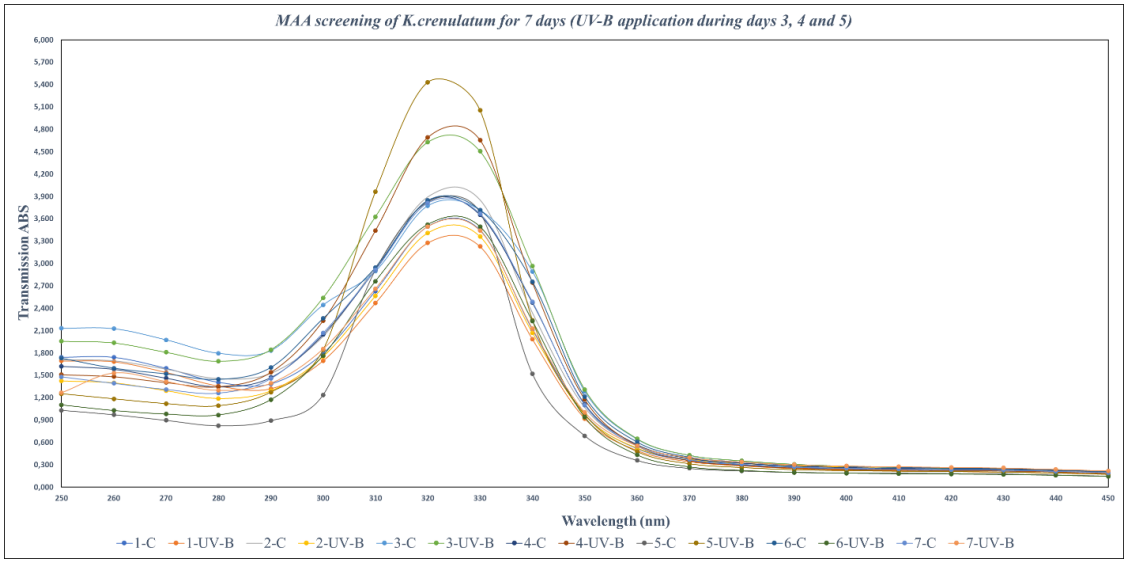

Figure 30: Spectrophotometric demonstration of *K.crenulatum* MAA accumulation obtained by exposure to f(UV-B) treatments for 7 days with the control group

The MAA screening result of *K.crenulatum* was the most promising result compared to other strains. It has been shown spectrally that all groups synthesize more MAA than other *Klebsormidium* strains. The highest MAA production was obtained after 72, 48, and 24 hours of UV-B application, respectively. Except for these 3 days, the other experimental groups had almost similar MAA production. The peaks taken are around 320nm, and the train between 260-270 nm, where precursor synthesis takes place, is very low compared to the peaks where MAA is located.

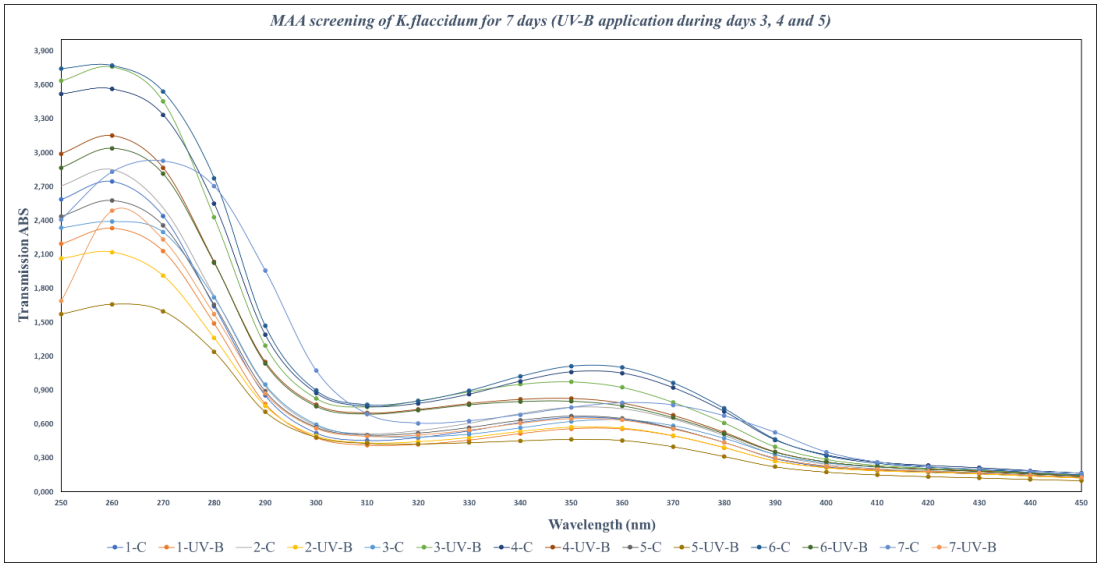

Figure 31: Spectrophotometric demonstration of *K.flaccidum* MAA accumulation obtained by exposure to f(UV-B) treatments for 7 days with the control group

Contrary to those obtained in the preliminary screening, very trace amounts of MAA production were observed in *K.flaccidum*, confirming the HPLC results. Potential gadusol peaks are significantly higher than other strains.

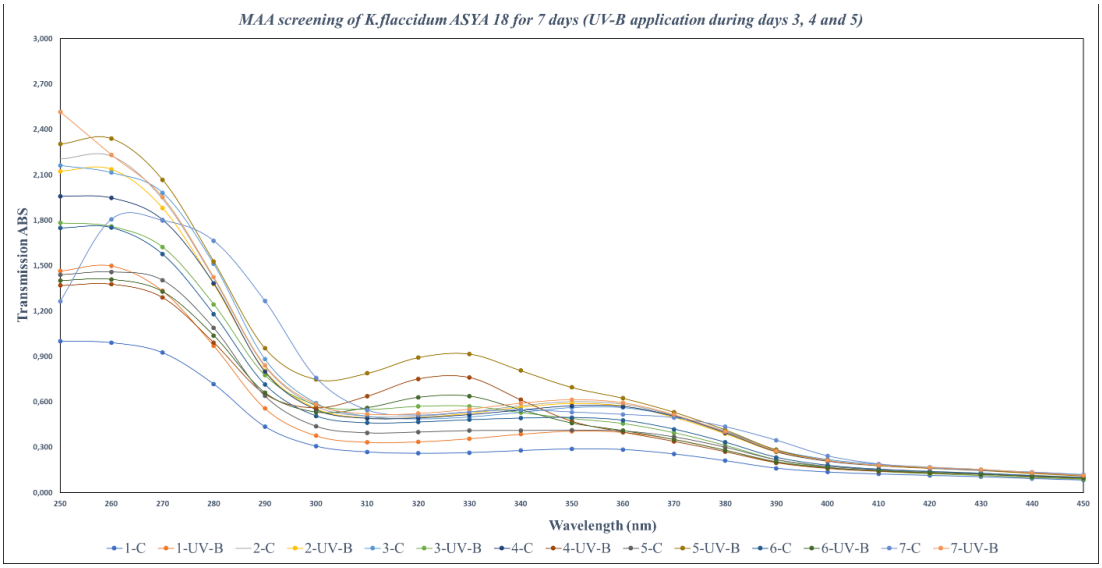

Figure 32: Spectrophotometric demonstration of *K.flaccidum* ASYA 18 MAA accumulation obtained by exposure to f(UV-B) treatments for 7 days with the control group

K.flaccidum ASYA 18 has a MAA production trend similar to *K.subtile* and *deserticola*. In the 320-330nm wavelength range, the 5th day, 4th day and 6th day of the main UV groups stand out in terms of MAA production. On the other hand, no MAA signal was detected in control groups like the mentioned strains. Additionally,

high amounts of precursor MAA were detected.

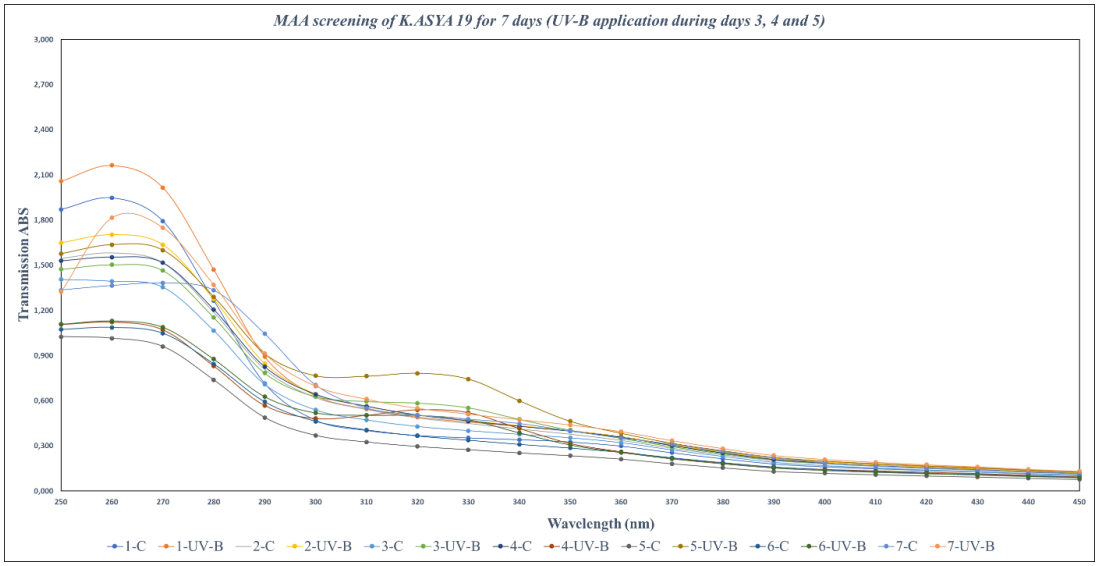

Figure 33: Spectrophotometric demonstration of *K.*ASYA 19 MAA accumulation obtained by exposure to f(UV-B) treatments for 7 days with control group

K. ASYA 19 showed a low MAA production compared to other *Klebsormidium* strains, just like *K.flaccidum*. Results correlated with preliminary MAA screening results. MAA production was observed as a result of 72, 48, and 24 hours of UV-B applications. MAA accumulation could not be detected in the control groups. In addition, it is clearly seen that the potential MAA production is at wavelengths of 320-330 nm. On the other hand, precursor MAA production between 260-270 nm wavelengths is much higher than main MAA production.

MAA screening of *Klebsormidium* strains was continued for 7 days, and MAA distribution during and after UV-B application (days 3, 4, and 5) was examined in detail. The data show that *K.crenulatum* was the species that accumulated the most MAA both under control conditions and during and after UV-B application. *K. subtile* and *K. deserticola* have a similar MAA pattern after UV-B application. *K. flaccidum, K. flaccidum* ASYA 18, and K. ASYA 19 had a much lower MAA production than the other strains. MAA production gradually decreased after UV-B application in all species and was almost not synthesized on Day 7, except for *K.crenulatum.* However, on day 6, MAA was still produced at significant levels in *Klebsormidium* strains, reflecting the major role of MAA during cellular recovery. At the same time, it is noted

that the effects of UV-B still continue and that MAA actively participates in these ongoing effects, considering the results.

3.3.2 Fluorescence Measurements

The fluorimetric growth of 6 different *Klebsormidium* strains was examined for 7 days with 2 different treatments: UV and Control group. The purpose of the experiment is to investigate the effect of UV exposure on the growth of different strains. In the first two days, both experimental groups were grown under control conditions.

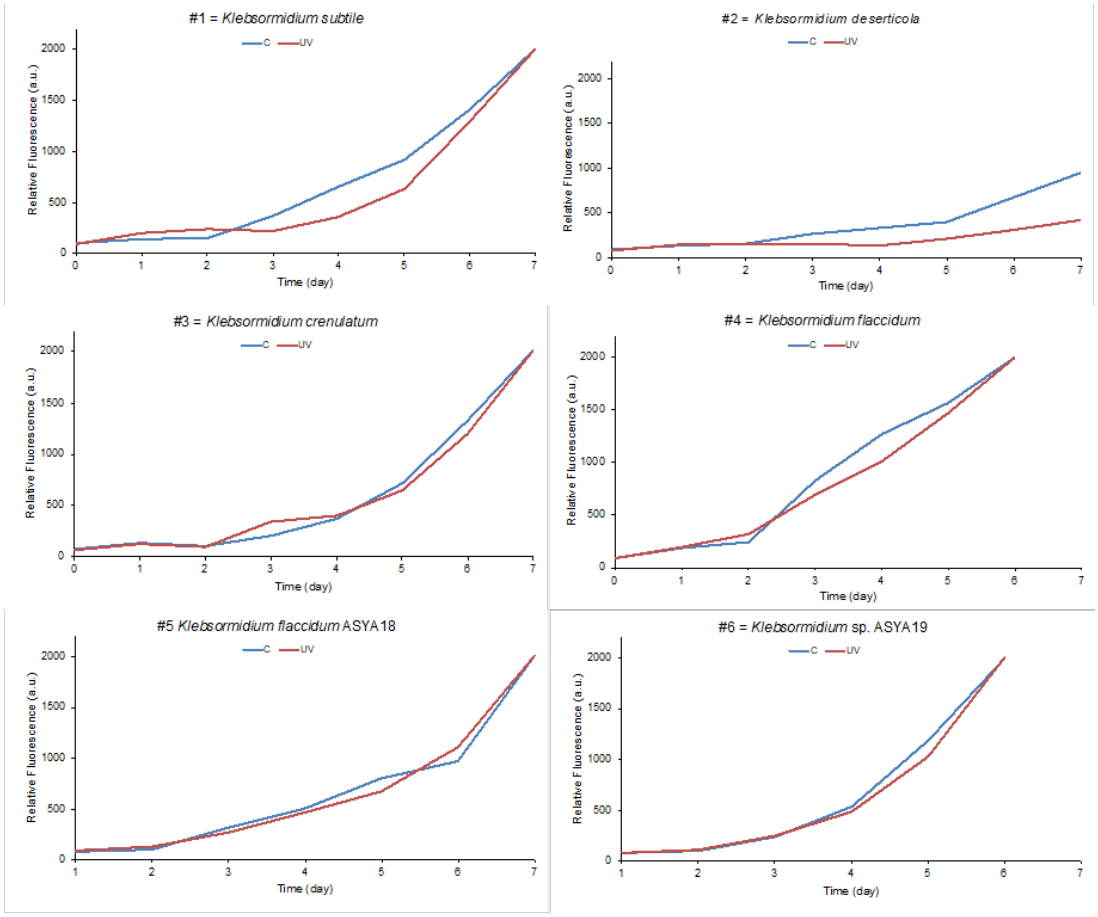

Figure 34: Fluorimetric growth chart of Klebsormidium strains under UV-B and Control conditions

In this context, based on the growth rates of K. ASYA 19, *K. flaccidum*, *K. flaccidum* ASYA 18, and *K. crenulatum*, respectively, they showed the same growth rate in the control group and the UVR group. However, *K. subtile* and *K.deserticola* strains were more affected by the harmful effects of UV-B based on growth compared to their control group. Day 3, that is, the start of UV-B application, was a factor that negatively

affected the growth of all *Klebsormidium* strains in the UVR experimental group. However, starting from the 48th hour (4th Experimental day), the growth rate of *K.subtile*, *K.crenulatum*, and *K.flaccidum* increased similarly with the control group. *K.flaccidum* ASYA 18 and *K.flaccidum* ASYA 19 are the strains least affected in terms of growth by 72-hour UV-B application compared to the control group. *K. deserticola* showed a sharp growth decrease after UV-B application, and it was observed that its cellular recovery after application took longer than other strains.

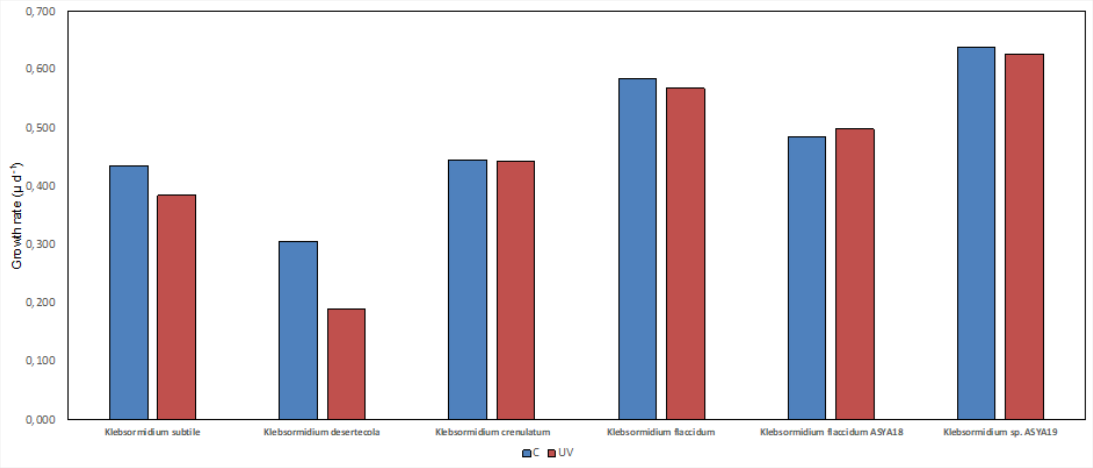

Figure 35: Growth rate of Klebsormidium strains under UV-B and Control conditions

When the growth rates of different strains exposed to UV and C environmental conditions during the experiment are examined, *Klebsormidium* sp. ASYA 19, *Klebsormidium flaccidum,* and *Klebsormidium flaccidum* ASYA 18 respectively stand out with 0,63, 0,57, and 0,50 growth rates in the UV group almost the same as the control group. These 3 Klebsormidium strains continued to grow positively even in UVR application, as in control conditions. The *K. deserticola* strain had the lowest growth rate with 0,19 for the UVR group and 0,30 for the control group. Additionally, its growth was almost halved against UV-B application. *K. subtile* strain is also sensitive to UV-B, and after 7 days of application, the growth rate, which was 0.44 in the control group, decreased to 0.38 in the UV group.

In this study, the effect of UV-B on the growth rates of *Klebsormidium* isolates taken from different regions was examined in detail. As a result of this examination, especially the growth rates of Antarctic and Arctic strains stand out compared to other strains, considering the control conditions. These strains did not respond negatively to

UV-B throughout the UVR application and their growth rates did not decrease. As mentioned in the studies conducted to date, there is a gap in the literature regarding the UV tolerance of green algae (Chiew-Yen et al., 2004). In a study, 1.1-5.2 W m^2 was applied to Antarctic *Klebsormidium* isolates, and complete inhibition was observed (Chiew-Yen et al., 2004). Although high-intensity UV-B has lethal effects on the cell, it should not be forgotten that the experimental parameters chosen are very important in fully explaining the cell's tolerance to UV-B. In addition, the parameter selected in the current study was 2W m^2 and no growth suppression was observed. Some polar *Klebsormidium* strains were virtually unaffected by high-energy UV-B, except for some partial decreases. Growth rate is a well-established and major parameter to examine the physiological performance of green algae under controlled and abiotic conditions (Gustavs et al., 2009). Growth rate summarizes all positive or negative processes in cell metabolism. Compared to the aero terrestrial green algae species such as *Chlorella* and *Chloroidium Stichococcus,* the growth rate of the Alpine isolate *K.fluitans* remained much lower than these species (0.6 μ) (Darienko et al., 2010), (Gustavs et al., 2010). However, *K. dissectum* ~0.5 μ and *K. crenulatum* ~0.3 μ from the Alps showed much higher growth than other *Klebsormidium* isolates (Karsten et al., 2010), (Karsten et al., 2012). When the results are examined, the Alpine isolate *K. crenulatum* has a growth rate of ~0.4, while Antarctic and arctic isolates have a growth rate of more than 0.4 even when exposed to UV-B. It was observed that only *K.deserticola* and *K.subtile* were seriously affected by UV-B and their growth decreased slightly compared to the control group. These species also have lower growth rates than *K. crenulatum* when comparing control groups.

3.3.3 PAM Measurements and Morphological Analysis

The bar charts present a study of the effective quantum yield (Y(II)) in various *Klebsormidium* strains under both control and UV-B stress conditions over seven days. Initially, all strains, including *Klebsormidium flaccidum*, *Klebsormidium flaccidum* ASYA 18 and Klebsormidium sp. ASYA 19, exhibits similar photosynthetic efficiencies, as indicated by their Y(II) values.

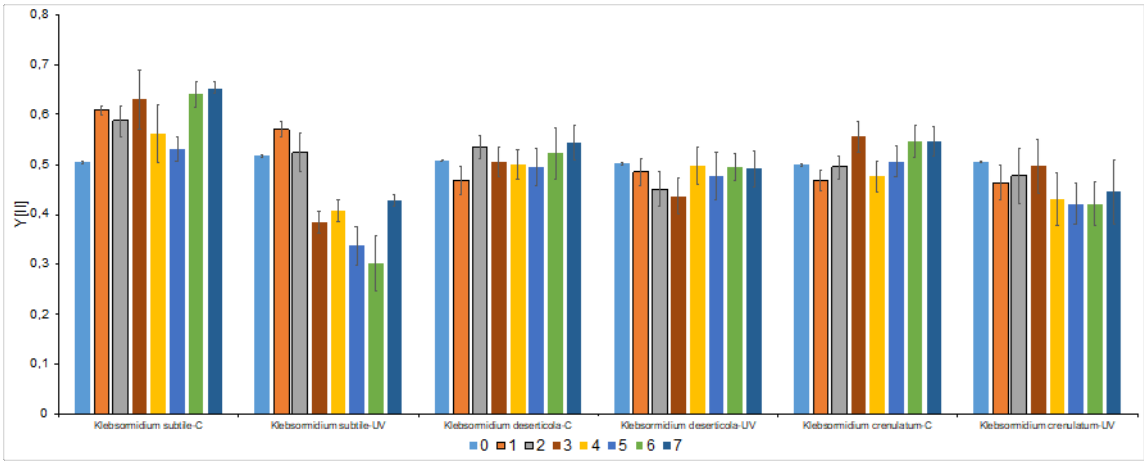

Figure 36: Illustration of the changing effective quantum yield rate [YII] between *K. subtile, K. deserticola*, and *K. crenulatum* strains during UV-B and control conditions.

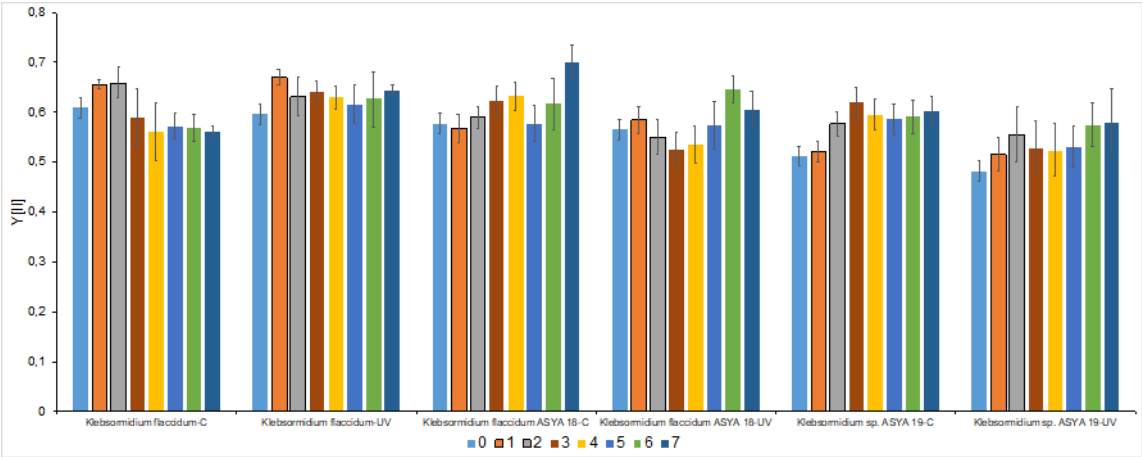

Figure 37: Illustration of the changing effective quantum yield rate [YII] between *K. flaccidum, K. flaccidum* ASYA 18, and K. ASYA 19 strains during UV-B and control conditions.

Upon 24 hours of UV-B exposure, a marked decrease in Y(II) is observed in several strains, particularly in the UVR group of *Klebsormidium deserticola* and *Klebsormidium crenulatum*, signifying a detrimental effect of UV-B radiation on the photosystem II (PSII). Interestingly, in the following 48 and 72 hours, which correspond to the 4th and 5th days of the experiment, there is a notable recovery in Y(II) values for strains such *as Klebsormidium flaccidum* ASYA 18-UV and *Klebsormidium* sp. ASYA 19-UV. This return suggests that certain Klebsormidium strains can activate repair mechanisms or undergo acclimatization processes to

mitigate the stress caused by UV-B radiation. As the experiment progresses to days 6 and 7, post-UV-B exposure, the Y(II) values across most strains stabilize or continue to improve. This trend is particularly evident in *Klebsormidium* sp. ASYA 19-UV, which shows a consistent recovery back to baseline levels, indicating resilience to UV-B stress or an effective adaptation strategy. In addition, it was generally seen that both the UV and control groups of *K. flaccidum, K. flaccidum* ASYA 18, and K. ASYA 19 strains had much more photosynthetic activity than other strains, and their photosynthetic activities decreased less in 72 hours of UV-B application than other strains.

PAM measurements typically provide information on the potential optimal quantum yield of PS II (F_v/F_m) to assess the physiological state of the microalgae under investigation (Hanelt, 1998). Photosynthesis has a fundamental role in the metabolism of plant cells. In many studies conducted to date, the photosynthetic mechanisms of UVR in micro and macroalgae have been examined (Karsten U.,2008). Therefore, the effect of UVR on the photosynthetic performance of *Klebsormidium* strains isolated from different geographical regions was investigated. In this research, it was seen that some *Klebsormidium* strains are more sensitive to UVR compared to control conditions, and some are resistant. The difference in this comparison is due to species-specific factors in the response to UVR, which is enhanced by the biochemical and physiological patterns provided by the habitat of the biogeography from which the species originated. A study conducted on *Prasiola crispa* isolated from the poles showed that the photosynthesis mechanism of this species works in a way that is resistant to UVR (Holzinger et al., 2006). This result is compatible with the polar species used in the current study, *Klebsormidium flaccidum, Klebsormidium flaccidum* ASYA 18, and *Klebsormidium* sp. ASYA 19. In a study conducted with *Hormidiella, Interfilum,* and *Klebsormidium* strains isolated from Germany, the effectiveness of UVR on photosynthesis was examined. The data clearly show that the optimal quantum yield of most *Interphyllum* and *Klebsormidium* strains, as well as Hormidiella, is unaffected or only slightly affected by UVR (Kitzing & Karsten (2015)). Many molecular events in microalgae are directly based on PS II or adjacent mechanisms. These include damage to the D1 protein located at the heart of PS II or the oxygen-evolving complex (Renger et al., 1986), the harvesting complex (Lorenz

et al., 1997), or the photo destruction of pigments (Strid et al., 1990). All of these phenomena can result in disruption of electron transfer to the PS II reaction center. hence, it blocks the energy flow between both photosystems (Bornman, J. F. (1989)). In addition, physiological effects that change with the effect of UVR can also cause morphological changes; a study shows dramatic changes in the chloroplast structure of UV-B in aquatic algae (Holzinger et al., 2004). In addition, this result is indicative of the morphological changes obtained as well as the change in photosynthetic performance with the effect of UVR. Finally, another study recently conducted on the *K.fluitans* isolate shows that UVR can only have minor effects on photosynthesis and respiration and that this species is resistant to UVR (Karsten et al.,2007).

Table 4: Visualization of morphological changes of different *Klebsormidium* strains before, during, and after UV-B application (100x).

Species	Pre-experiment (Day 1)	Post-UV-B Application (Day 5)	End of the experiment (Day7)
Klebsormidium subtile	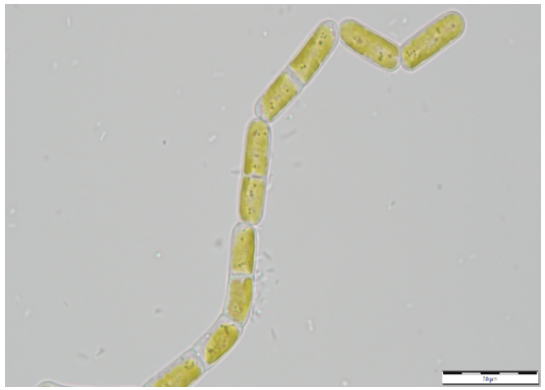	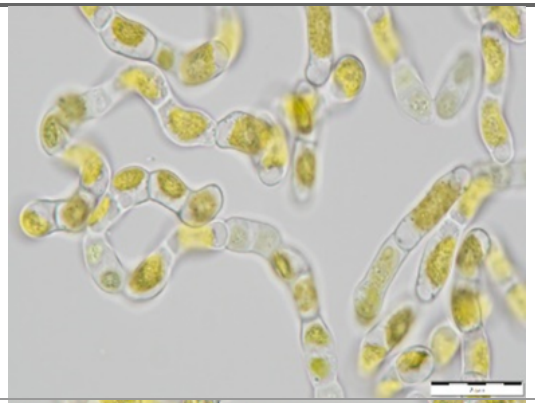	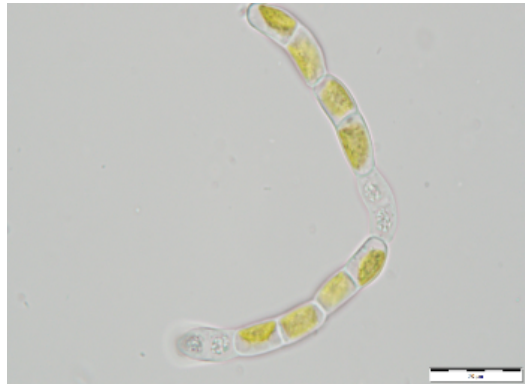
Klebsormidium deserticola		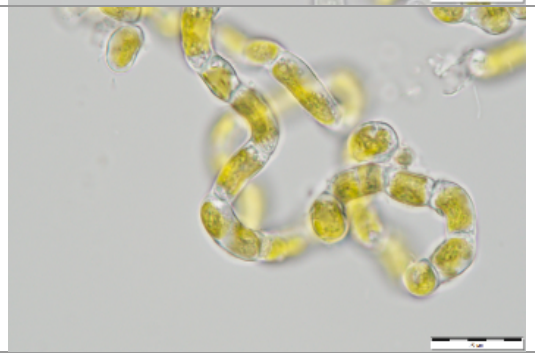	
Klebsormidium crenulatum	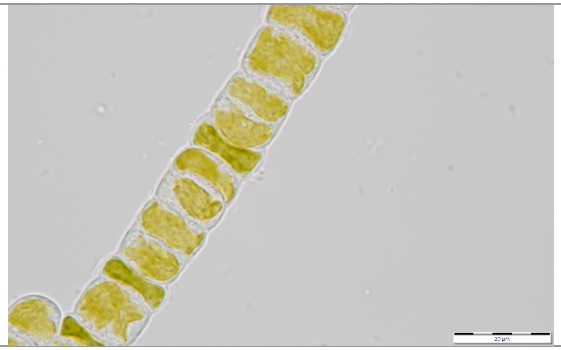		

Species	Pre-experiment (Day 1)	Post-UV-B Application (Day 5)	End of the experiment (Day7)
Klebsormidium flaccidum	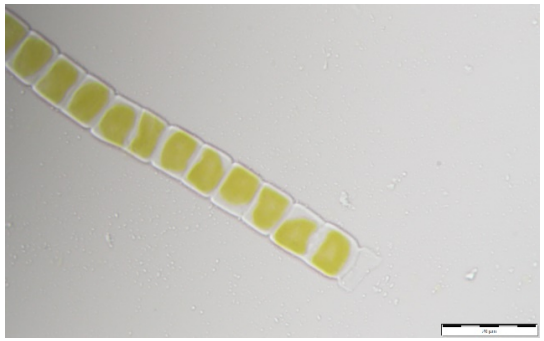	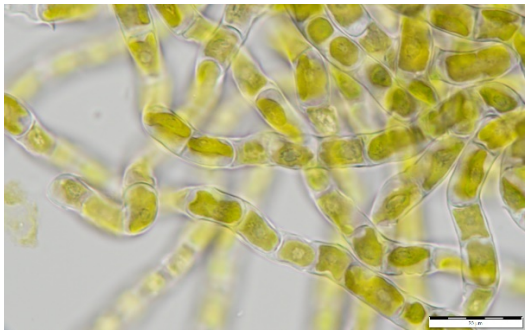	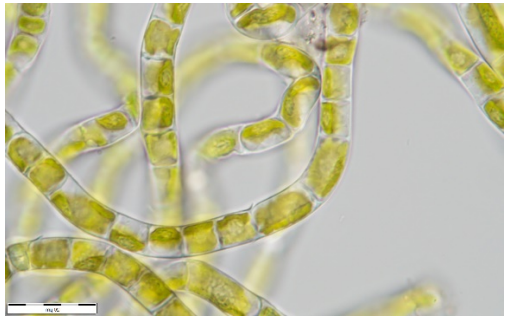
***Klebsormidium flaccidium* ASYA18**	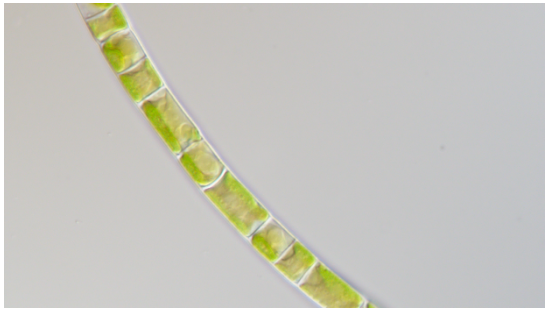	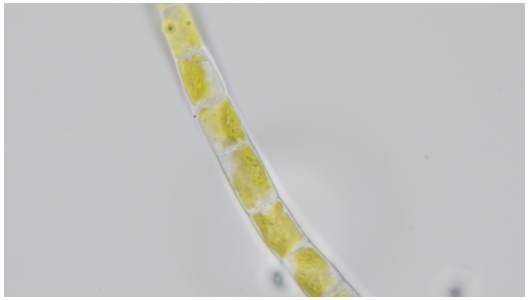	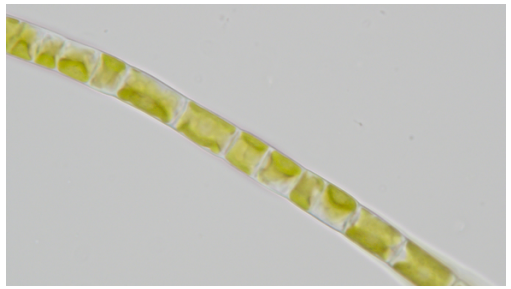
***Klebsormidium* sp. ASYA19**	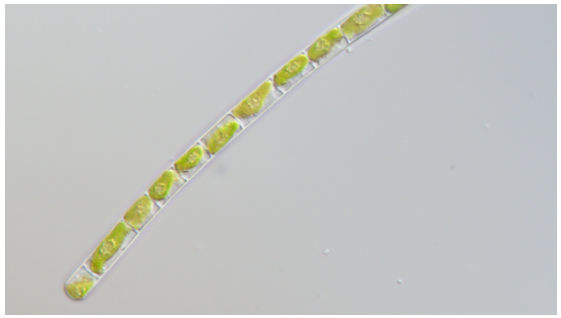	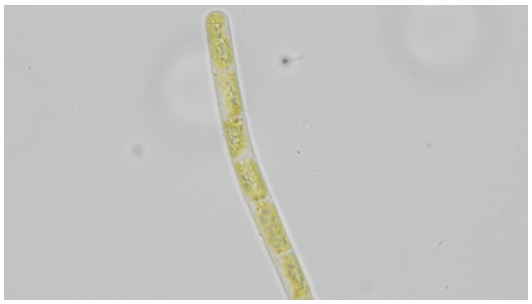	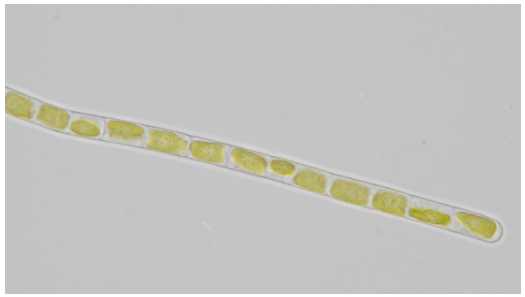

Morphology also plays a key role in the response to UV-B under the experimental conditions. In particular, the morphology of some *Klebsormidium* strains was affected in different ways after UV-B application. For example, the plastid ratio in the cells of the *K.subtile* strain is reduced and the cells are swollen. At the same time, its filaments have changed from a smooth linear structure to an indefinable state that has curled in on itself. In addition, 2 days after UV-B application, the morphology of the cells began to return to normal state, and the filament structure was observed to be close to its state at the beginning of the experiment. *K. deserticola* showed almost a similar morphological change as *K.subtile*. Differently, cellular deterioration is still much higher than *K.subtile* even on the 7th day of the experiment. In *K.crenulatum*, after UV-B application, cell fragmentation and pigmentation differences, unlike filament structure and cellular differentiation, are clearly visible. For the other 3 strains (*Klebsormidium flaccidum*, *Klebsormidium flaccidum* ASYA 18, and *Klebsormidium* sp. ASYA 19), apart from minor pigmentation differences, no deterioration or differentiation in the cell structure or filament structure was observed.

3.3.4 Purification of MAAs

Two types of standards were employed for HPLC detection of MAAs in Klebsormidium strains. The biological standards were used as biomass from different sources: A lichen (*Lichina pygmaea*), a macroalga (*Mastocarpus stellatus*) and (*Prasiola* sp.), fish (*Plectropomus leopardus*), and a Haddock were used as MAA standard shown in table x.

Table 5: a) Detailed representation of biological standards used for MAA and retention time, area peak WL values obtained by HPLC. b) Detailed representation of concentration, retention time, and area peak WL values obtained by HPLC of industrial standards

Standards	Name	MAA	RT [min]	Area	peak WL [nm]
Lichina pygmaea	F3 1:10	Mycosporin-Glycine	2,033	850,5	309,5
Mastocarpus stellatus	MS6 1:10	Shinorin	1,526	1241,5	332
Prasiola	Pra	Prasiolin	1,872	1125,1	323,5
Plectropomus leopardus	PL	Astertina-330	1,666	4473	330
Haddock	SF1	Palythin	1,519	87,1	319

Industrial standards are limited for MAA compounds. Only three standards could be obtained from the laboratory of Prof. Karsten (University of Rostock) The industrial standards and their HPLC-related determination parameters are shown below (Table 3.2).

MAA	conc. [mM]	RT [min]	Area	peak WL [nm]
Palythin	0,005	1,518	130,2	319,5
	0,05	1,518	1294,4	319
	0,1	1,517	2564,8	319
Shinorin	0,005	1,527	241,7	332,5
	0,05	1,525	2455,7	332
	0,1	1,524	4669,6	332
Porphyra-334	0,005	2,033	161,9	333
	0,05	2,029	1635,3	332
	0,5	1,997	12773	323

The purification assessment was validated comparatively using biological and industrial standards before taking test samples. Standards previously obtained from different organisms such as *Prasiola* sp. *Mastocarpus stellatus* were weighed up to 10mg and MAAs were obtained using the extraction method explained in the method section. Additionally, industrial standards of major MAAs such as Palythin, Shinorin, and Porphyra-334 were used as a secondary correction factor to strengthen the data reliability and facilitate the determination of possible MAAs.

Table 6: Retention time and absorption maxima values obtained by HPLC of the MAAs accumulated in the test samples after the 72nd hour of UV-B exposure.

Species	max. RT [min]	max. RT [s]	peak WL [nm]
K.flaccidum ASYA 18	1,901	114,1	323,5
K. subtile	1,915	114,9	323,5
K. ASYA 19	1,922	115,3	323,5
K. deserticola	1,939	116,3	323,5
K. flaccidum	1,943	116,6	323,5
K. crenulatum	1,937	116,2	318

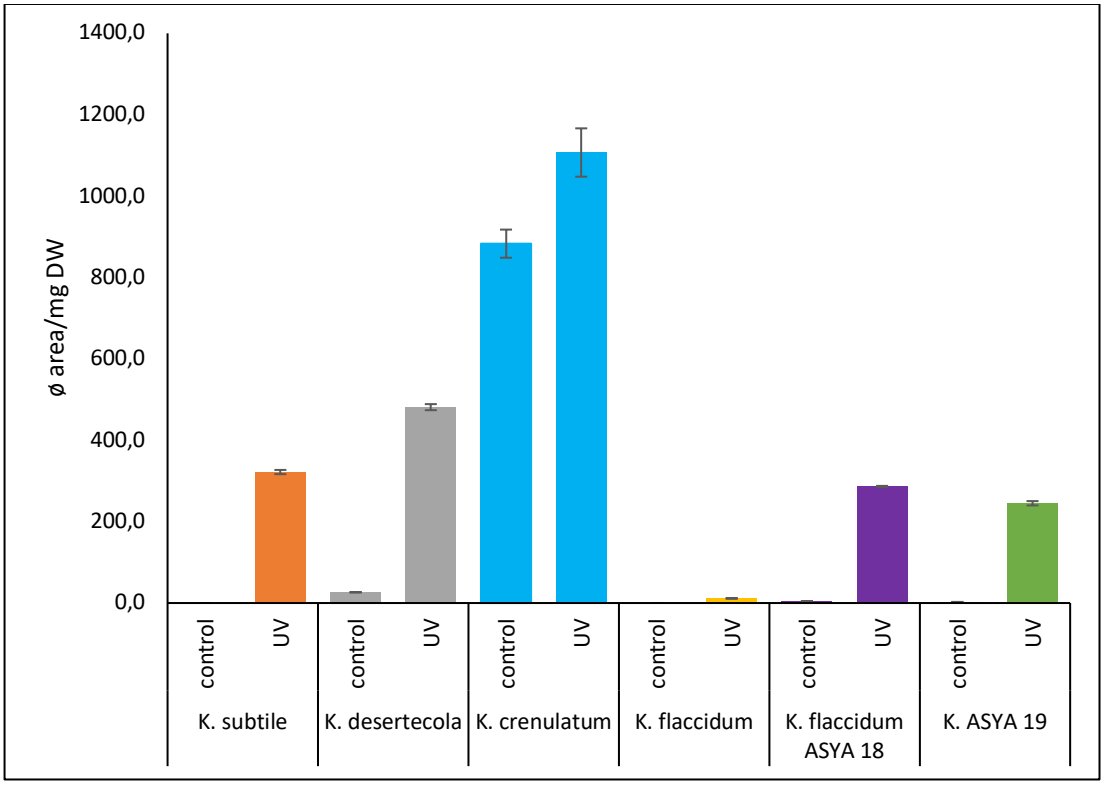

Figure 38: MAA distribution of *Klebsormidium* strains after 72 hours of UV-B treatment and control groups after HPLC purification

As can be seen in Fig.38., at the 72nd hour of UV-B application, all *Klebsormidium* strains accumulated more MAA compared to the control group. Specifically, *K.crenulatum* stands out against other strains with the highest MAA concentration it accumulates after this application. Interestingly, MAAs were found in this strain even in the control group, and its MAA rate was found to be higher than the MAA accumulation of other strains after UVR application. In addition, as expected for other *Klebsormidium* strains, either 0 or a trace amount of MAA concentration was found in

the control groups. After *K.crenulatum, K.deserticola, K.subtile, K. flaccidum* ASYA 18 and K. ASYA 19 come respectively. *K. flaccidum* accumulated almost no MAA after UV-B application compared to other groups.

As detailed in Table 6 The results obtained from the other 5 strains, except *K.crenulatum*, show that Prasiolin type MAA is predominantly produced in these species. Elutes obtained from *K.crenulatum* could not be detected due to the difference in both RT and WL values. This is an indication that there may be a new type of MAA or a type of MAA that has already been detected in the literature but cannot be determined by our biological standards.

As a result of the previous preliminary screening, UV-B was determined as the appropriate condition to increase MAA production in *Klebsormidium* strains. In addition, as a result of this preliminary screening and spectral scanning showing the 7-day change of MAA production, 72-hour UV-B application was determined as the main parameter for HPLC for all species. The results show that mostly *Klebsormidium* strains have maximum MAA production as a result of 72-hour UV-B application. Therefore, MAA derivatization was determined by HPLC at the point where MAA production was maximum. Studies have shown that only a very few microalgae species in the chlorophytic lineage of green algae produce MAAs, and the structure of these synthesized MAAs is not complex and they are derived from gadusol, a precursor molecule for MAA production (Hartmann et al., 2016). On the other hand, phenolic compounds rather than MAAs are found in the streptophyte lineage, including *Klebsormidium*. Since *Klebsormidium* is one of the most pioneering representatives of this group in the evolutionary process, it carries more primitive features in its structure than other group members. The *Zygnematophyceae* family, which is a descendant of streptophytes, is one of the most well-known and has been proven by scientists to accumulate phenolic compounds in their structures as defense molecules against UV radiation (Remias et al., 2012). In a study, scientists worked with *K.crenulatum*, which was also used in this study and gave promising results and discovered 2 new MAA types, klebsormidin A and klebsormidin B, that can be purified at different retention times (Hartmann et al., 2020). Additionally, the absorption spectra of these discovered MAA species are at 322nm. To induce MAA, they used UV-A and UV-B in combination and supported it with PAR. When the parameters used were examined, it

was seen that the intensity of UV-B was only 0.45 Wm^2. In the current study, the UV-B intensity value used was 2 Wm^2 and UV-A was used only as a stress factor to increase MAA in preliminary scans. The reason why *K.crenulatum* has a different MAA than the previously discovered MAAs due to increasing UV-B intensity may be due to the fact that MAAs change their diversity according to environmental conditions.

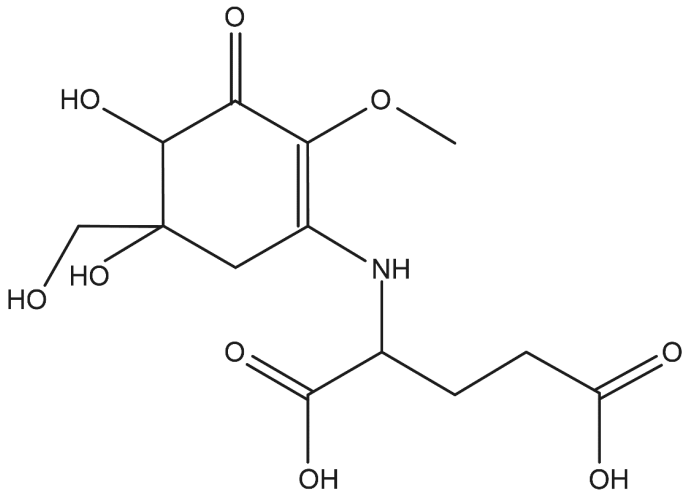

Figure 39: Structural representation of Prasiolin, which has an absorption maximum at a wavelength of 324nm and an extinction coefficient of 12.393 M^{-1} cm^{-1}

Except for *K.crenulatum*, clear peaks were obtained at 323.5nm with the UVR effect in other *Klebsormidium* strains. This result shows that these strains are the source of Prasiolin. Prasiolin has a low extinction coefficient value, which provides its photoprotective feature by increasing photostability (Conde et al., 2000). At the same time, the reason why the MAA capacity in *K.subtile, K.deserticola, K.flaccidum*, and 2 other Antarctic *Klebsormidium* variants is lower than in *K. crenulatum* may be hidden in the morphology of the *Klebsormidium* species. Because these species have self-shading abilities to avoid excessive UV radiation by aggregates, thanks to their matte, biofilm-forming ability (Karsten, U., & Holzinger, A. (2014)). Thus, they can cope with their physical adaptation features against UV and intense light stress without the need for MAA production.

3.4. Bioplastic Production with UV-Blocking Capacity

3.4.1 Preparation and Optimization of Bioactive Film

Table 7: Optimization of casted microalgae-derived films under different conditions and different microalgae origins

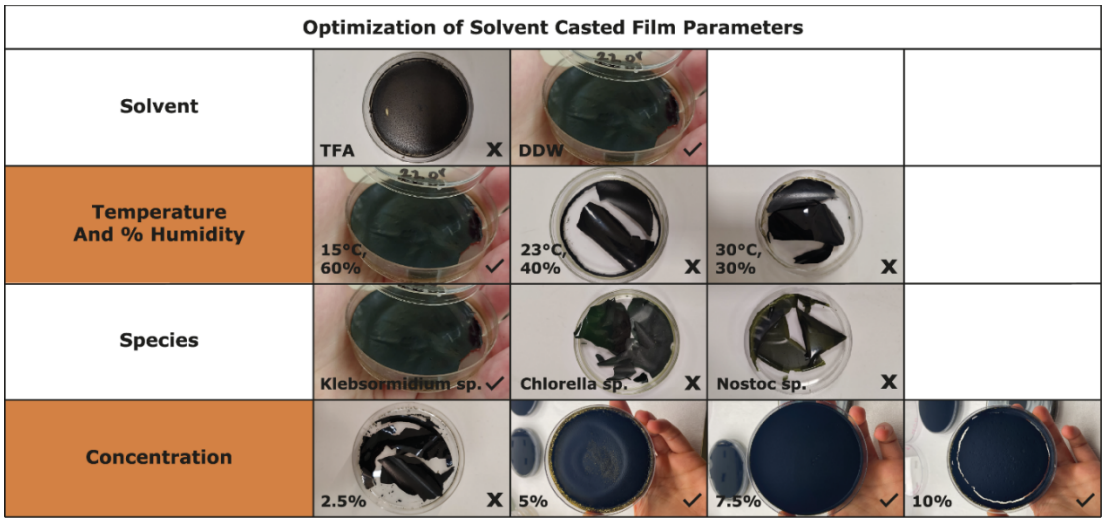

At the beginning of the study, different solvents and different microalgae sources were used. Trifluoroacetic acid (TFA) is widely used in the solvent casting method to increase the polymerization and bond number of the components in the mixture. However, it was observed that mixtures made with TFA could not be converted into films and prevented polymerization due to its harmful effect on microalgae solutions. In water-based films, Nostoc, Chlorella, and *Klebsormidium* species have been tried as biomass sources for the film. In this preliminary study, different drying temperatures (15°C, 23°C and 30°C) and different humidity conditions (30, 40, 60%) were tested and 15°C temperature and 60% humidity environment were determined as the optimum condition for film polymerization. In addition, under these conditions, the fact that the films made with *Klebsormidium* biomass stand out compared to other films in terms of structural and film-forming capacity made them the biomass source chosen for the study.

Finally, the optimum concentration to be used in bioplastic film was determined between 5%, 7.5%, and 10%. In these 3 concentrations, Crude *Klebsormidium* Biomass formed a water-based film. Therefore, the appropriate concentration was

determined by mechanical testing. In this determination, stress and strain values were the factors that enabled selection. Accordingly, 5% *Klebsormidium* biomass stood out significantly from other concentrations according to both stress and strain values. At the same time, the fact that it contains less biomass than other concentrations also contributed to the applicability of the study.

Figure 40: Image of all film groups made directly from Klebsormidium and prepared with PVA and Glycerol additives.

3.4.2 Mechanical Properties of the Film

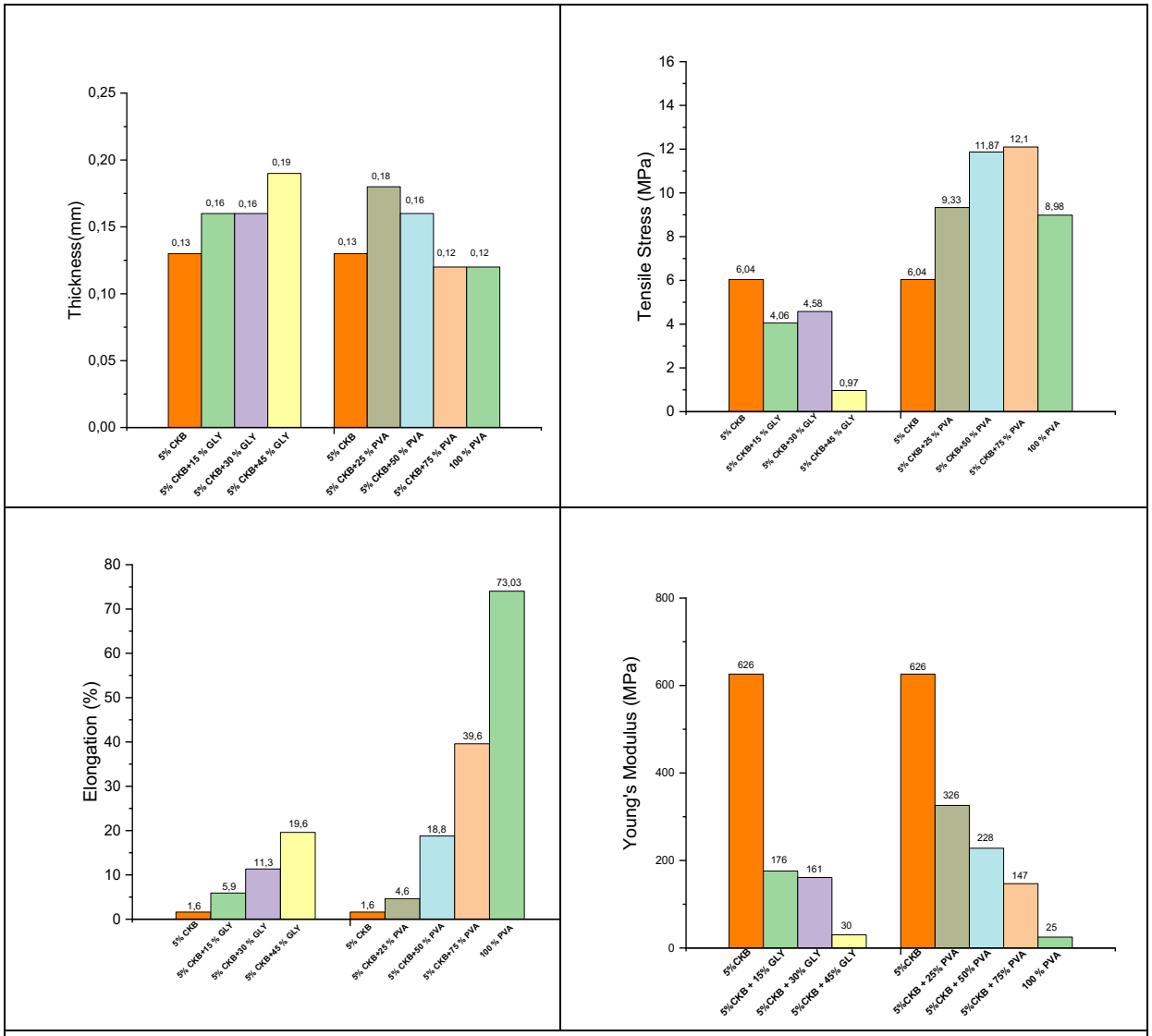

Figure 41: Mechanical properties of CKB, CKB+GLY and CKB+PVA film

The film thickness was determined with a digital micrometer, with measurements taken at a minimum of five random points on each film. The average of these measurements provided the final thickness value for each sample. 5% CKB has a thickness of 0.13 mm, whereas the films with 15% and 30% glycerol added have the same thickness, that is, 0.16 mm. The thickness of the *Klebsormidium* film to which 45% glycerol was added was determined as 0.19, which is the thickest of all groups. The thicknesses of the 5%CKB+25% PVA, 5%CKB+50%PVA, and 5%CKB+75%PVA groups were found to be 0.18, 0.16, and 0.12, respectively. The result shows that as the distribution of the PVA ratio in the film increases, the thickness

decreases, while as the Glycerol ratio added to the film increases, the film thickness increases at the same ratio. These thickness values were found to be nearly 3.5 times lower than the thickness of the film obtained using 4% starch (Lopes et al., 2021).

Tensile strength and elongation at break are critical parameters that measure a material's resistance to forces that can cause it to stretch and ultimately break. These properties are particularly important for the practical performance of bioplastics, where flexibility and durability are key. An evaluation of Glycerol and PVA's contribution to the flexibility and robustness of the Crude *Klebsormidium* Biomass (CKB) matrix was conducted. The mechanical integrity of bioplastics is pivotal for their practical application. Consequently, the incorporation of Glycerol and Polyvinyl Alcohol (PVA) into the Crude *Klebsormidium* Biomass (CKB) matrix to enhance its flexibility and sturdiness was scrutinized. As displayed in Figure 3.23, pure CKB films demonstrated a tensile strength of 6.04 MPa. A recent study reported that increasing algae concentrations increased tensile stress. Increasing the red algae (Gelidium corneum) concentration in rice bran protein-based films (5.0%) up to 3.0% increased the tensile strength and caused the films to reduce the elongation at break (Shin et al., 2011). Films augmented with glycerol at 15%, 30%, and 45% displayed varying tensile strengths of 4.06 MPa, 4.58 MPa, and 0.97 MPa, respectively, altering their mechanical properties (Dick et al., 2015; Paolicelli et al., 2018; Yu et al., 2008; Gozan & Noviasari 2018). In contrast, films doped with PVA at 25%, 50%, 75%, and pure PVA, showed enhanced tensile strengths of 9.33 MPa, 11.87 MPa, 12.1 MPa, and 8.98 MPa, respectively, indicating the reinforcing effect of PVA (Khalis 2018; Dianursanti et al., 2019; Sabathini et al., 2018; Edhirej et al., 2017). Analysis of tensile stress revealed that the addition of Glycerol and PVA led to the highest elongation in 5%CKB- 45%GLY and 5%CKB- 75% PVA films. Specifically, the 75% PVA composition exhibited the strongest tensile stress, while the 45% Glycerol variant showed a lower tensile stress strength of 0.97MPa. The introduction of 30% glycerol decreased tensile strength to 6.04 MPa and 4.4 MPa but increased the material's elongation property significantly from 1.6 to 11.3, suggesting 30% as the optimal glycerol content for mechanical performance (Onen et al. 2020; Edhirej et al., 2017; Park & Lee, 2022). A previous study confirms these results, showing that the rate of elongation at break increases as the algae content decreases (Jo, W. S et al., 2014).

This comparative analysis demonstrates that CKB can be effectively mixed with PVA and glycerol to engineer bioplastics with adjustable mechanical properties. Furthermore, Young's modulus, which gauges the rigidity of the films, showed that pure CKB films possessed the highest modulus, indicating a greater resistance to deformation, followed by films with 25% and 50% PVA, respectively. It is also clearly seen that the elasticity modulus gradually decreased with the increasing concentration of additives such as PVA and glycerol added to 5% CKB. Studies have shown so far that the side effect of increasing concentrations of plasticizers such as glycerol is reflected in the decrease of the elasticity modulus (Sanyang et al., 2016), (Tapia-Blácido et al., 2013)

Chemical Characterization (FT-IR)

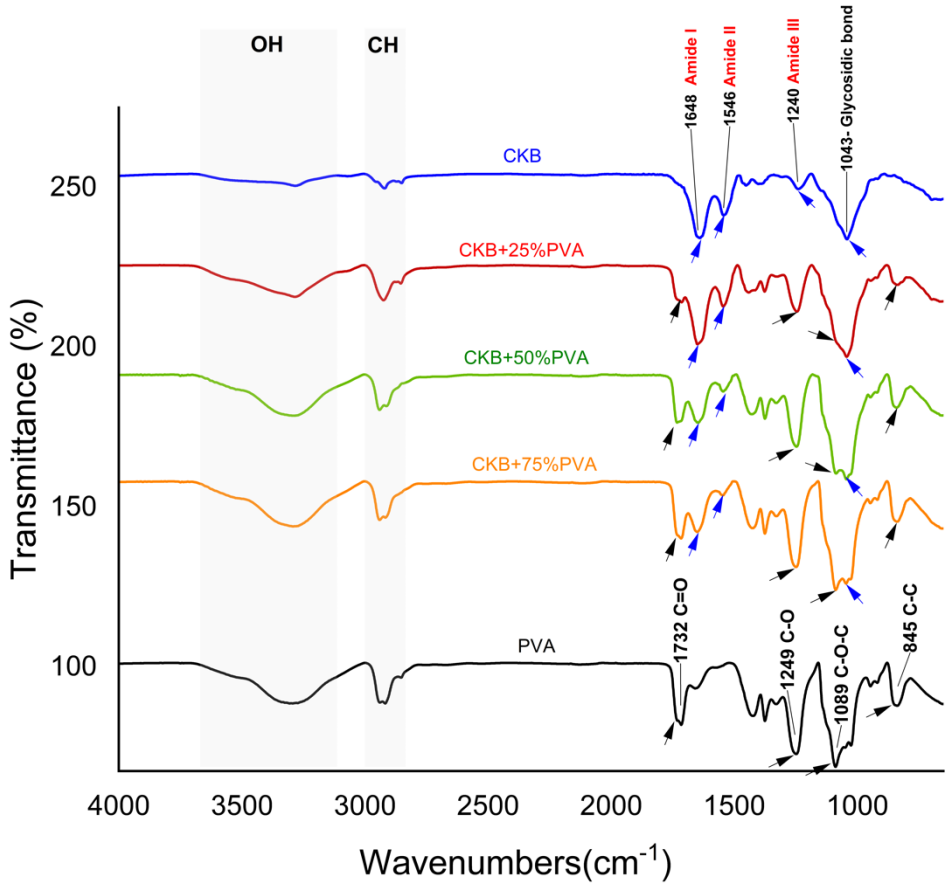

Figure 42: Functional group analysis of CKB and CKB+PVA film with FTIR

The Fourier-transform infrared spectroscopy (FTIR) analysis of pure polyvinyl alcohol (PVA) films revealed characteristic absorption peaks. The prominent peak at 3293 cm-

^{1} corresponds to hydroxyl (OH) group stretching, while peaks at 2940 cm^{-1} and 1715 cm^{-1} are indicative of CH stretching and carbonyl (C=O) stretching, respectively. Peaks at 1374 cm^{-1} represent CH2 bending, and the peak at 1087 cm^{-1} is associated with CO stretching vibrations (Wang et al., 2020; Mansur et al., 2008).

In the FTIR spectrum of Crude *Klebsormidium* Biomass (CKB), distinct absorption peaks were noted at 1648 cm^{-1} and 1562 cm^{-1}, corresponding to amide I and amide II bands, with another peak at 1041 cm^{-1} linked to glycosidic bonds (Kondo et al., 2016; Movasaghi et al., 2008; Miglio et al., 2013; Liu et al., 2020; Murdock & Wetzel, 2009).

A broad absorption band spanning from 3675 cm^{-1} to 3009 cm^{-1} was observed, attributable to the O–H groups in PVA. These bands are primarily due to the vibrations of hydrogen bonding within and between PVA chains, and with CKB (Cai et al., 2019; Chandrakala et al., 2014; Jayaramudu et al., 2018). For PVA/CKB bioplastics, the absorption bands of Amide I, Amide II, and carbohydrate (glycosidic bonds) from CKB, along with characteristic PVA bands at 1715 cm^{-1} (C=O) and 1084 cm^{-1} (O-C-O), confirmed the successful integration of PVA into the CKB matrix (Abureesh et al., 2016; Pistoriu et al., 2008; Mansur et al.).

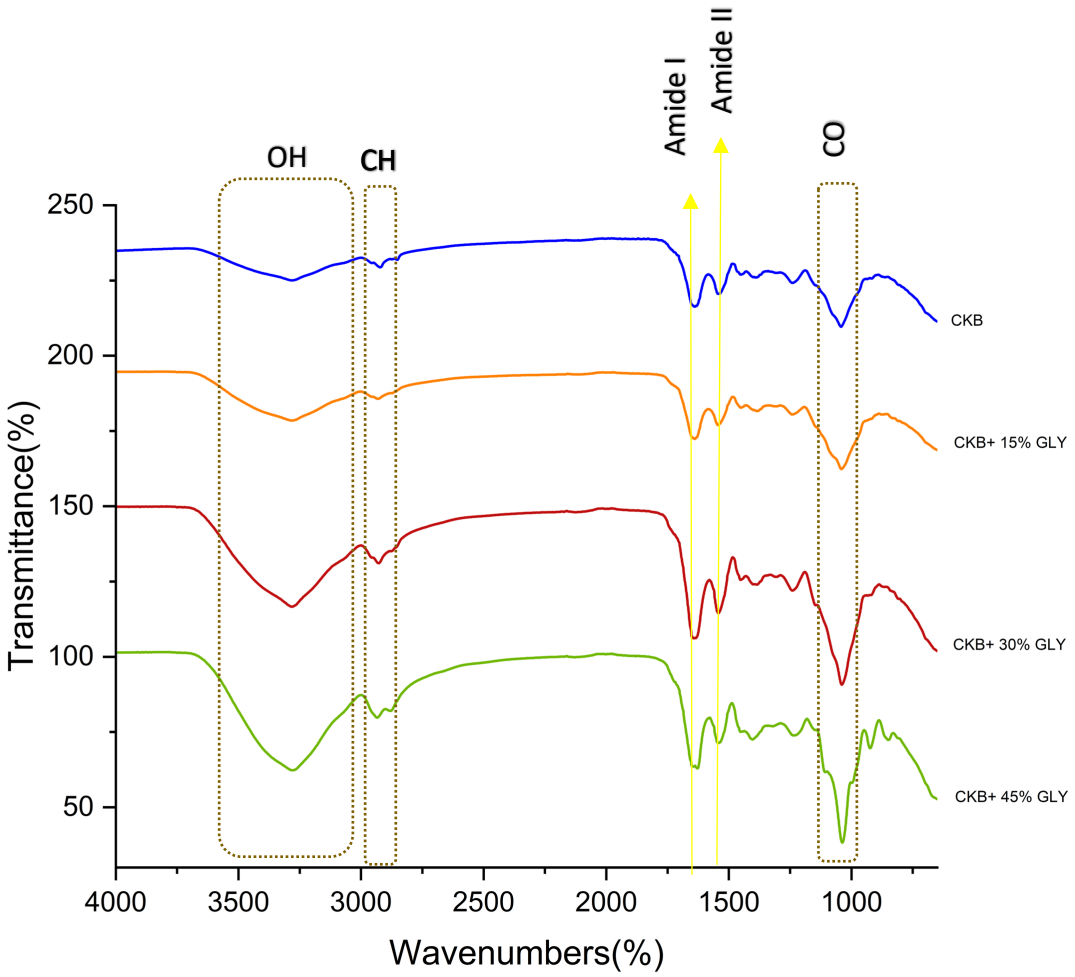

Figure 43: Functional group analysis of CKB and CKB+GLY film with FTIR

Glycerol, or propane-1,2,3-triol, features a chemical structure with two primary alcohol groups and one secondary alcohol group, reflected in the FTIR peak at 1040 cm^{-1} for primary alcohols and at 1110 cm^{-1} for the C-O stretching vibrations typical of secondary alcohols. Peaks within the 2800-3000 cm^{-1} range arise from the C-H bonds of methyl and methylene groups in glycerol (Barbosa, 2007; Teixeira et al., 2021).

In all samples, a broad absorption between 3500-2930 cm^{-1} was indicative of hydrogen bonding via the O-H groups. As glycerol concentration increased, both the intensity and breadth of the absorption bands were enhanced, suggesting the formation of additional hydrogen bonds between glycerol and CKB molecules (Yekta et al., 2020; Cao et al., 2018; Dick et al., 2015; Liang & Wang).

3.4.4 DSC (Differential Scanning Calorimetry)

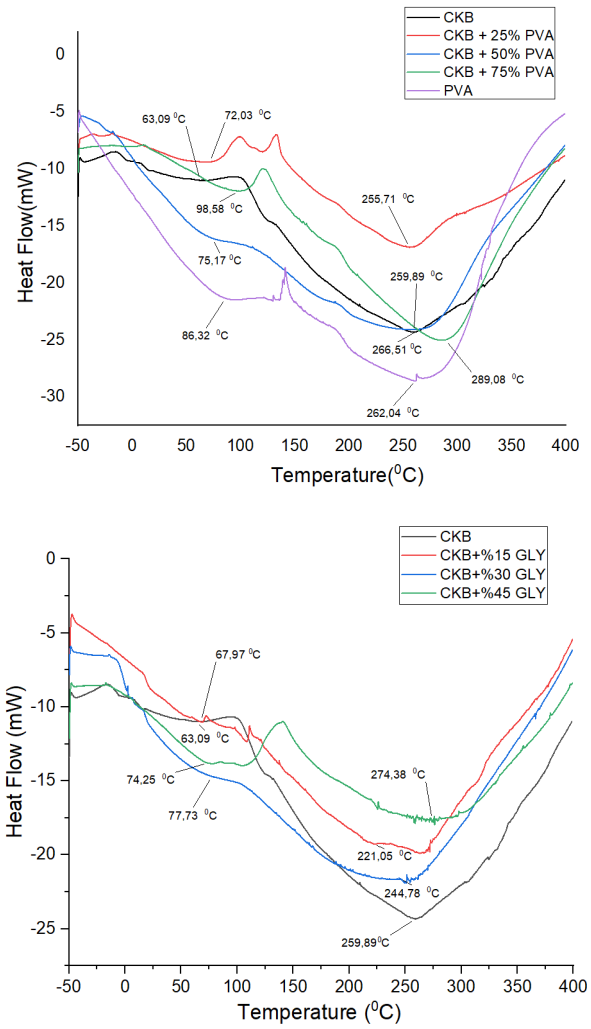

Figure 44: DSC analysis of films with plasticizers type at different concentrations

Differential Scanning Calorimetry (DSC) charts show the thermal behavior of *Klebsormidium* microalgae-based bioplastics containing different concentrations of glycerol (GLY) and polyvinyl alcohol (PVA), formed with only *Klebsormidium* biomass (CKB). In the first graph, the curves represent the thermal transitions of CKB and CKB+PVA doped films. Pure *Klebsormidium* shows a certain thermal profile with a certain heat flow trend as the temperature increases, with a thermal decomposition point of 259.89°C. PVA concentrations show a change in thermal profile compared to the pure sample. The addition of PVA positively affects the thermal stability and

overall structure of bioplastics. As PVA concentration increases, the heat flow endotherm changes, indicating changes in the melting and decomposition temperatures of the films. This may be due to increased intermolecular interactions between microalgae and PVA molecules, potentially increasing the stiffness and thermal resistance of the films. This can be explained by the fact that the thermal decomposition of the 5%CKB+75%PVA group reaches up to 289.08°C. In the second graph, the thermal behaviors of the CKB and CKB+GLY groups are depicted comparatively. With the addition of 15% glycerol, the thermal behavior changes, indicating that glycerol changes the thermal stability and interaction within the bioplastic matrix (221.05°C). At 45% glycerol, there is a significant deviation in the curve; This suggests a significant effect on thermal properties potentially due to glycerol acting as a plasticizer, which can reduce the interaction between bioplastic chains and lower the glass transition temperature (tg=74.25°C).

Table 8: Glass transition (Tg) and melting (Tm) temperatures of films.

Samples	**Tg (°C)**	**Tm (°C)**
CKB	63,09	259,89
CKB + 15% GLY	67,97	221,05
CKB + 30% GLY	77,73	244,78
CKB + 45% GLY	74,25	274,38
CKB + 25% PVA	72,03	255,71
CKB + 50% PVA	75,17	266,51
CKB + 75% PVA	98,58	289,08
PVA	86,32	262,04

Tg is one of the most important thermal properties of polymers, defining the temperature at which polymer chains begin to move. Below Tg, polymer chains are rigid and have much less mobility. Tg is affected by the molecular structure, molar mass, crystallinity, and thermal history of the polymers (Ahmad Z. et al., 2023). Table 3.5 shows that the glass transition temperature of pure CKB films without additives was found to be 63.09°C. Tg temperature gradually increased up to 45% in the Glycerol additive group and then decreased to 74.25°C. In the PVA groups, Tg was determined as 72.03°C, 75.17°C, and 98.58°C at 25%, 50% and 75%, respectively.

The results show that the glass transition temperature of the microalgae-based film increased in correlation with the added PVA concentration.

3.4.5 TGA (Thermogravimetric Analysis)

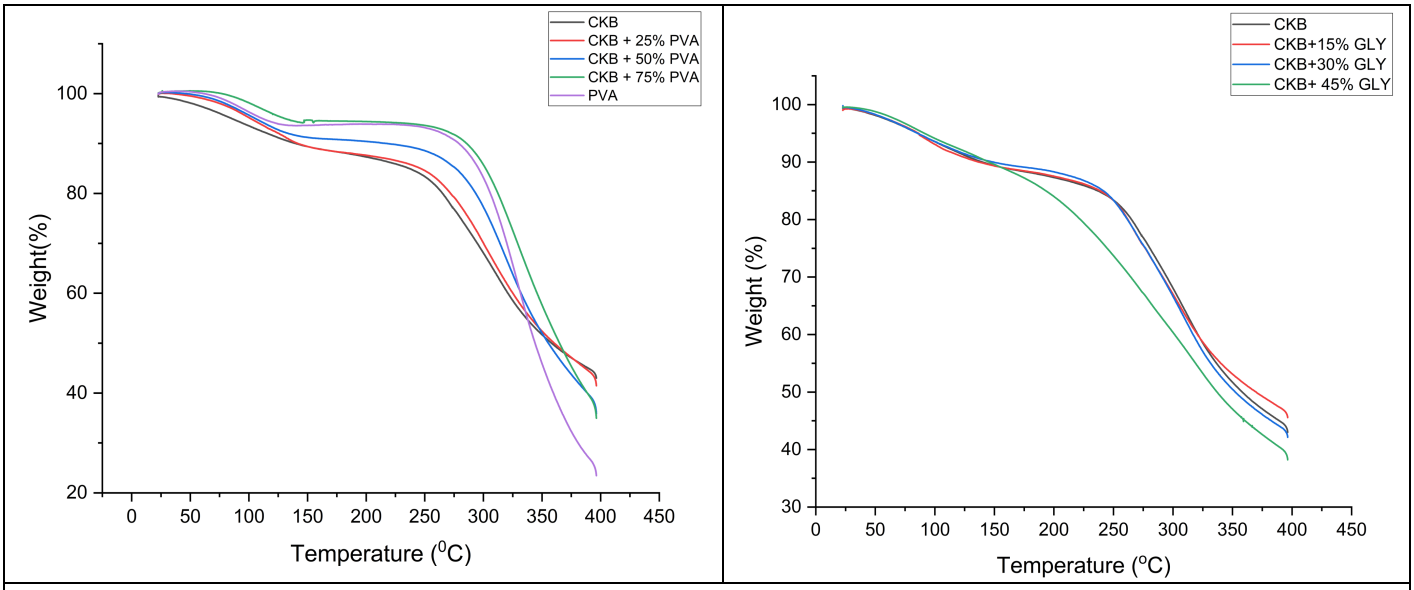

Figure 45: Thermogravimetric analysis of films with plasticizers type at different concentrations

The thermal stability of films made from Crude *Klebsormidium* Biomass (CKB) was assessed using thermogravimetric analysis, with findings detailed in Figure 45 and Table 9. This analysis aimed to identify the temperatures at which the materials decompose, and the proportion of residues left at the highest rate of degradation (Abotbina et al., 2021). The resulting data revealed a consistent pattern of mass loss across films composed of CKB, as well as those with 15% and 30% glycerol content. However, films with a higher glycerol content of 45% showed a significantly higher rate of mass loss. Each sample underwent three distinct phases of degradation. The first phase of mass reduction was noted below 158 °C, likely due to the evaporation of moisture and dehydroxylation. Following this temperature, a weight decrease was connected to the evaporation of plasticizers, indicating an escalation in mass loss correlating with rising levels of plasticizers (Abotbina et al., 2021; Edhirej et al., 2017; Suppakul et al., 2013; Dang et al., 2015).

Table 9: Weight loss of all samples

Temperature Range	**CKB**	**CKB+ %15 GLY**	**CKB + %30 GLY**	**CKB + %45 GLY**	**CKB + %25 PVA**	**CKB + %50 PVA**	**CKB + %75 PVA**	**%100 PVA**
23-158°C	10,37	10,15	9,86	10,81	9,84	9,84	5,71	5,97
158-255°C	6,48	6,72	7,52	16,01	10,29	10,13	14,51	18,45
255-392°C	38,14	35,46	35,18	32,98	36,37	41,42	41,29	49,89
Total Lost (%)	54,99	52,33	52,56	59,8	56,5	61,39	61,51	74,31

In summary, the total mass loss for films containing Crude *Klebsormidium* Biomass (CKB) and glycerol (GLY) varied from 52.33% to 59.8%, closely aligning with the control sample's degradation rate of 54.99%. Conversely, films with added Polyvinyl Alcohol (PVA) exhibited a greater reduction in mass, with rates spanning from 56.5% to 61.39%.

The data indicated that an escalation in the proportion of PVA used as a plasticizer corresponded with an increase in overall mass loss upon degradation. In contrast, augmenting the glycerol content to 30% was linked to a diminished rate of degradation in the bioplastic films.

3.4.6 Scanning Electron Microscopy (SEM) Analysis

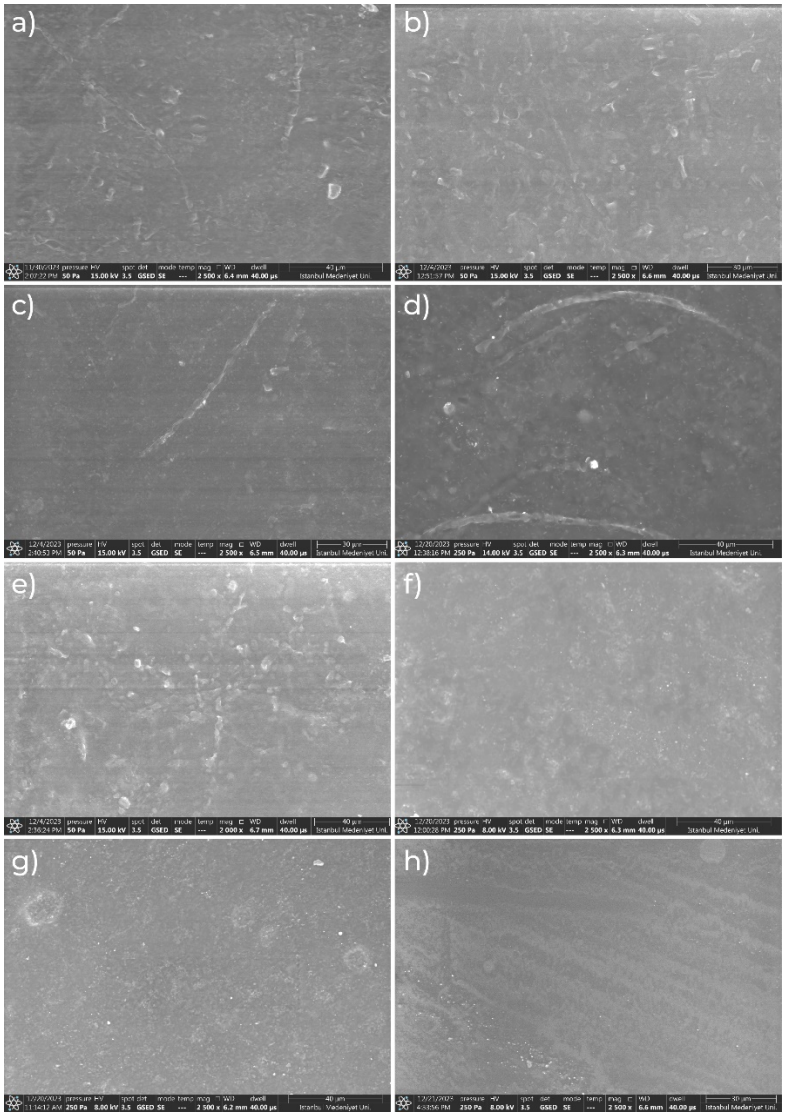

Figure 46: SEM morphology images of CKB, CKB+GLY, and CKB+PVA film groups. The morphologies of the films are represented by a)5%CKB, b)5%CKB-15%GLY, c)5%CKB-30%GLY, d) 5%CKB-45%GLY, e) 5%CKB-25%PVA, f) 5%CKB-50%PVA, g) 5%CKB- 75PVA, h) %100PVA.

The SEM images of the films prepared with different additives were examined, and the cell morphology of *Klebsormidium* microalgae was observed in all samples except the 100% PVA sample. Filamentous cells of *Klebsormidium* were found most abundantly in the 5%CKB sample. Cell morphology is partially preserved. It was similar to the cell density observed in glycerol groups. At the same time, it is clearly seen that *Klebsormidium* cells are less present in the structure at decreasing

concentrations in the PVA groups. At the same time, no cracking was observed in any of the samples, only the *Klebsormidium* cells in the film were observed to have a supporting role in the material matrix. However, there is no aggregation or overlapping cells in the structure, and the cell distribution is smooth and in a certain orientation.

3.4.7 DPPH Radical Scavenging Capacity

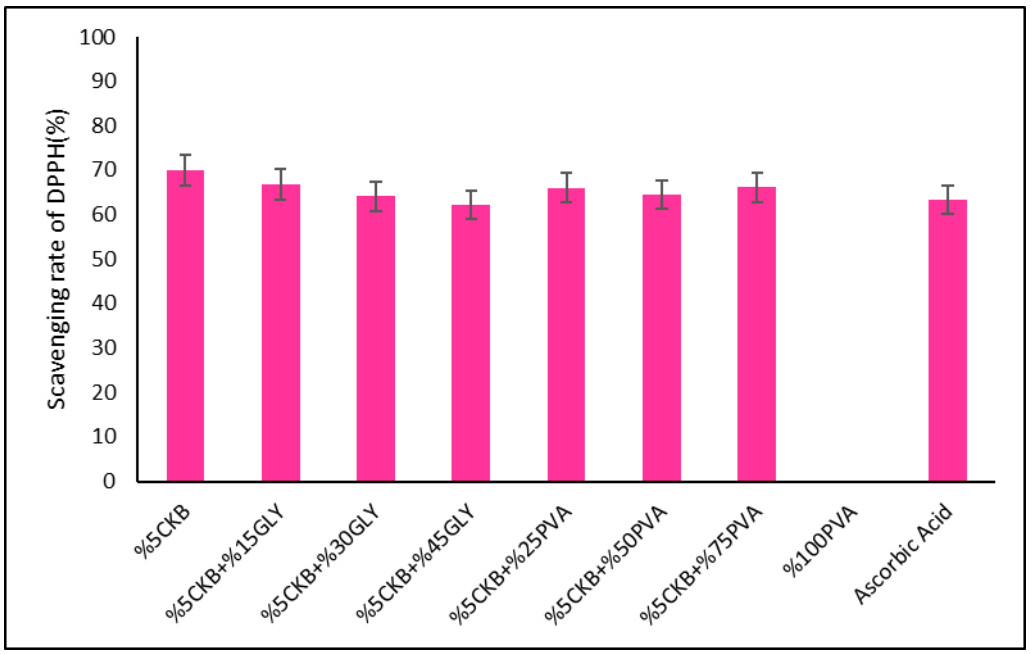

Figure 47: DPPH Radical Scavenging Capacity of CKB, CKB+GLY, CKB+PVA film groups

The antioxidant capacity of films prepared at different concentrations was examined and it is noteworthy that a high level of antioxidant effect was observed in all film groups. When the results are detailed, it can be clearly said that the 5%CKB film has the highest radical scavenging capacity (69%). As the concentration of glycerol added as an additives agent and plasticizer increased, it showed a decreasing trend (62%), while in the PVA group, as the concentration increased, the antioxidant effect decreased slightly and remained almost constant (lowest 64%). When the results are compared to the very low concentration of ascorbic acid in the prepared film samples, it can be clearly said that the bioactive films obtained have a high antioxidant potential. Additionally, no antioxidant effect was detected in the 100% PVA film used as the control group (Ali, A., & Ahmed, S. (2021)). As a result, all bioactive films prepared

at 5mg/mL concentration showed almost the same antioxidant effect as ascorbic acid prepared at 5µg/mL.

Although there is no study to date to determine the antioxidant effect of *Klebsormidium* species, it has been confirmed that microalgae have high antioxidant capacities after a study on *Tetradesmus obliquus*, a green microalgae species (Guedes et al., 2013). Additionally, in another study, it was observed that starch-based films obtained using *Heterochlorella luteoviridis* and *Dunaliella tertiolecta* biomass reduced the oxidation rate of oils during storage (Carissimi et al., 2018). Additionally, another study stated that as the microalgae content increases, the antioxidant effect of the bioactive film increases (Tedeschi et al.,2021). The results show that while 5%CKB had the highest antioxidant capacity, the other films also showed that they had high antioxidant capacity with small decreases.

3.4.8 UV Blocking Capacity of Microalgae Biomass and Bio-active Film

Figure 48 depicts the synthesis patterns of Mycosporine-like Amino Acids (MAAs) by the microalgae Klebsormidium sp. ASYA19, cultivated under intense photosynthetically active radiation (PAR) within a photobioreactor. Weekly sampling followed by extraction of MAAs shows distinct trends. The progression of MAA accumulation is represented through color coding: day 7 is marked in blue, day 14 in orange, day 21 in gray, and day 28 in yellow. There is a discernible escalation in MAA production leading up to day 21, which is likely due to the heightened biosynthetic activity during the late exponential growth phase of the algae, coinciding with the 21st day.

The absorption peaks of MAAs are generally expected within a range of 280-360 nm; however, this specific dataset highlights a concentration of peak activity within the narrower spectrum of 320-330 nm. This observation underscores that Klebsormidium sp. ASYA19 most effectively generates MAAs at these wavelengths under elevated PAR conditions. The peak in MAA production noted on day 21 diminishes by day 28, suggesting a downshift in biosynthetic activity as the algae approach the stationary phase of growth, which typically follows the late exponential phase. Consequently, the optimal window for harvesting MAAs from Klebsormidium sp. ASYA19 under such

growth conditions appears to be just before the transition to the stationary phase, particularly at the identified wavelength range where MAA synthesis is most prolific.

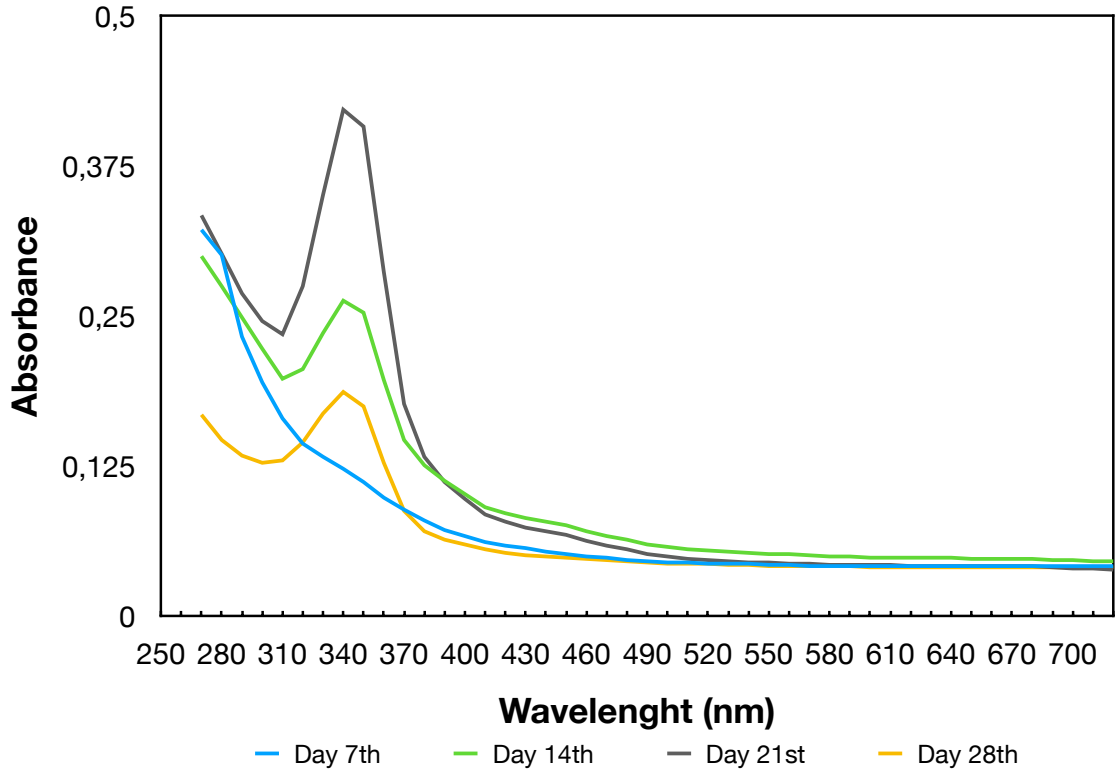

Figure 48: Evaluation of MAA potential of *Klebsormidium* sp. ASYA19 grown with high PAR in the photobioreactor

Figure 49 displays the efficacy of different bio-composite films in shielding against UV radiation, particularly emphasizing the effectiveness of MAAs sourced from Klebsormidium cells harvested on the 21st day—a time identified as peak MAA production. The biocomposite labeled as 5%CKB shows a pronounced ability to absorb UV radiation, with a notable peak at the 320-330 nm wavelength. This finding underscores the CKB film's potential as an exceptional option for applications demanding strong UV protection. Conversely, films with 15GLY and 30GLY additives demonstrate a somewhat diminished but still notable UV-blocking ability.

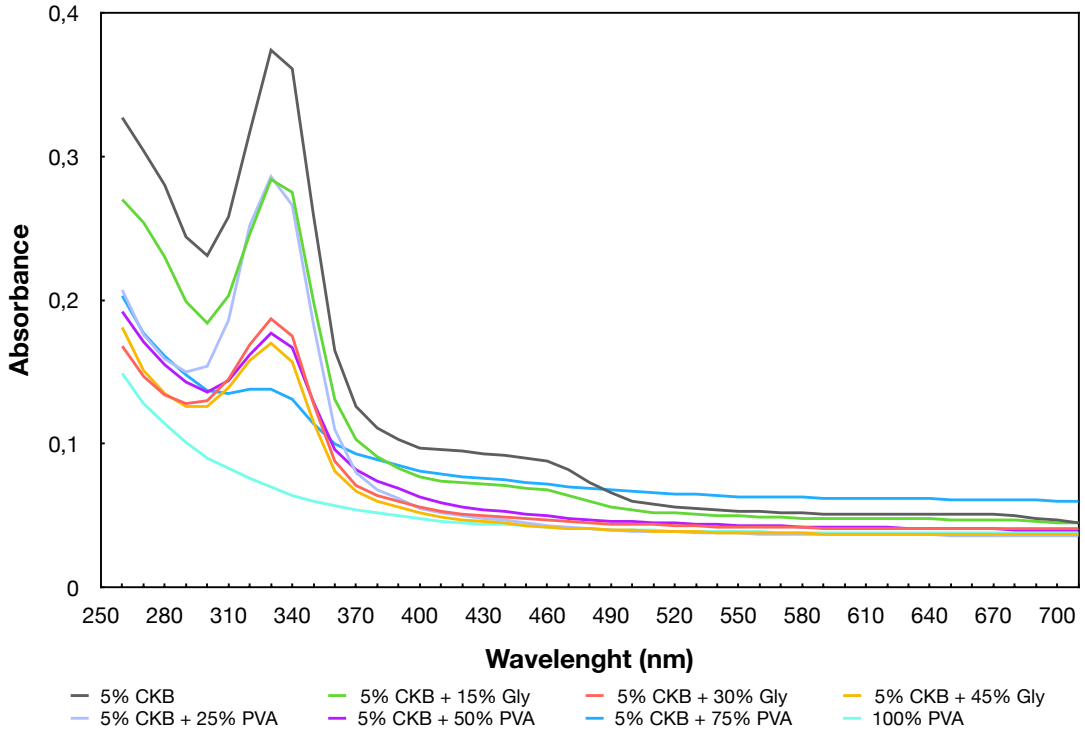

Figure 49: Evaluation of MAA-based UV-Blocking capacity of bioplastic films obtained from *Klebsormidium* biomass obtained with different sources and additives

An observable pattern across the films is that the UV protection tends to wane as the concentration of additives increases. This trend is quite apparent in films integrated with PVA, where, despite a consistent level of protection provided by all concentrations, the overall UV-blocking performance is somewhat less across the spectrum when compared to CKB. The 100% PVA film served as a control and was not anticipated to possess UV-blocking attributes.

In essence, the CKB biocomposite outperforms the others in terms of UV protection, particularly around the 320-330 nm wavelength, while the efficacy of other films with additives varies. Specifically, the PVA-enhanced films demonstrate a reduction in UV-blocking potential as the concentration of the additive surges, yet they maintain a baseline level of this protective characteristic.

3.4.9 Evaluation of Water Content, Swelling Extent, Solubility, Density, and Water Contact Angle of the Film

Film groups	Water content (%)	Swelling degree (%)	Solubility (%)	Density (g/cm3)	WCA
%5CKB-1	4,8%±0,57	49,98%±0,96	25,63%±0,72	1,33±0,12	67,8±1,5
%5CKB+%15GLY	6,92%±0,99	42,5%±2,92	48,39%±5,69	1,35±0,10	67,4±2,1
%5CKB+%30GLY	8,34%±0,39	34,98%±0,63	45%±2,90	1,39±0,07	63,8±2,5
%5CKB+%45GLY	8,56%±0,58	30,6%±0,54	44,11%±0,95	1,49±0,08	60,8±1,2
%5CKB+%25PVA	8,02%±0,49	38,28%±2,27	60,8%±5,95	1,4±0,06	69,7±1,5
%5CKB+%50PVA	8,88%±0,96	21,5%±4,05	62,1%±7,82	1,5±0,06	72,5±0,15
%5CKB+%75PVA	9,36%±0,26	20,73%±4,85	79,34%±2,83	1,52±0,17	67,5±2,7
%100PVA	-	-	100,00%	1,61±0,35	32,6±3,5

Table 10: Explanatory representation of Water Content, Swelling Extent, Solubility, Density, and Water Contact Angle values of the obtained bioactive films.

The water content of the film is the macroscopic characterization of the total water molecules in the film form (Gan et al., 2022). Firstly, when the water content was examined, it was found to be .4.8% in the 5%CKB group, and it was observed that it increased in a non-correlated manner with increasing glycerol and PVA additives. All films have a water content below 10%, confirming their potential for use as food and pharmaceutical packaging. Additionally, due to the solubility of 100% PVA, water content and swelling degree values could not be reached. Secondly, for a swelling degree, there is a trend starting from 5% CKB (50%) and decreasing to 20.73% in the 5%CKB + 75%PVA group. It has been noted that although the values are consistent within the additive groups, there is a wide range. When the solubility is examined, the 5% CKB group has the lowest solubility with 25.63%. In glycerol groups, it varies between 48.39%±5.69 and 44.11%±0.95, which is information that shows that the solubility increases as the glycerol contribution increases. On the other hand, in the PVA group, the solubility varies between 60.8%±5.95 and 79.34%±2.83 (excluding 100% PVA). This increasing solubility rate in the film structure as the PVA ratio increases indicates the unique solubility of PVA in water. When the results are carefully examined, it is seen that the films obtained have high solubility capacity, which makes them advantageous for use in application areas (Tan et al., 2015), (Li et al., 2014). Film density generally increased linearly as plasticizer concentration increased. Regarding the contact angle, it has been observed that, as a general opinion, glycerol decreases

the contact angle at concentrations added to the film due to its hydrophilic character. For the PVA group films, the changes in the contact angle are not sufficient to be taken into consideration and no correlation is observed.

4. CONCLUSION and FUTURE PROSPECT

In this study, the MAA production of strains belonging to the Klebsormidiaceae family isolated from different geographical regions (Antarctica, Arctic, Alps, Alaska, and Atacama) against UV radiation and the changing physiological performances (mainly photosynthetic) of these strains against UV radiation were discussed. In addition, bioplastic-derived films were produced using the biomass of *Klebsormidium sp* ASYA 19, which was determined as the strain with the highest biomass performance. In addition, the UV-blocking effects provided by MAAs were determined by mechanical and thermal development studies of this produced film with various additives.

In this study, it was basically seen that six different *Klebsormidium* strains; *Klebsormidium subtile, Klebsormidium deserticola, Klebsormidium crenulatum, Klebsormidium flaccidum, Klebsormidium flaccidium* ASYA 18, and *Klebsormidium* sp ASYA 19 showed different amounts of biomass accumulation pattern at different temperatures (5,15 and 23°C). When all temperature groups and biomass accumulations are compared, *Klebsormidium* sp ASYA19 shows the highest biomass accumulation at 15°C, which reveals a high potential for material production. However, based on all strains, it was determined that 23°C was the common ambient temperature for all strains.

Klebsormidium strains, whose growth at the specified temperature and photosynthetic performance were determined to affect UV radiation, showed interesting physiological responses among themselves when compared to the control groups. The main polar species, *Klebsormidium* sp ASYA19, *Klebsormidium* flaccidium ASYA18, and *Klebsormidium* flaccidum 2Wm^2, were almost unaffected by UV-B radiation and showed a high degree of UV-B tolerance in terms of both growth and photosynthetic performance, and morphological examinations confirm this result. This result clearly reflected the metabolic adaptations of species living in polar regions that are more sensitive and permeable to UV radiation.

Studies conducted to date have evaluated *Klebsormidium* species as having high potential in terms of MAA production, especially against UV-B. However, this study showed that MAA production in *Klebsormidium* strains is not only synthesized against UV-B (*K.crenulatum*) but also that it is not a dominant metabolite in dealing with (polar) UV-B tolerance in some of these strains. Especially based on HPLC results, the fact that *Klebsormidium crenulatum* produces MAA even under control conditions shows that MAA is used as an osmolyte and nitrogen store in metabolism. The simultaneous increase in MAA concentration with increasing UV-B radiation shows that MAA has a major role in resistance to UV-B in this strain. On the other hand, in polar species, strains with high UV-B tolerance did not produce MAA at the expected rate. This shows that they defend against UV-B by utilizing different mechanisms such as exopolysaccharides and cells forming biofilms and mat forms.

Another step of this study was to present it as a bioplastic-derived film from the biomass of *Klebsormidium* sp. ASYA 19. Following the optimization study, appropriate drying temperature, solvent, and biomass concentrations were determined and the film-forming capacity of microalgae biomass on its own was proven based on its mechanical properties. In order to improve the structural, mechanical, and thermal properties of the film, glycerol, and polyvinyl alcohol plasticizers, which are frequently used in the literature, were used as additives to the film in certain proportions.

Strikingly, a high tensile stress value was obtained with 5% CKB. Especially with the increasing glycerol concentration, the initial tensile stress value in the film decreased and the elongation rate increased significantly. This result revealed that glycerol significantly increased the flexibility of the film structure. However, the results of the PVA group were observed to be much more promising. It was observed that with increasing PVA ratios, both tensile stress and elongation ratio in the film structure increased. This result confirmed that PVA contributed positively to mechanical strength more than the glycerol-doped film groups obtained, as it contributed to the film in both parameters. It has been observed that the thermal stabilization of the films obtained and reinforced with PVA increases as the PVA contribution increases, which again makes it stand out from the glycerol groups lowering the melting temperature over 30% of addition.

The bioactive properties of the microalgae-based films have also attracted attention based on the results. The high antioxidant effect of films in general, even at low concentrations, and the increase in UV-blocking (MAA-based) properties as doping decreases are findings that may expand the use of films in the industry. At the same time, its low water content and high solubility indicate that the film can be a good alternative to the petroleum-based or other green products commonly used today.

As a result, in this study, the physiological responses to UV radiation and MAA production potential of *Klebsormidium* strains isolated from different extreme geographical conditions were evaluated for the first time. At the same time, a film with a UV-blocking effect provided by MAAs was produced from *Klebsormidium* sp. ASYA 19, which has high biomass production. This study has been an indication for future studies to focus specifically on the basic coping mechanism of the *Klebsormidiaceae* family against UV radiation. It also shows that *Klebsormidium* is a potential candidate for popularizing green production and increasing alternative products. In future studies, product developments are made more comprehensively and factors such as stability, color, and odor are carefully taken into account. It has a high potential to be a pioneer in the production of new microalgae-based bioplastics.

5. REFERENCES

Ali, A., & Ahmed, S. (2021). Eco-friendly natural extract loaded antioxidative chitosan/polyvinyl alcohol-based active films for food packaging. *Heliyon*, *7*(3).

Ali, S. S., Abdelkarim, E. A., Elsamahy, T., Al-Tohamy, R., Li, F., Kornaros, M., ... & Sun, J. (2023). Bioplastic production in terms of life cycle assessment: A state-of-the-art review. *Environmental Science and Ecotechnology*, 100254.

Andrady, A. L., & Neal, M. A. (2009). Applications and societal benefits of plastics. *Philosophical Transactions of the Royal Society B: Biological Sciences*, *364*(1526), 1977-1984.

Arróniz-Crespo, M., Sinha, R. P., Martínez-Abaigar, J., Núñez-Olivera, E., & Häder, D. P. (2005). Ultraviolet radiation-induced changes in mycosporine-like amino acids and physiological variables in the red alga Lemanea fluviatilis. *Journal of Freshwater Ecology*, *20*(4), 677-687.

Babele, P. K., Singh, G., Singh, A., Kumar, A., Tyagi, M. B., & Sinha, R. P. (2017). UV-B radiation and temperature stress-induced alterations in metabolic events and defense mechanisms in a bloom-forming cyanobacterium Microcystis aeruginosa. *Acta Physiologiae Plantarum*, *39*, 1-11.

Balskus, E. P., & Walsh, C. T. (2010). The genetic and molecular basis for sunscreen biosynthesis in cyanobacteria. *Science*, *329*(5999), 1653-1656.

Bandaranayake, W. (1998). Mycosporines: are they nature's sunscreens?. *Natural Product Reports*, *15*(2), 159-172.

Barreiro, C., & Barredo, J. L. (2018). Carotenoids production: a healthy and profitable industry. *Microbial Carotenoids: Methods and Protocols*, 45-55.

Becker, E. W. (2007). Micro-algae as a source of protein. *Biotechnology advances*, *25*(2), 207-210.

Bernillon, J., Parussini, E., Letoublon, R., Favre-Bonvin, J., & Arpin, N. (1990). Flavin-mediated photolysis of mycosporines. Phytochemistry, 29(1), 81-84.

Bhatia, S., Sharma, K., Namdeo, A. G., Chaugule, B. B., Kavale, M., & Nanda, S. (2010). Broad-spectrum sun-protective action of Porphyra-334 derived from Porphyra vietnamensis. *Pharmacognosy research*, *2*(1), 45.

Böhm, G. A., Pfleiderer, W., Böger, P., & Scherer, S. (1995). Structure of a novel oligosaccharide-mycosporine-amino acid ultraviolet A/B sunscreen pigment from the terrestrial cyanobacterium Nostoc commune. *Journal of Biological Chemistry*, *270*(15), 8536-8539.

Borburema, H. D., Graiff, A., Marinho-Soriano, E., & Karsten, U. (2022). Photosynthetic performance, growth, pigment content, and photoprotective compounds of the mangrove macroalgae Bostrychia calliptera and Bostrychia montagnei (Rhodophyta) under light stress. *Frontiers in Marine Science*, *9*, 989454.

Bornman, J. F. (1989). New trends in photobiology: Target sites of UV-B radiation in photosynthesis of higher plants. *Journal of Photochemistry and Photobiology B: Biology*, *4*(2), 145-158.

Borowitzka, M. A. (2013). High-value products from microalgae—their development and commercialisation. *Journal of applied phycology*, *25*, 743-756.

Bradford, M. M. (1976). A rapid and sensitive method for the quantitation of microgram quantities of protein utilizing the principle of protein-dye binding. *Analytical biochemistry*, *72*(1-2), 248-254.

Brand-Williams, W., Cuvelier, M. E., & Berset, C. L. W. T. (1995). Use of a free radical method to evaluate antioxidant activity. *LWT-Food science and Technology*, *28*(1), 25-30.

Brennan, L., & Owende, P. (2010). Biofuels from microalgae—a review of technologies for production, processing, and extractions of biofuels and co-products. *Renewable and sustainable energy reviews*, *14*(2), 557-577.

Carissimi, M., Flôres, S. H., & Rech, R. (2018). Effect of microalgae addition on active biodegradable starch film. *Algal Research*, *32*, 201-209.

Carreto, J. I., & Carignan, M. O. (2011). Mycosporine-like amino acids: relevant secondary metabolites. Chemical and ecological aspects. *Marine drugs*, *9*(3), 387-446.

Chandra, R., Pons-Faudoa, F. P., Saldívar, R. P., & Rittmann, B. E. (2020). Effect of ultra-violet exposure on production of mycosporine-like amino acids and lipids by Lyngbya purpurem. *Biomass and bioenergy*, *134*, 105475.

Chen, G. Q., & Patel, M. K. (2012). Plastics derived from biological sources: present and future: a technical and environmental review. *Chemical reviews*, *112*(4), 2082-2099.

Chia, W. Y., Tang, D. Y. Y., Khoo, K. S., Lup, A. N. K., & Chew, K. W. (2020). Nature's fight against plastic pollution: Algae for plastic biodegradation and bioplastics production. *Environmental Science and Ecotechnology*, *4*, 100065.

Chiew-Yen, W., Wan-Loy, C., Marchant, H., & Siew-Moi, P. (2004). Growth response, biochemical composition and fatty acid profiles of four Antarctic microalgae subjected to UV radiation stress. *Malaysian Journal of Science*, *23*(2), 103-118.

Cockell, C. S., & Knowland, J. (1999). Ultraviolet radiation screening compounds. *Biological Reviews*, *74*(3), 311-345.

Conde, F. R., Churio, M. S., & Previtali, C. M. (2000). The photoprotector mechanism of mycosporine-like amino acids. Excited-state properties and photostability of porphyra-334 in aqueous solution. *Journal of Photochemistry and Photobiology B: Biology*, *56*(2-3), 139-144.

Conde, F.R. *et al.* (2007) Experimental study of the excited-state properties and photostability of the mycosporine-like amino acid palythine in aqueous solution. *Photochemical and Photobiological Sciences* 6, 669–674

Convey, P., Bindschadler, R., Di Prisco, G., Fahrbach, E., Gutt, J., Hodgson, D. A., ... & Acce Consortium. (2009). Antarctic climate change and the environment. *Antarctic Science*, *21*(6), 541-563.

Cordero, R. R., Feron, S., Damiani, A., Redondas, A., Carrasco, J., Sepúlveda, E., ... & Seckmeyer, G. (2022). Persistent extreme ultraviolet irradiance in Antarctica despite the ozone recovery onset. *Scientific reports*, *12*(1), 1266.

Darienko, T., Gustavs, L., Mudimu, O., Menendez, C. R., Schumann, R., Karsten, U., ... & Proeschold, T. (2010). Chloroidium, a common terrestrial coccoid green alga previously assigned to Chlorella (Trebouxiophyceae, Chlorophyta). *European Journal of Phycology*, *45*(1), 79-95.

De la Coba, F., Aguilera, J., Figueroa, F. L., De Gálvez, M. V., & Herrera, E. (2009). Antioxidant activity of mycosporine-like amino acids isolated from three red macroalgae and one marine lichen. *Journal of Applied Phycology*, *21*, 161-169.

Del Mondo, A., Sansone, C., & Brunet, C. (2022). Insights into the biosynthesis pathway of phenolic compounds in microalgae. *Computational and Structural Biotechnology Journal*, *20*, 1901-1913.

Dionisio-Sese, M. L. (2010). Aquatic microalgae as potential sources of UV-screening compounds. *Philipp. J. Sci*, *139*(1), 5-16.

Döhler, G., Hoffmann, M., & Stappel, U. (1995). Pattern of proteins after heat shock and UV-B radiation of some temperate marine diatoms and the Antarctic Odontella weissflogii. *Botanica Acta*, *108*(2), 93-98.

Dunlap, W. C., & Shick, J. M. (1998). Ultraviolet radiation-absorbing mycosporine-like amino acids in coral reef organisms: a biochemical and environmental perspective. *Journal of Phycology*, *34*(3), 418-430.

Emadian, S. M., Onay, T. T., & Demirel, B. (2017). Biodegradation of bioplastics in natural environments. *Waste management*, *59*, 526-536.

Fan, X., Bai, L., Zhu, L., Yang, L., & Zhang, X. (2014). Marine algae-derived bioactive peptides for human nutrition and health. *Journal of Agricultural and Food Chemistry*, *62*(38), 9211-9222.

Fu, W., Guðmundsson, Ó., Paglia, G., Herjólfsson, G., Andrésson, Ó. S., Palsson, B. Ø., & Brynjólfsson, S. (2013). Enhancement of carotenoid biosynthesis in the green microalga Dunaliella salina with light-emitting diodes and adaptive laboratory evolution. *Applied microbiology and biotechnology*, *97*, 2395-2403.

Gan, J., Guan, C., Zhang, X., Sun, L., Zhang, Q., Pan, S., ... & Chen, H. (2022). The Preparation of Anti-Ultraviolet Composite Films Based on Fish Gelatin and Sodium Alginate Incorporated with Mycosporine-like Amino Acids. *Polymers*, *14*(15), 2980.

Gandini, A., & Belgacem, M. N. (2012). The state of the art of polymers from renewable resources. *Handbook of Biopolymers and Biodegradable Plastics: Properties, procession and applications, 1st ed., Boston, William Andrew Publishing*, 71-85.

Garcia-Pichel, F., Prufert-Bebout, L., & Muyzer, G. (1996). Phenotypic and phylogenetic analyses show Microcoleus chthonoplastes to be a cosmopolitan cyanobacterium. *Applied and Environmental Microbiology*, *62*(9), 3284-3291.

Gastineau, R., Davidovich, N. A., Hallegraeff, G. M., Probert, I., & Mouget, J. L. (2014). *Reproduction in microalgae* (pp. 1-28). CRC Press.

Genty, B., Briantais, J. M., & Baker, N. R. (1989). The relationship between the quantum yield of photosynthetic electron transport and quenching of chlorophyll fluorescence. *Biochimica et Biophysica Acta (BBA)-General Subjects*, *990*(1), 87-92.

Geraldes, V. *et al.* (2020) Genetic and biochemical evidence for redundant pathways leading to mycosporine-like amino acid biosynthesis in the cyanobacterium sphaerospermopsis torques-reginae ITEP-024. *Algae* 35, 177–187

Gleason, D. F. (1993). Differential effects of ultraviolet radiation on green and brown morphs of the Caribbean coral Porites astreoides. *Limnology and Oceanography*, *38*(7), 1452-1463.

Gopu, M., & Selvam, K. (2020). Polysaccharides from marine red algae Amphiroa rigida and their biomedical potential: An in-vitro study. *Biocatalysis and Agricultural Biotechnology*, *29*, 101769.

Gröniger, A., Hallier, C., & Häder, D. P. (1999). Influence of UV radiation and visible light on Porphyra umbilicalis: photoinhibition and MAA concentration. *Journal of applied phycology*, *11*, 437-445.

Guedes, A. C., Gião, M. S., Seabra, R., Ferreira, A. S., Tamagnini, P., Moradas-Ferreira, P., & Malcata, F. X. (2013). Evaluation of the antioxidant activity of cell extracts from microalgae. *Marine drugs*, *11*(4), 1256-1270.

Gustavs, L., Eggert, A., Michalik, D., & Karsten, U. (2010). Physiological and biochemical responses of green microalgae from different habitats to osmotic and matric stress. *Protoplasma*, *243*, 3-14.

Gustavs, L., Schumann, R., Eggert, A., & Karsten, U. (2009). In vivo growth fluorometry: accuracy and limits of microalgal growth rate measurements in ecophysiological investigations. *Aquatic microbial ecology*, *55*(1), 95-104.

Hanelt, D. (1998). Capability of dynamic photoinhibition in Arctic macroalgae is related to their depth distribution. *Marine Biology*, *131*, 361-369.

Hartmann, A., Glaser, K., Holzinger, A., Ganzera, M., & Karsten, U. (2020). Klebsormidin A and B, two new UV-sunscreen compounds in green microalgal Interfilum and Klebsormidium species (Streptophyta) from terrestrial habitats. Front Microbiol 11: 499.

Hartmann, A., Holzinger, A., Ganzera, M., & Karsten, U. (2016). Prasiolin, a new UV-sunscreen compound in the terrestrial green macroalga Prasiola calophylla (Carmichael ex Greville) Kützing (Trebouxiophyceae, Chlorophyta). *Planta*, *243*, 161-169.

Heo, S. J., Ko, S. C., Cha, S. H., Kang, D. H., Park, H. S., Choi, Y. U., ... & Jeon, Y. J. (2009). Effect of phlorotannins isolated from Ecklonia cava on melanogenesis and their protective effect against photo-oxidative stress induced by UV-B radiation. *Toxicology in vitro*, *23*(6), 1123-1130.

Holzinger, A., & Karsten, U. (2013). Desiccation stress and tolerance in green algae: consequences for ultrastructure, physiological and molecular mechanisms. *Frontiers in plant science*, *4*, 327.

Holzinger, A., Karsten, U., Lütz, C., & Wiencke, C. (2006). Ultrastructure and photosynthesis in the supralittoral green macroalga Prasiola crispa from Spitsbergen (Norway) under UV exposure. *Phycologia*, *45*(2), 168-177.

Holzinger, A., Lütz, C., Karsten, U., & Wiencke, C. (2004). The effect of ultraviolet radiation on ultrastructure and photosynthesis in the red macroalgae Palmaria palmata and Odonthalia dentata from Arctic waters. *Plant Biology*, *6*(05), 568-577.

Hotter, V., Glaser, K., Hartmann, A., Ganzera, M., & Karsten, U. (2018). Polyols and UV-sunscreens in the Prasiola-clade (Trebouxiophyceae, Chlorophyta) as metabolites for stress response and chemotaxonomy. *Journal of phycology*, *54*(2), 264-274.

Hoyer, K., Karsten, U., & Wiencke, C. (2002). Induction of sunscreen compounds in Antarctic macroalgae by different radiation conditions. *Marine Biology*, *141*, 619-627.

Huang, J. J., Lin, S., Xu, W., & Cheung, P. C. K. (2018). Enhancement of the production of bioactive microalgal metabolites by ultraviolet radiation (UVA 365 nm). *Journal of agricultural and food chemistry*, *66*(39), 10215-10224.

Hupel, M., Lecointre, C., Meudec, A., Poupart, N., & Gall, E. A. (2011). Comparison of photoprotective responses to UV radiation in the brown seaweed Pelvetia canaliculata and the marine angiosperm Salicornia ramosissima. *Journal of Experimental Marine Biology and Ecology*, *401*(1-2), 36-47.

Ignat, I., Volf, I., & Popa, V. I. (2011). A critical review of methods for characterisation of polyphenolic compounds in fruits and vegetables. *Food chemistry*, *126*(4), 1821-1835.

Inoue-Sakamoto, K., Nazifi, E., Tsuji, C., Asano, T., Nishiuchi, T., Matsugo, S., ... & Sakamoto, T. (2018). Characterization of mycosporine-like amino acids in the cyanobacterium Nostoc verrucosum. *The Journal of General and Applied Microbiology*, *64*(5), 203-211.

Ishihara, K., Watanabe, R., Uchida, H., Suzuki, T., Yamashita, M., Takenaka, H., ... & Sakamoto, T. (2017). Novel glycosylated mycosporine-like amino acid, 13-O-(β-galactosyl)-porphyra-334, from the edible cyanobacterium Nostoc sphaericum-protective activity on human keratinocytes from UV light. *Journal of Photochemistry and Photobiology B: Biology*, *172*, 102-108.

Jamróz, E., Kopel, P., Juszczak, L., Kawecka, A., Bytesnikova, Z., Milosavljević, V., ... & Adam, V. (2018). Development and characterisation of furcellaran-gelatin films containing SeNPs and AgNPs that have antimicrobial activity. *Food Hydrocolloids*, *83*, 9-16.

Jeffrey, S. T., & Humphrey, G. F. (1975). New spectrophotometric equations for determining chlorophylls a, b, c1 and c2 in higher plants, algae and natural phytoplankton. *Biochemie und physiologie der pflanzen*, *167*(2), 191-194.

Jo, W. S., Song, N. B., Lee, J. H., & Song, K. B. (2014). Physical properties and antimicrobial activities of a persimmon peel/red algae composite film containing grapefruit seed extract. *Food Science and Biotechnology*, *23*, 1169-1172.

Johnsson, N., & Steuer, F. (2018). Bioplastic material from microalgae: Extraction of starch and PHA from microalgae to create a bioplastic material.

Joshi, D., Mohandass, C., & Dhale, M. (2018). Effect of UV-B radiation and desiccation stress on photoprotective compounds accumulation in marine Leptolyngbya sp. *Applied biochemistry and biotechnology*, *184*, 35-47.

Jung, K. A., Lim, S. R., Kim, Y., & Park, J. M. (2013). Potentials of macroalgae as feedstocks for biorefinery. *Bioresource technology*, *135*, 182-190.

Karentz, D., McEuen, F. S., Land, M. C., & Dunlap, W. C. (1991). Survey of mycosporine-like amino acid compounds in Antarctic marine organisms: potential protection from ultraviolet exposure. *Marine Biology*, *108*, 157-166.

Karsten, U. (2008). Defense strategies of algae and cyanobacteria against solar ultraviolet radiation. In *Algal chemical ecology* (pp. 273-296). Berlin, Heidelberg: Springer Berlin Heidelberg.

Karsten, U., & Holzinger, A. (2012). Light, temperature, and desiccation effects on photosynthetic activity, and drought-induced ultrastructural changes in the green alga Klebsormidium dissectum (Streptophyta) from a high alpine soil crust. *Microbial ecology*, *63*, 51-63.

Karsten, U., & Holzinger, A. (2014). Green algae in alpine biological soil crust communities: acclimation strategies against ultraviolet radiation and dehydration. *Biodiversity and Conservation*, *23*, 1845-1858.

Karsten, U., Holzinger, A., & Lütz, C. (2016). Ecophysiological performance of the aeroterrestrial green alga Klebsormidium crenulatum (Klebsormidiophyceae, Streptophyta) isolated from alpine soil crusts. *Journal of Phycology*, 52(6), 989-997.

Karsten, U., Klimant, I., & Holst, G. (1996). A new in vivo fluorimetric technique to measure growth of adhering phototrophic microorganisms. *Applied and Environmental Microbiology*, *62*(1), 237-243.

Karsten, U., Lembcke, S., & Schumann, R. (2007). The effects of ultraviolet radiation on photosynthetic performance, growth and sunscreen compounds in aeroterrestrial biofilm algae isolated from building facades. *Planta*, *225*, 991-1000.

Karsten, U., Lütz, C., & Holzinger, A. (2010). Ecophysiological performance of the aeroterrestrial green alga Klebsormidium crenulatum (Charophyceae, Streptophyta) isolated from an alpine soil crust with an emphasis on desiccation stress 1. *Journal of Phycology*, *46*(6), 1187-1197.

Katoch, M. *et al.* (2016) Heterologous production of cyanobacterial mycosporine-like amino acids mycosporine-ornithine and mycosporine-lysine in Escherichia coli. *Appl Environ Microbiol* 82, 6167–6173

Kessler, E. (1985). Upper limits of temperature for growth in Chlorella (Chlorophyceae). *Plant systematics and evolution*, *151*, 67-71.

Koller, M., Maršálek, L., de Sousa Dias, M. M., & Braunegg, G. (2017). Producing microbial polyhydroxyalkanoate (PHA) biopolyesters in a sustainable manner. *New biotechnology*, *37*, 24-38.

Kraan, S. (2012). Algal polysaccharides, novel applications and outlook. In *Carbohydrates-comprehensive studies on glycobiology and glycotechnology*. IntechOpen.

Kumari, S., Satapathy, S., Datta, M., & Kumar, S. (2022). Adaptation of microalgae to temperature and light stress. In *Plant stress: Challenges and management in the new decade* (pp. 123-134). Cham: Springer International Publishing.

Lawrence, K. P., Long, P. F., & Young, A. R. (2018). Mycosporine-like amino acids for skin photoprotection. *Current Medicinal Chemistry*, *25*(40), 5512-5527.

Lawrence, K.P. *et al.* (2018) Mycosporine-Like Amino Acids for Skin Photoprotection. *Curr Med Chem* 25, 5512

Lee, K. Y., & Mooney, D. J. (2012). Alginate: properties and biomedical applications. *Progress in polymer science*, *37*(1), 106-126.

Levine, I. A., & Fleurence, J. (Eds.). (2018). *Microalgae in health and disease prevention*. Academic Press.

Li, J. H., Miao, J., Wu, J. L., Chen, S. F., & Zhang, Q. Q. (2014). Preparation and characterization of active gelatin-based films incorporated with natural antioxidants. *Food Hydrocolloids*, *37*, 166-173.

Littlepage, J. L. (1965). Oceanographic investigations in McMurdo sound, Antarctica. *Biology of the Antarctic seas II*, *5*, 1-37.

Lopes, J., Goncalves, I., Nunes, C., Teixeira, B., Mendes, R., Ferreira, P., & Coimbra, M. A. (2021). Potato peel phenolics as additives for developing active starch-based films with potential to pack smoked fish fillets. *Food Packaging and Shelf Life*, *28*, 100644.

Lorenz, M., Schubert, H., & Forster, R. M. (1997). In vitro-and in vivo-effects of ultraviolet-B radiation on the energy transfer in phycobilisomes. *Photosynthetica*, *33*(3-4), 517-527.

Mathiot, C., Ponge, P., Gallard, B., Sassi, J. F., Delrue, F., & Le Moigne, N. (2019). Microalgae starch-based bioplastics: Screening of ten strains and plasticization of unfractionated microalgae by extrusion. *Carbohydrate polymers*, *208*, 142-151.

Mikhailyuk, T., Holzinger, A., Massalski, A., & Karsten, U. (2014). Morphology and ultrastructure of Interfilum and Klebsormidium (Klebsormidiales, Streptophyta) with special reference to cell division and thallus formation. *European journal of phycology*, *49*(4), 395-412.

Milledge, J. J., Staple, A., & Harvey, P. J. (2015). Slow pyrolysis as a method for the destruction of Japanese wireweed, Sargassum muticum. *Environment and Natural Resources Research*, *5*(1), 28-37.

Mimouni, V., Ulmann, L., Pasquet, V., Mathieu, M., Picot, L., Bougaran, G., ... & Schoefs, B. (2012). The potential of microalgae for the production of bioactive molecules of pharmaceutical interest. *Current pharmaceutical biotechnology*, *13*(15), 2733-2750.

Morgan-Kiss, R. M., Priscu, J. C., Pocock, T., Gudynaite-Savitch, L., & Huner, N. P. (2006). Adaptation and acclimation of photosynthetic microorganisms to permanently cold environments. *Microbiology and molecular biology reviews*, *70*(1), 222-252.

Nagarajan, V., Mohanty, A. K., & Misra, M. (2016). Perspective on polylactic acid (PLA) based sustainable materials for durable applications: Focus on toughness and heat resistance. *ACS Sustainable Chemistry & Engineering*, *4*(6), 2899-2916.

Navarro, N. P., Mansilla, A., Figueroa, F. L., Korbee, N., Jofre, J., & Plastino, E. (2014). Short-term effects of solar UV radiation and NO3-supply on the accumulation of mycosporine-like amino acids in Pyropia columbina (Bangiales, Rhodophyta) under spring ozone depletion in the sub-Antarctic region, Chile. *Botanica Marina*, *57*(1), 9-20.

Neale, P. J. (2000). Spectral weighting functions for quantifying effects of UV radiation in marine ecosystems. *The effects of UV radiation in the marine environment*, *10*, 72.

Nunes, C., Maricato, É., Cunha, Â., Nunes, A., da Silva, J. A. L., & Coimbra, M. A. (2013). Chitosan–caffeic acid–genipin films presenting enhanced antioxidant activity and stability in acidic media. *Carbohydrate Polymers*, *91*(1), 236-243.

Núñez-Pons, L., Avila, C., Romano, G., Verde, C., & Giordano, D. (2018). UV-protective compounds in marine organisms from the Southern Ocean. *Marine drugs*, *16*(9), 336.

Onen Cinar, S., Chong, Z. K., Kucuker, M. A., Wieczorek, N., Cengiz, U., & Kuchta, K. (2020). Bioplastic production from microalgae: a review. *International journal of environmental research and public health*, *17*(11), 3842.

Oren, A. (1997). Mycosporine-like amino acids as osmotic solutes in a community of halophilic cyanobacteria. *Geomicrobiology Journal*, *14*(3), 231-240.

Oren, A., & Gunde-Cimerman, N. (2007). Mycosporines and mycosporine-like amino acids: UV protectants or multipurpose secondary metabolites? *FEMS microbiology letters*, *269*(1), 1-10.

Pandey, J. K., Lee, C. S., & Ahn, S. H. (2010). Preparation and properties of bio-nanoreinforced composites from biodegradable polymer matrix and cellulose whiskers. *Journal of Applied Polymer Science*, *115*(4), 2493-2501.

Pandey, J. K., Reddy, K. R., Kumar, A. P., & Singh, R. P. (2005). An overview on the degradability of polymer nanocomposites. *Polymer degradation and stability*, *88*(2), 234-250.

Philp, J. C., Bartsev, A., Ritchie, R. J., Baucher, M. A., & Guy, K. (2013). Bioplastics science from a policy vantage point. *New biotechnology*, *30*(6), 635-646.

Piao, M. J., Ahn, M. J., Kang, K. A., Kim, K. C., Zheng, J., Yao, C. W., ... & Hyun, J. W. (2014). Phloroglucinol inhibits ultraviolet B radiation-induced oxidative stress in the mouse skin. *International journal of radiation biology*, *90*(10), 928-935.

Pittman, J. K., Dean, A. P., & Osundeko, O. (2011). The potential of sustainable algal biofuel production using wastewater resources. *Bioresource technology*, *102*(1), 17-25.

Plaza, M., Cifuentes, A., & Ibáñez, E. (2008). In the search of new functional food ingredients from algae. *Trends in food science & technology*, *19*(1), 31-39.

Pope, M.A. *et al.* (2015) O-methyltransferase is shared between the pentose phosphate and shikimate pathways and is essential for mycosporine-like amino acid biosynthesis in Anabaena variabilis ATCC 29413. *ChemBioChem* 16, 320–327

Portwichi, A. and Garcia-Pichel2, F. (2003) *Biosynthetic pathway of mycosporines (mycosporine-like amino acids) in the cyanobacterium Chlorogloeopsis sp. strain PCC 6912*, 42

Rangel, K. C., Villela, L. Z., de Castro Pereira, K., Colepicolo, P., Debonsi, H. M., & Gaspar, L. R. (2020). Assessment of the photoprotective potential and toxicity of Antarctic red macroalgae extracts from Curdiea racovitzae and Iridaea cordata for cosmetic use. *Algal Research*, *50*, 101984.

Rastogi, R. P., & Incharoensakdi, A. (2014). Analysis of UV-absorbing photoprotectant mycosporine-like amino acid (MAA) in the cyanobacterium Arthrospira sp. CU2556. *Photochemical & Photobiological Sciences*, *13*, 1016-1024.

Rastogi, R. P., Madamwar, D., & Incharoensakdi, A. (2015). Sun-screening bioactive compounds mycosporine-like amino acids in naturally occurring cyanobacterial biofilms: role in photoprotection. *Journal of Applied Microbiology*, *119*(3), 753-762.

Remias, D., Schwaiger, S., Aigner, S., Leya, T., Stuppner, H., & Lütz, C. (2012). Characterization of an UV-and VIS-absorbing, purpurogallin-derived secondary pigment new to algae and highly abundant in M esotaenium berggrenii (Z ygnematophyceae, Chlorophyta), an extremophyte living on glaciers. *FEMS microbiology ecology*, *79*(3), 638-648.

Renger, G., Voss, M., Gräber, P., & Schulze, A. (1986). Effect of UV irradiation on different partial reactions of the primary processes of photosynthesis. In *Stratospheric ozone reduction, solar ultraviolet radiation and plant life* (pp. 171-184). Springer Berlin Heidelberg.

Rhim, J. W., Park, H. M., & Ha, C. S. (2013). Bio-nanocomposites for food packaging applications. *Progress in polymer science*, *38*(10-11), 1629-1652.

Rosic, N.N. (2012) Phylogenetic analysis of genes involved in mycosporine-like amino acid biosynthesis in symbiotic dinoflagellates*Applied Microbiology and Biotechnology*, 9429–37

Ryan, K. G., McMinn, A., Mitchell, K. A., & Trenerry, L. (2002). Mycosporine-like amino acids in Antarctic sea ice algae, and their response to UVB radiation. *Zeitschrift für Naturforschung C*, *57*(5-6), 471-477.

Ryšánek, D., Elster, J., Kováčik, L., & Škaloud, P. (2016). Diversity and dispersal capacities of a terrestrial algal genus Klebsormidium (Streptophyta) in polar regions. *FEMS Microbiology Ecology*, *92*(4), fnw039.

Saba, N., Jawaid, M., & Al-Othman, O. (2017). An overview on polylactic acid, its cellulosic composites and applications. *Current Organic Synthesis*, *14*(2), 156-170.

Samolov, E., Mikhailyuk, T., Lukešová, A., Glaser, K., Büdel, B., & Karsten, U. (2019). Usual alga from unusual habitats: Biodiversity of Klebsormidium (Klebsormidiophyceae, Streptophyta) from the phylogenetic superclade G isolated from biological soil crusts. *Molecular phylogenetics and evolution*, *133*, 236-255.

Santiesteban-Romero, B., Martínez-Ruiz, M., Sosa-Hernández, J. E., Parra-Saldívar, R., & Iqbal, H. M. (2022). Microalgae Photo-Protectants and Related Bio-Carriers Loaded with Bioactive Entities for Skin Applications—An Insight of Microalgae Biotechnology. *Marine Drugs*, *20*(8), 487.

Sanyang, M. L., Sapuan, S. M., Jawaid, M., Ishak, M. R., & Sahari, J. (2016). Effect of plasticizer type and concentration on physical properties of biodegradable films based on sugar palm (Arenga pinnata) starch for food packaging. *Journal of food science and technology*, *53*, 326-336.

Sathasivam, R., Radhakrishnan, R., Hashem, A., & Abd_Allah, E. F. (2019). Microalgae metabolites: A rich source for food and medicine. *Saudi journal of biological sciences*, *26*(4), 709-722.

Seaburg, K. G., Parked, B. C., Wharton jr, R. A., & Simmons Jr, G. M. (1981). TEMPERATURE-GROWTH RESPONSES OF ALGAL ISOLATES FROM ANTARCTIC OASES 1. *Journal of Phycology*, *17*(4), 353-360.

Sen, S., & Mallick, N. (2021). Mycosporine-like amino acids: Algal metabolites shaping the safety and sustainability profiles of commercial sunscreens. *Algal Research*, *58*, 102425.

Shang, J. L., Zhang, Z. C., Yin, X. Y., Chen, M., Hao, F. H., Wang, K., ... & Qiu, B. S. (2018). UV-B induced biosynthesis of a novel sunscreen compound in solar radiation and desiccation tolerant cyanobacteria. *Environmental Microbiology*, *20*(1), 200-213.

Shen, J., Jiang, C., Yan, Y., Liu, B., & Zu, C. (2017). Effect of increased UV-B radiation on carotenoid accumulation and total antioxidant capacity in tobacco (Nicotiana tabacum L.) leaves. *Genet. Mol. Res*, *16*(1).

Shetty, P., Gitau, M. M., & Maróti, G. (2019). Salinity stress responses and adaptation mechanisms in eukaryotic green microalgae. *Cells*, *8*(12), 1657.

Shin, Y. J., Jang, S. A., & Song, K. B. (2011). Preparation and mechanical properties of rice bran protein composite films containing gelatin or red algae. *Food Science and Biotechnology*, *20*, 703-707.

Singh, A., Čížková, M., Bišová, K., & Vítová, M. (2021). Exploring mycosporine-like amino acids (MAAs) as safe and natural protective agents against UV-induced skin damage. *Antioxidants*, *10*(5), 683.

Singh, A., Nigam, P. S., & Murphy, J. D. (2011). Mechanism and challenges in commercialisation of algal biofuels. *Bioresource technology*, *102*(1), 26-34.

Singh, A., Nigam, P. S., & Murphy, J. D. (2011). Renewable fuels from algae: an answer to debatable land based fuels. *Bioresource technology*, *102*(1), 10-16

Singh, A., Tyagi, M. B., & Kumar, A. (2017). Cyanobacteria growing on tree barks possess high amount of sunscreen compound mycosporine-like amino acids (MAAs). *Plant physiology and biochemistry*, *119*, 110-120.

Singh, N. K., & Dhar, D. W. (2011). Microalgae as second generation biofuel. A review. *Agronomy for Sustainable Development*, *31*, 605-629.

Singh, S. P. (2009). *Study on mycosporine-like amino acids (MAAs) in cyanobacteria: A biochemical, bioinformatics and molecular biology approach* (Doctoral dissertation, Friedrich-Alexander-Universität Erlangen-Nürnberg (FAU)).

Singh, S.P. *et al.* (2010) Genome mining of mycosporine-like amino acid (MAA) synthesizing and non-synthesizing cyanobacteria: A bioinformatics study. *Genomics* 95, 120–128

Sinha, R. P., & Häder, D. P. (2002). Life under solar UV radiation in aquatic organisms. *Advances in Space Research*, *30*(6), 1547-1556.

Sirisha, V. L., & D'Souza, J. S. (2016). Polysaccharide-based nanoparticles as drug delivery systems. *Marine OMICS*, 663-702.

Škaloud, P., Lukešová, A., Malavasi, V., Ryšánek, D., Hrčková, K., & Rindi, F. (2014). Molecular evidence for the polyphyletic origin of low pH adaptation in the genus Klebsormidium (Klebsormidiophyceae, Streptophyta). *Plant Ecology and Evolution*, *147*(3), 333-345.

Skjånes, K., Rebours, C., & Lindblad, P. (2013). Potential for green microalgae to produce hydrogen, pharmaceuticals and other high value products in a combined process. *Critical reviews in biotechnology*, *33*(2), 172-215.

Smith Jr, W. O., & Gordon, L. I. (1997). Hyperproductivity of the Ross Sea (Antarctica) polynya during austral spring. *Geophysical Research Letters*, *24*(3), 233-236.

Spence, E. *et al.* (2012) Redundant Pathways of Sunscreen Biosynthesis in a Cyanobacterium. *ChemBioChem* 13, 531–533

Starr, R. C., & Zeikus, J. A. (1993). UTEX—The culture collection of algae at the University of Texas at Austin 1993 List of cultures 1. *Journal of phycology*, *29*, 1-106.

Strid, Å., Chow, W. S., & Anderson, J. M. (1990). Effects of supplementary ultraviolet-B radiation on photosynthesis in Pisum sativum. *Biochimica et Biophysica Acta (BBA)-Bioenergetics*, *1020*(3), 260-268.

Tan, J. B. L., & Lim, Y. Y. (2015). Critical analysis of current methods for assessing the in vitro antioxidant and antibacterial activity of plant extracts. *Food chemistry*, *172*, 814-822.

Tapia-Blácido, D. R., do Amaral Sobral, P. J., & Menegalli, F. C. (2013). Effect of drying conditions and plasticizer type on some physical and mechanical properties of amaranth flour films. *LWT-Food Science and Technology*, *50*(2), 392-400.

Tedeschi, A. M., Di Caprio, F., Piozzi, A., Pagnanelli, F., & Francolini, I. (2021). Sustainable bioactive packaging based on thermoplastic starch and microalgae. *International Journal of Molecular Sciences*, *23*(1), 178.

Teoh, M. L., Chu, W. L., Marchant, H., & Phang, S. M. (2004). Influence of culture temperature on the growth, biochemical composition and fatty acid profiles of six Antarctic microalgae. *Journal of Applied Phycology*, *16*, 421-430.

Teoh, M. L., Phang, S. M., & Chu, W. L. (2013). Response of Antarctic, temperate, and tropical microalgae to temperature stress. *Journal of Applied Phycology*, *25*, 285-297.

Thompson, R. C., Moore, C. J., Vom Saal, F. S., & Swan, S. H. (2009). Plastics, the environment and human health: current consensus and future trends. *Philosophical Transactions of the Royal Society B: Biological Sciences*, 364(1526), 2153-2166.

Torres, S., Navia, R., Campbell Murdy, R., Cooke, P., Misra, M., & Mohanty, A. K. (2015). Green composites from residual microalgae biomass and poly (butylene adipate-co-terephthalate): processing and plasticization. *ACS Sustainable Chemistry & Engineering*, *3*(4), 614-624.

Vincent, W. F., & Quesada, A. (2012). Cyanobacteria in high latitude lakes, rivers and seas. In *Ecology of cyanobacteria II: their diversity in space and time* (pp. 371-385). Dordrecht: Springer Netherlands.

Vincent, W. F., & Roy, S. (1993). Solar ultraviolet-B radiation and aquatic primary production: damage, protection, and recovery. *Environmental Reviews*, *1*(1), 1-12.

Vroman, I., & Tighzert, L. (2009). Biodegradable polymers. *Materials*, *2*(2), 307-344.

Wada, N., Sakamoto, T., & Matsugo, S. (2013). Multiple roles of photosynthetic and sunscreen pigments in cyanobacteria focusing on the oxidative stress. *Metabolites*, *3*(2), 463-483.

Wada, N., Sakamoto, T., & Matsugo, S. (2015). Mycosporine-like amino acids and their derivatives as natural antioxidants. *Antioxidants*, *4*(3), 603-646.

Wang, B., Li, Y., Wu, N., & Lan, C. Q. (2008). CO 2 bio-mitigation using microalgae. *Applied microbiology and biotechnology*, *79*, 707-718.

Weihs, P., Schmalwieser, A. W., & Schauberger, G. (2013). UV effects on living organisms. *Environmental Toxicology: Selected Entries from the Encyclopedia of Sustainability Science and Technology*, 609-688.

Weis, E., & Berry, J. A. (1987). Quantum efficiency of photosystem II in relation to 'energy'-dependent quenching of chlorophyll fluorescence. *Biochimica et Biophysica Acta (BBA)-Bioenergetics*, *894*(2), 198-208.

Wijesekara, I., Pangestuti, R., & Kim, S. K. (2011). Biological activities and potential health benefits of sulfated polysaccharides derived from marine algae. *Carbohydrate polymers*, *84*(1), 14-21.

Wu, Y., Polvani, L. M., & Seager, R. (2013). The importance of the Montreal Protocol in protecting Earth's hydroclimate. *Journal of Climate*, *26*(12), 4049-4068.

Zacher, K., Roleda, M. Y., Hanelt, D., & Wiencke, C. (2007). UV effects on photosynthesis and DNA in propagules of three Antarctic seaweeds (Adenocystis utricularis, Monostroma hariotii and Porphyra endiviifolium). *Planta*, *225*, 1505-1516.

Zaki, N. A. A., Mahmud, S., & Omar, A. F. (2018, August). Ultraviolet protection properties of commercial sunscreens and sunscreens containing zno nanorods. In *Journal of Physics: Conference Series* (Vol. 1083, No. 1, p. 012012). IOP Publishing.

Zavřel, T., Očenášová, P., Sinetova, M. A., & Červený, J. (2018). Determination of storage (starch/glycogen) and total saccharides content in algae and cyanobacteria by a phenol-sulfuric acid method. *Bio-protocol*, *8*(15), e2966-e2966.

Zia, K. M., Zuber, M., & Ali, M. (Eds.). (2017). *Algae based polymers, blends, and composites: chemistry, biotechnology and materials science*. Elsevier.